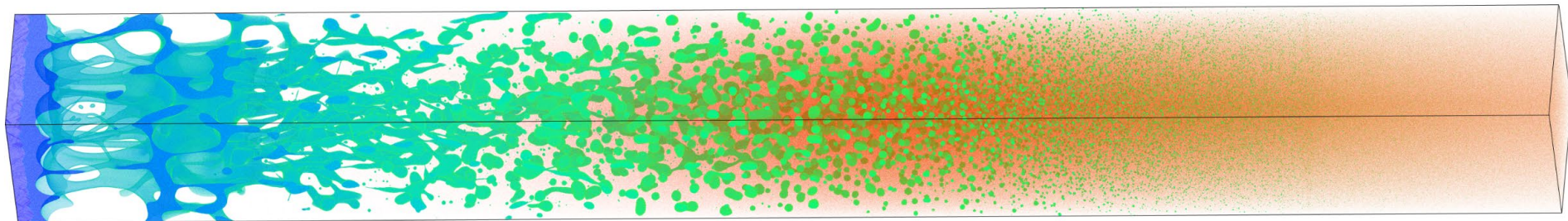
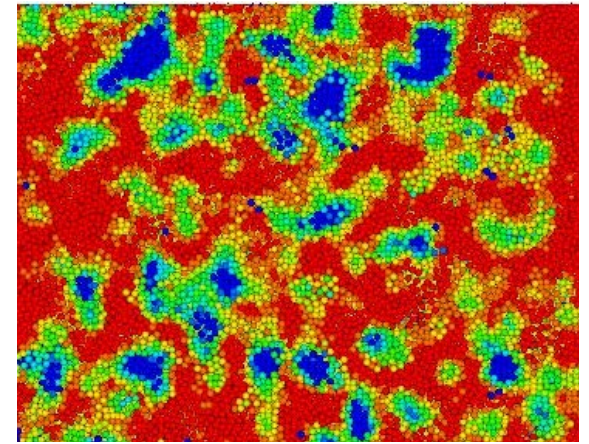
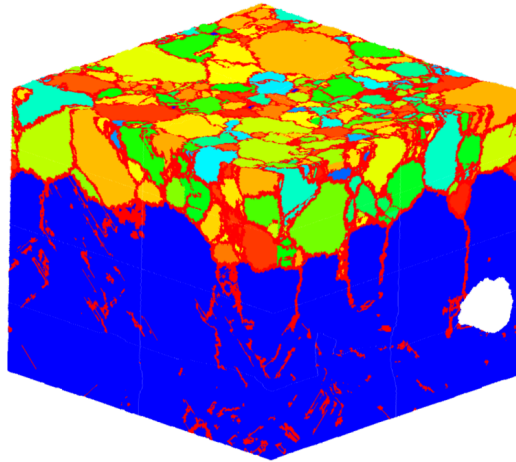
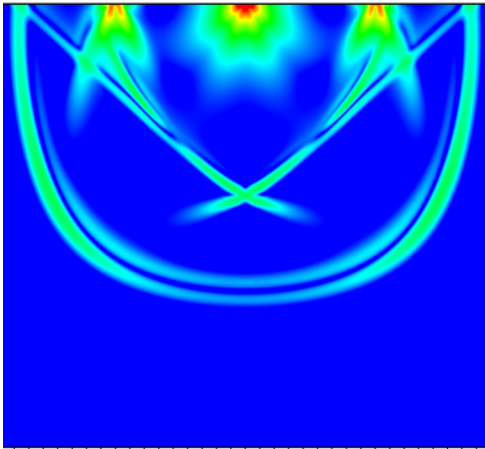


Laser-induced thermal processes: heat transfer, thermoelastic waves, melting, spallation, evaporation, and phase explosion (basic mechanisms and illustrations from atomistic modeling)

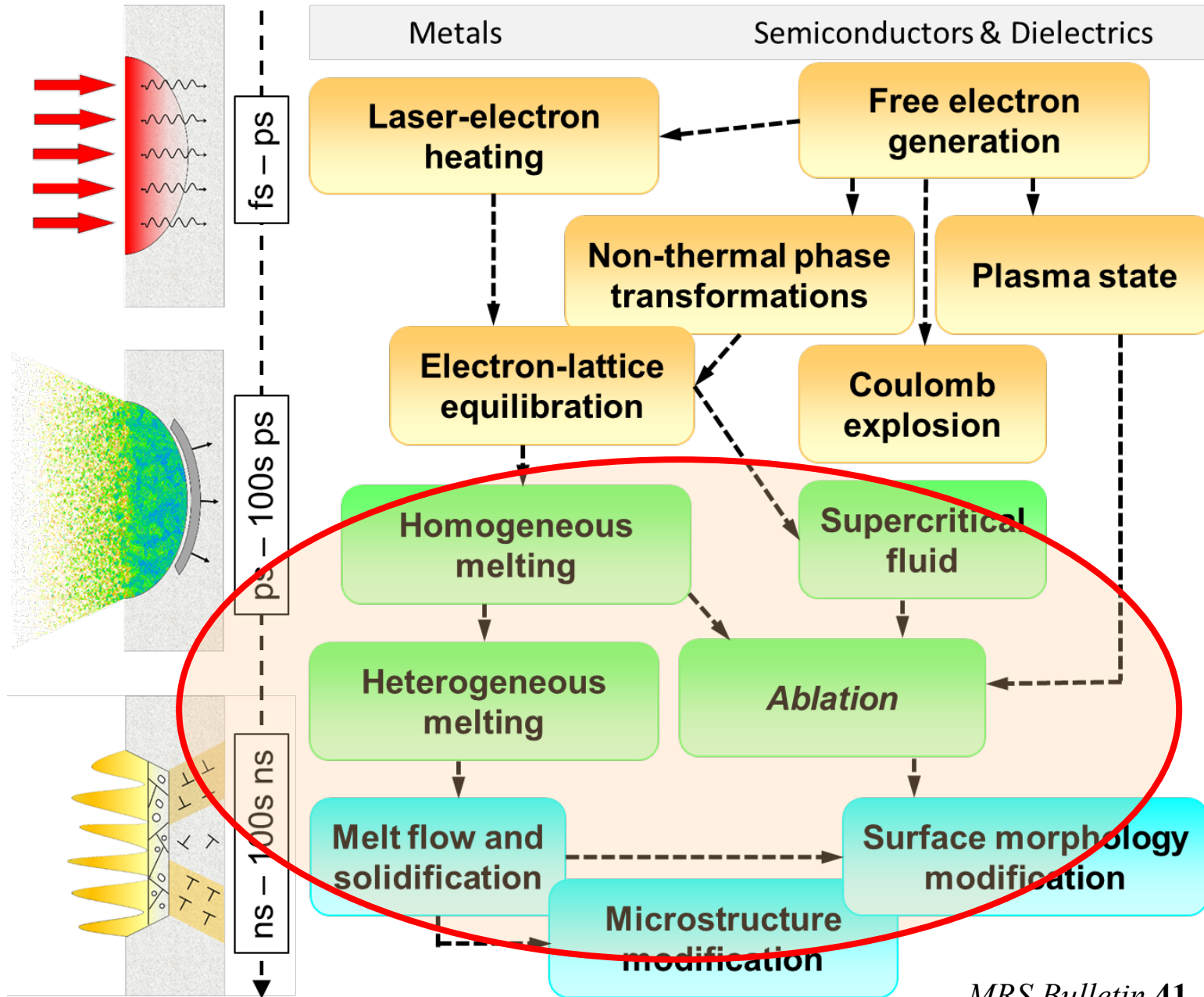
Leonid Zhigilei

University of Virginia

Department of Materials Science and Engineering



Processes involved in laser interaction with materials



Thermal processes in laser-materials interactions

Implications of **rapid, localized** heating by laser pulses

Heat transfer after laser excitation



dimensionality of heat transfer, electron-phonon nonequilibrium

Laser-induced stresses



photomechanical effects, spallation

Melting



superheating, homogeneous & heterogeneous melting

Solidification



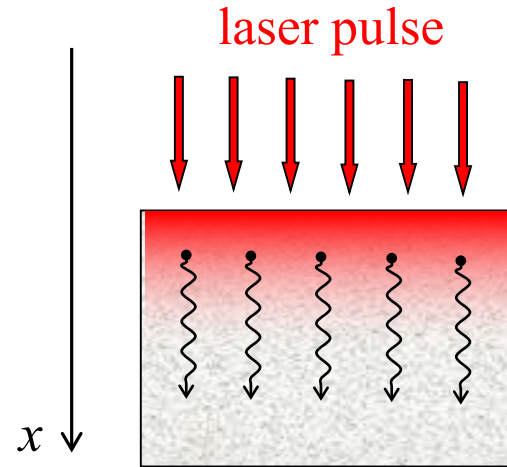
metastable phases, unusual microstructure

Vaporization



explosive boiling / “phase explosion”

Laser energy deposition and heat transfer



Fourier's law for heat transfer:

$$q_x = -k \frac{\partial T(x, t)}{\partial x} \quad \text{- heat flux [Jm}^{-2}\text{s}^{-1}\text{]}$$

$$\rho c_p \frac{\partial T(x, t)}{\partial t} = \frac{\partial}{\partial x} \left[k(T) \frac{\partial T(x, t)}{\partial x} \right] + S(x, t)$$

laser →

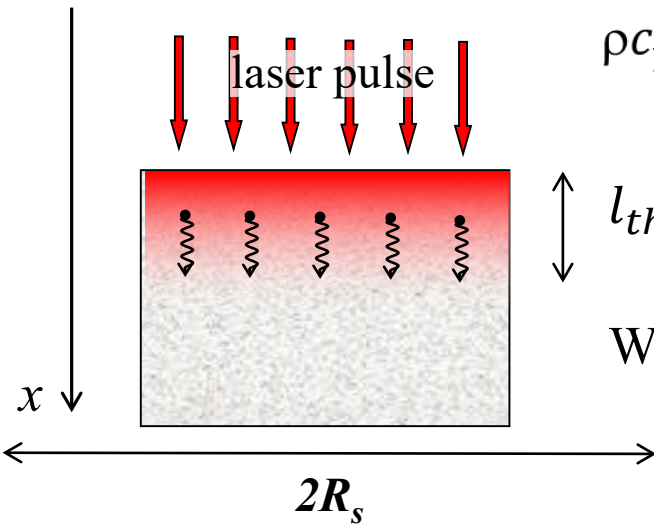
ρ is density [kgm^{-3}]; k is thermal conductivity [$\text{W m}^{-1}\text{K}^{-1}$], c_p is specific heat [$\text{Jkg}^{-1}\text{K}^{-1}$]

if k is constant

$$\frac{\partial T(x, t)}{\partial t} = D \frac{\partial^2 T(x, t)}{\partial x^2} + S(x, t)$$

where $D = k/\rho c_p$ is diffusion coefficient [m^2/s]

Dimensionality of heat transfer



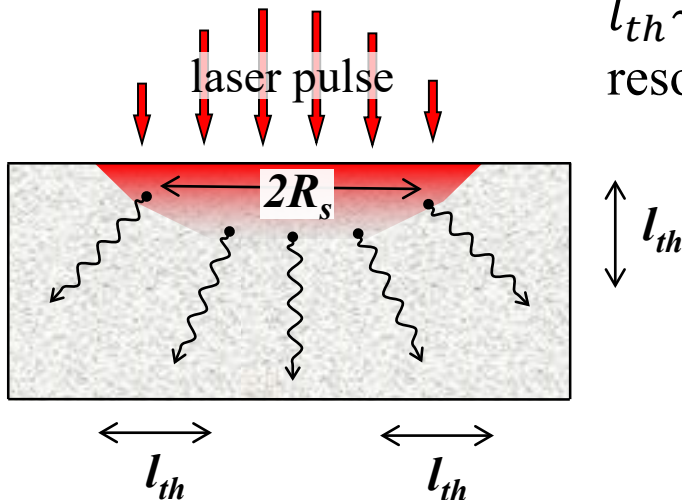
$$\rho c_p \frac{\partial T(x, t)}{\partial t} = \frac{\partial}{\partial x} \left[k(T) \frac{\partial T(x, t)}{\partial x} \right] + S(x, t)$$

$$l_{th} = \sqrt{2k \tau / \rho c_p} = \sqrt{2D\tau} \quad \text{- characteristic length of heat diffusion}$$

When are the estimations based on 1D heat transfer valid?

when $l_{th} \ll R_s$, 1D approximation is valid

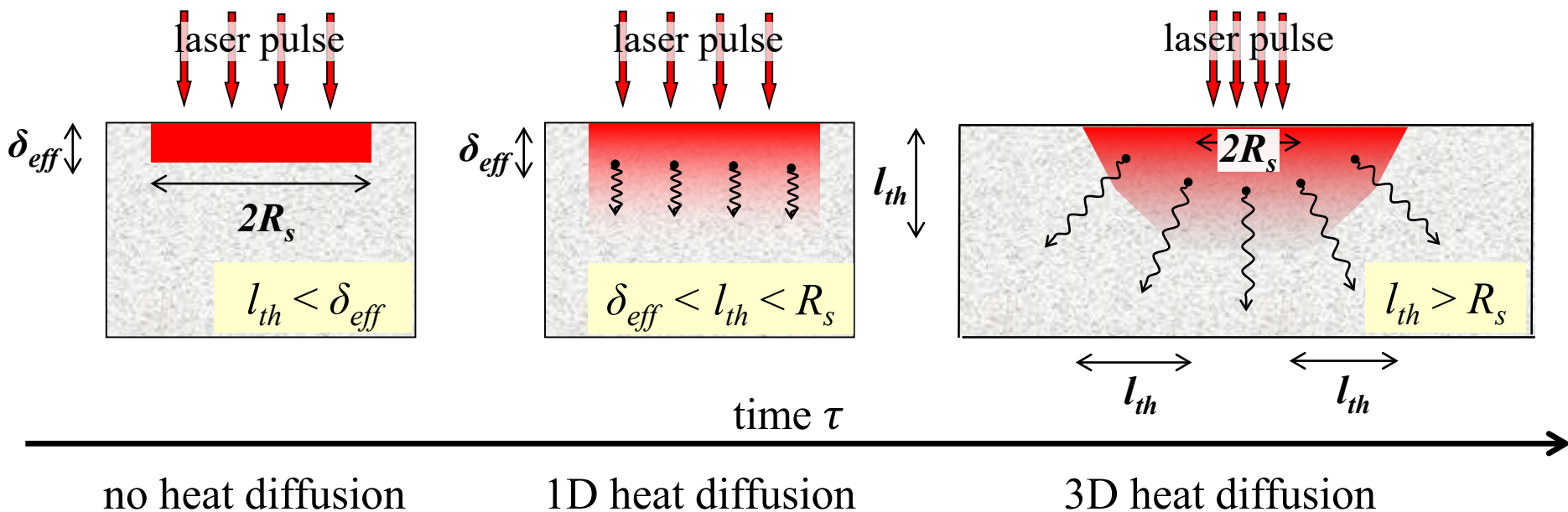
Example: using k and c_p typical for metals, we can estimate $l_{th} \sim 0.1 - 1 \mu m$ for $\tau \sim 1 - 10 ns$ (typical melting – resolidification time) \rightarrow 1D is valid for $R_s \approx 10 - 100 \mu m$



Otherwise, if $l_{th} \sim R_s$ or $l_{th} > R_s$ we have to consider 2D or 3D heat transfer:

$$\rho c_p \frac{\partial T(\vec{r}, t)}{\partial t} = \nabla \cdot [k(T) \nabla T(\vec{r}, t)] + S(\vec{r}, t)$$

Dimensionality of heat transfer: Implications for F_{th} (τ_p)



δ_{eff} - effective depth of energy deposition:

$$\delta_{eff} = \left(\frac{128}{\pi}\right)^{\frac{1}{8}} \left(\frac{\kappa_0^2 \cdot C_l}{T_f \cdot G^2 \gamma}\right)^{\frac{1}{4}} \quad C_e = \gamma T_e$$

$$k_e = k_0 T_e / T_l$$

Corkum *et al.*, *Phys. Rev. Lett.* **61**, 2886, 1988

For Ni (large G):

$$l_{opt} = 13.5 \text{ nm}$$

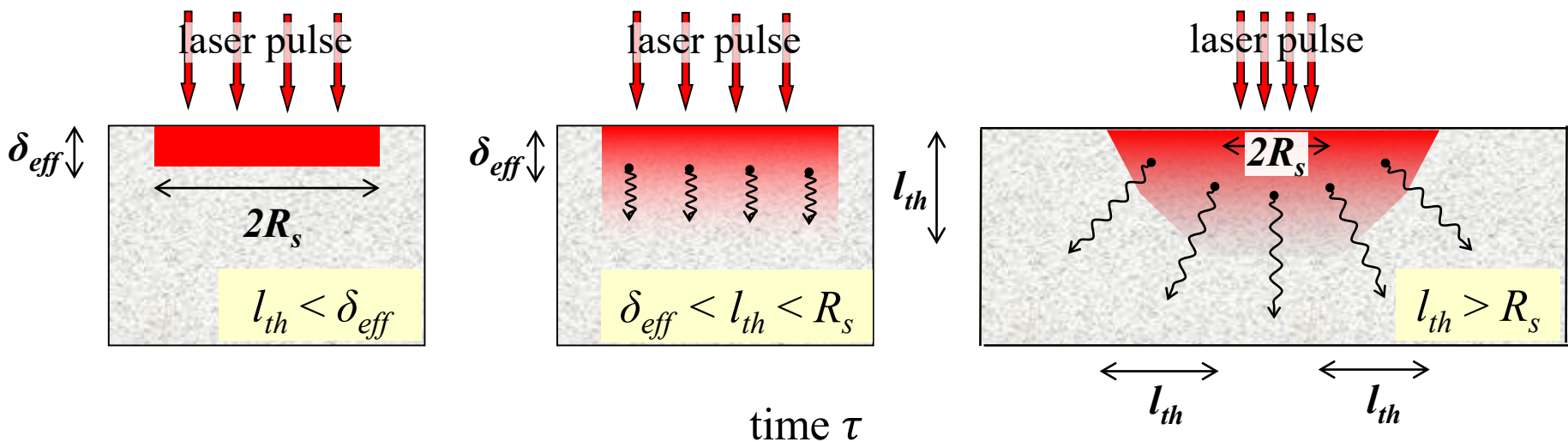
$$\delta_{eff} \approx 50 \text{ nm}$$

For Ag (small G):

$$l_{opt} = 12 \text{ nm}$$

$$\delta_{eff} \approx 350 - 100 \text{ nm}$$

Dimensionality of heat transfer: Implications for F_{th} (τ_p)



no heat diffusion

1D heat diffusion

3D heat diffusion

δ_{eff} - effective depth of energy deposition:

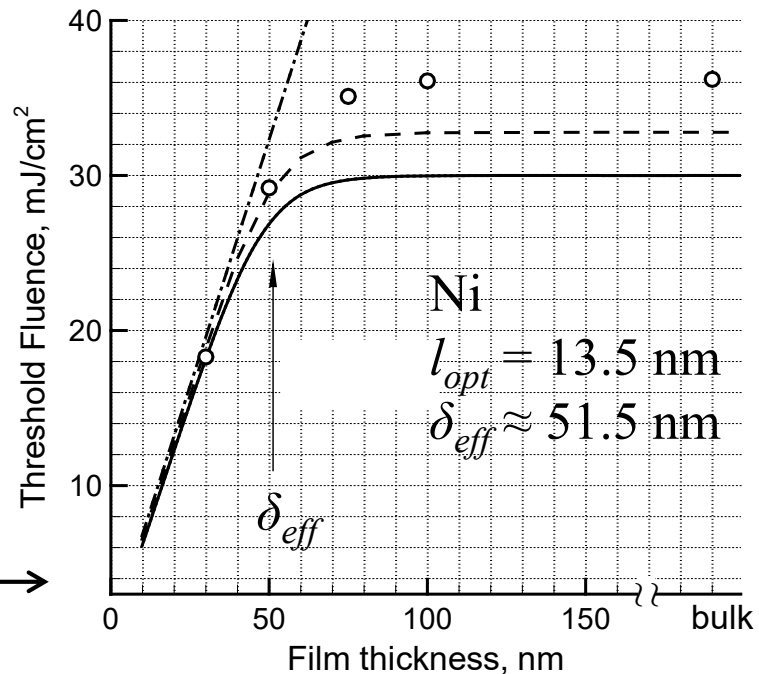
$$\delta_{eff} = \left(\frac{128}{\pi}\right)^{\frac{1}{8}} \left(\frac{\kappa_0^2 \cdot C_l}{T_f \cdot G^2 \gamma}\right)^{\frac{1}{4}}$$

$$C_e = \gamma T_e$$

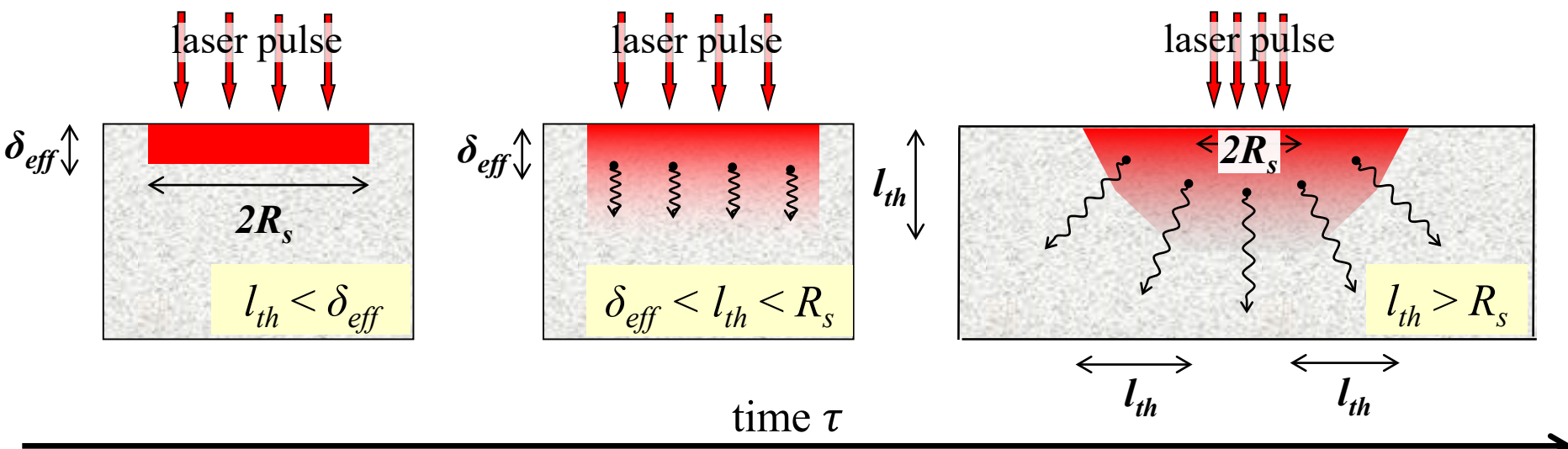
$$k_e = k_0 T_e / T_l$$

Corkum *et al.*, *Phys. Rev. Lett.* **61**, 2886, 1988

Ivanov and Zhigilei, *Appl. Phys. A* **79**, 977, 2004



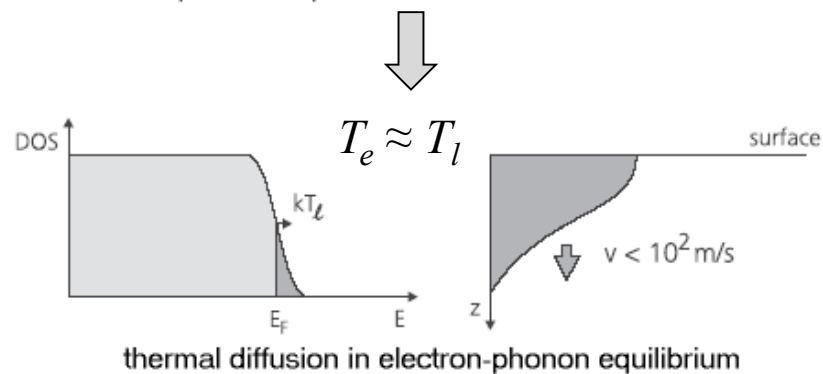
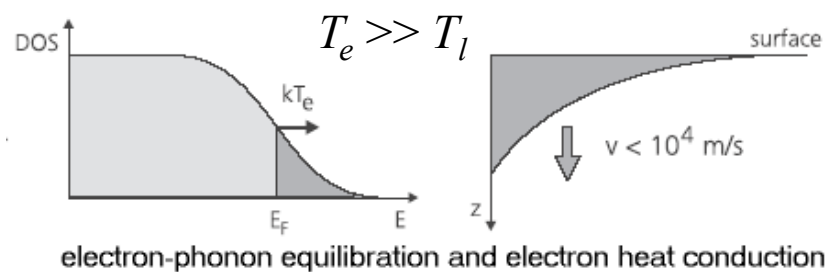
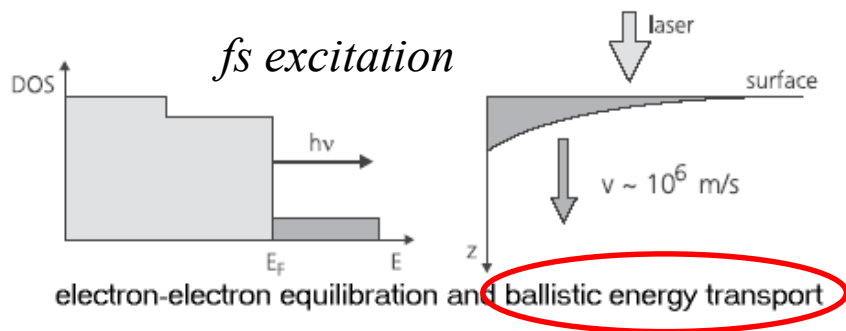
Dimensionality of heat transfer: Implications for F_{th} (τ_p)



no heat diffusion

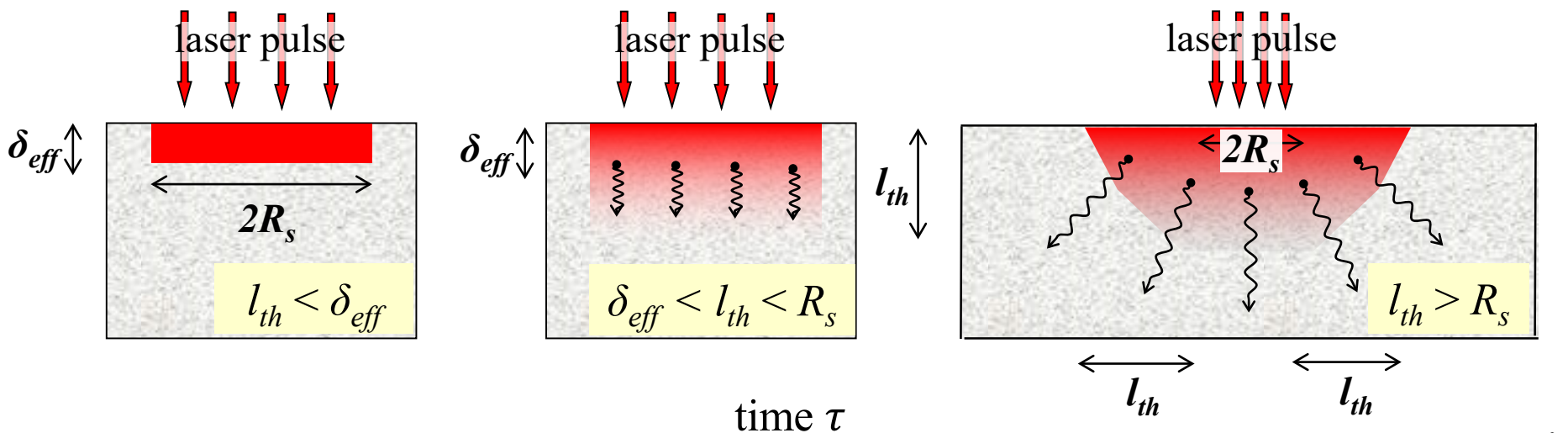
1D heat diffusion

3D heat diffusion



Hohlfeld *et al.*, *Chem. Phys.* **251**, 237, 2000

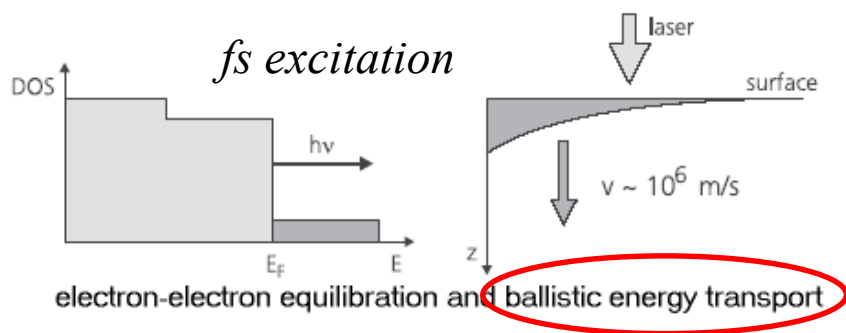
Dimensionality of heat transfer: Implications for F_{th} (τ_p)



no heat diffusion

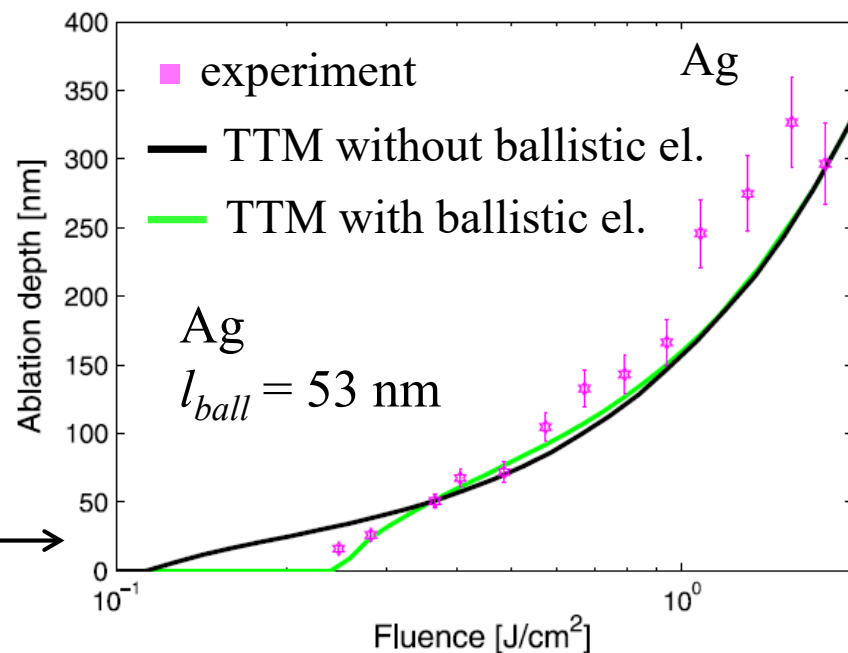
1D heat diffusion

3D heat diffusion

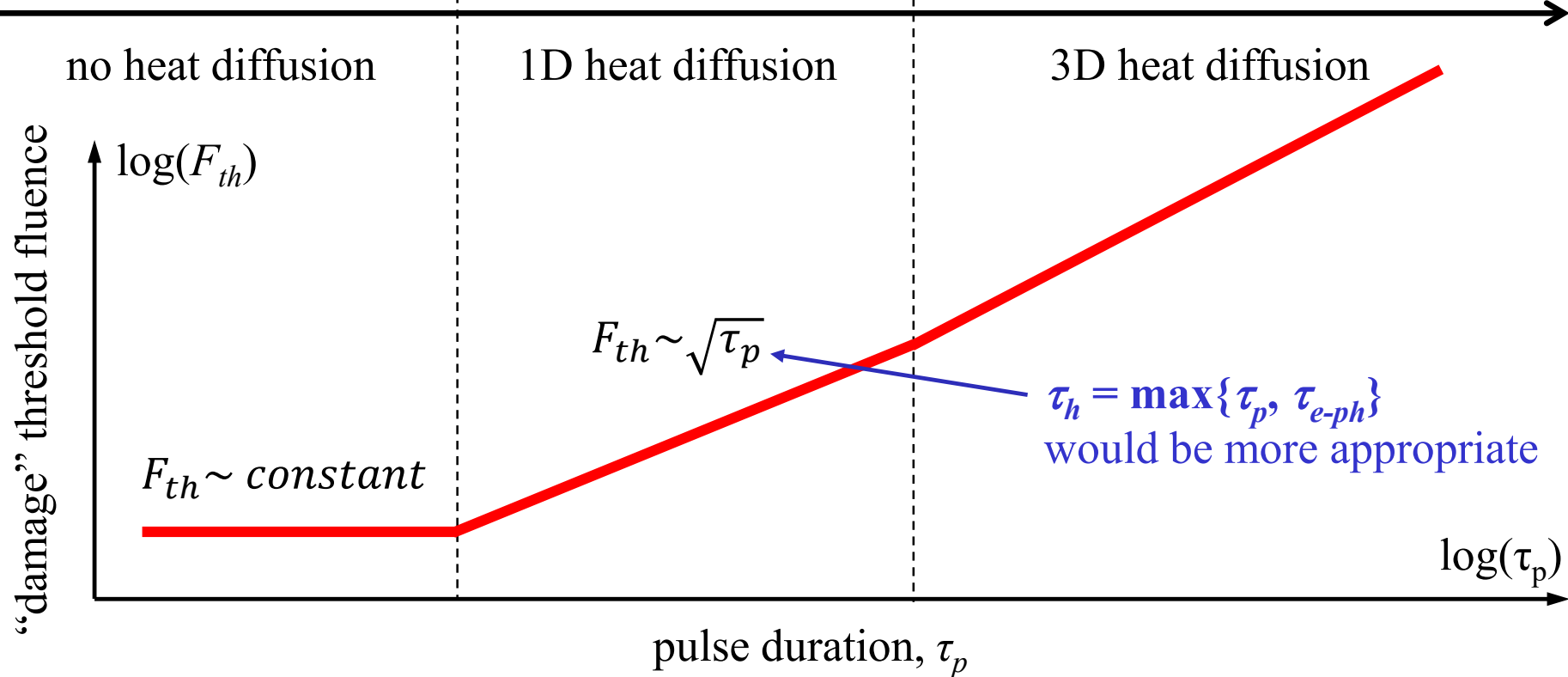
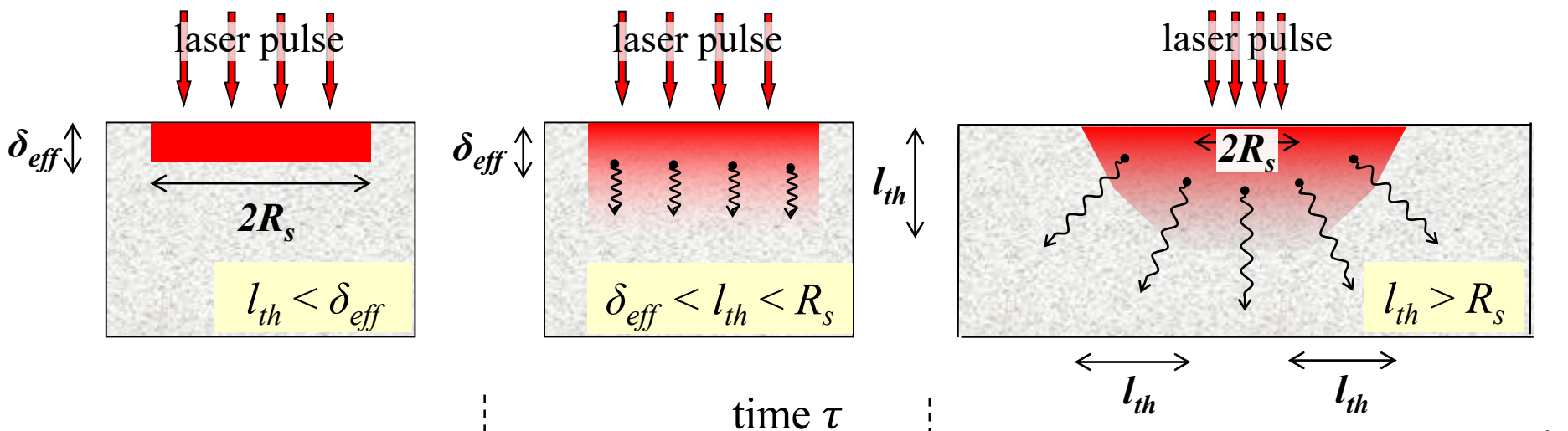


Hohlfeld *et al.*, *Chem. Phys.* **251**, 237, 2000

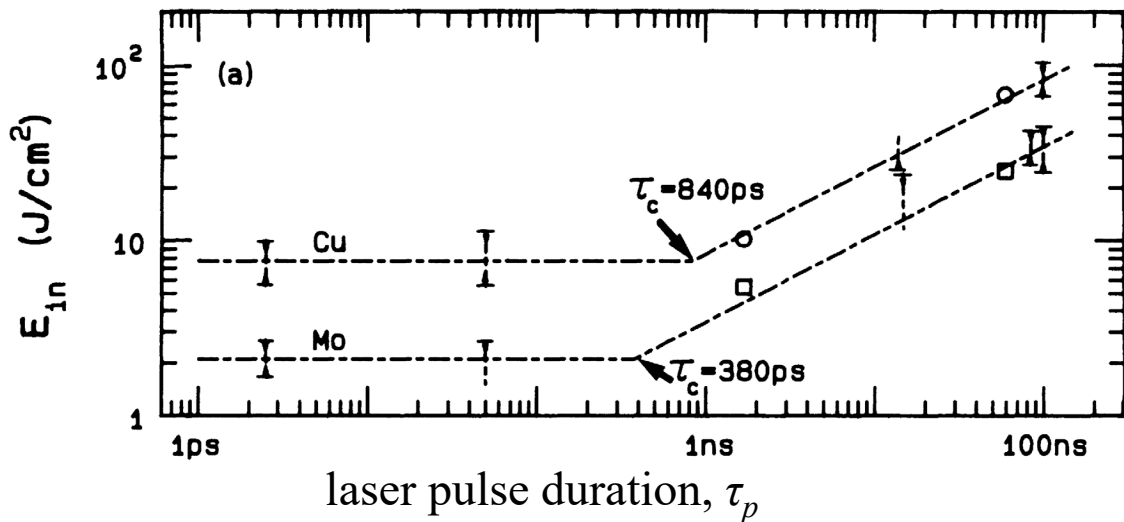
Byskov-Nielsen *et al.*, *Appl Phys A* **103**, 447, 2011 →



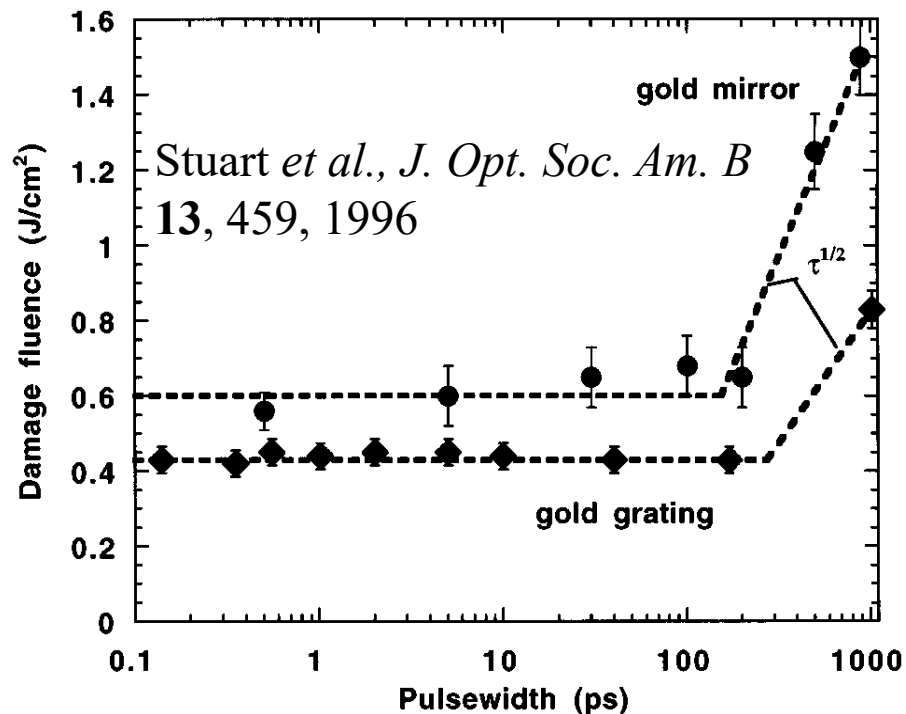
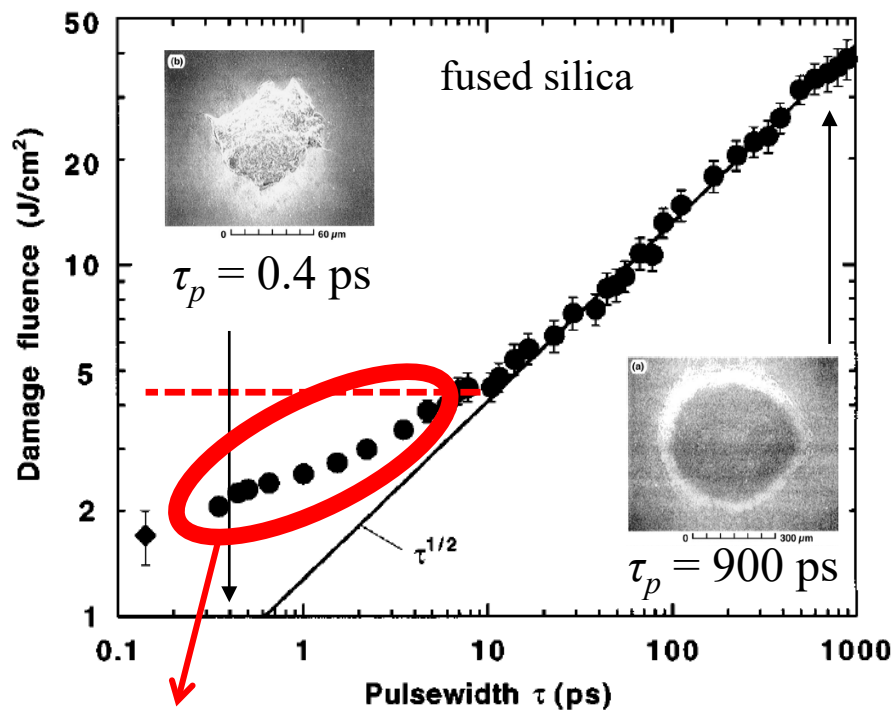
Dimensionality of heat transfer: Implications for F_{th} (τ_p)



Dimensionality of heat transfer: Implications for $F_{th}(\tau_p)$



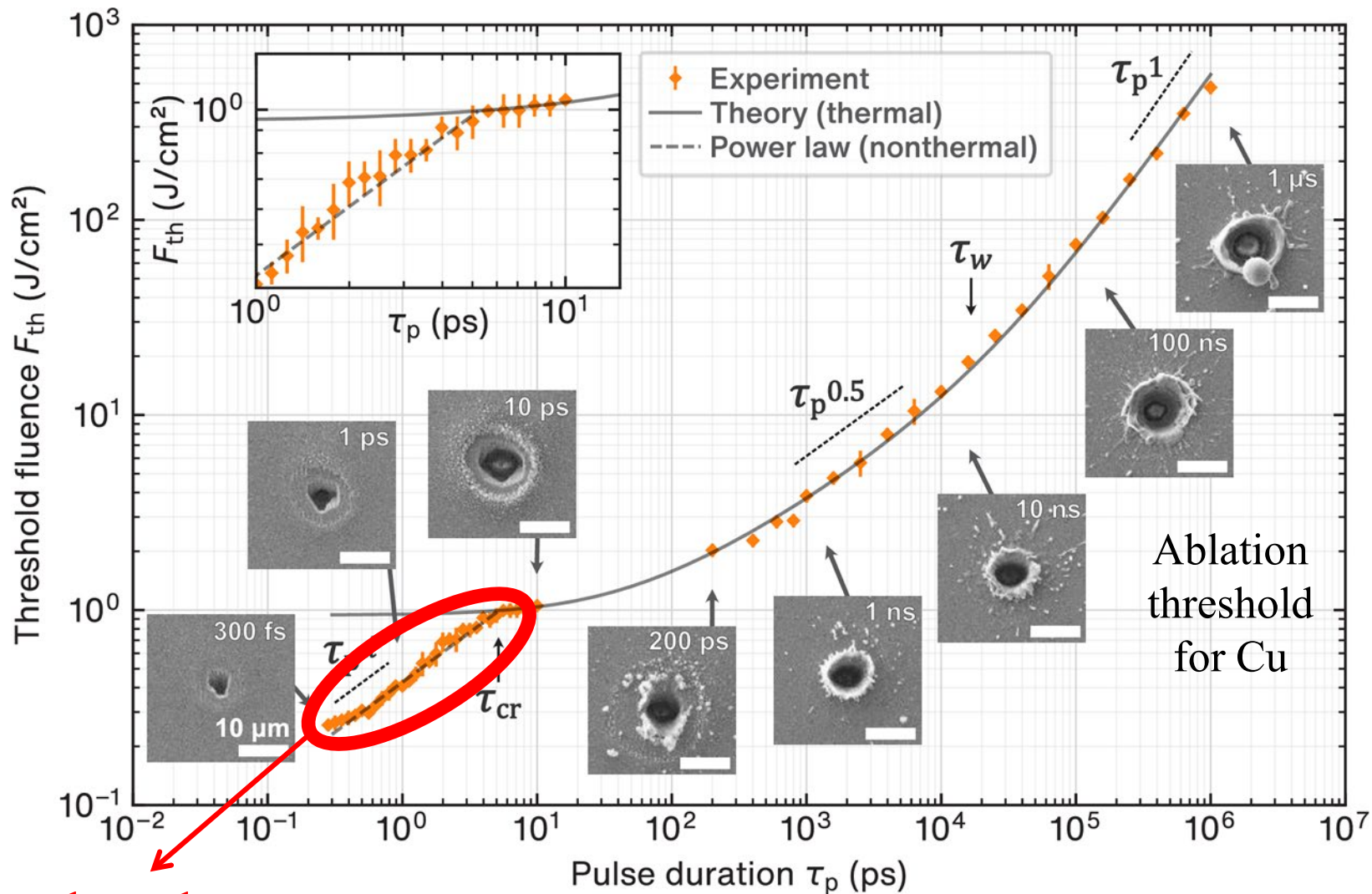
Corkum *et al.*, *Phys. Rev. Lett.* **61**, 2886, 1988



Stuart *et al.*, *J. Opt. Soc. Am. B* **13**, 459, 1996

nonthermal ablation

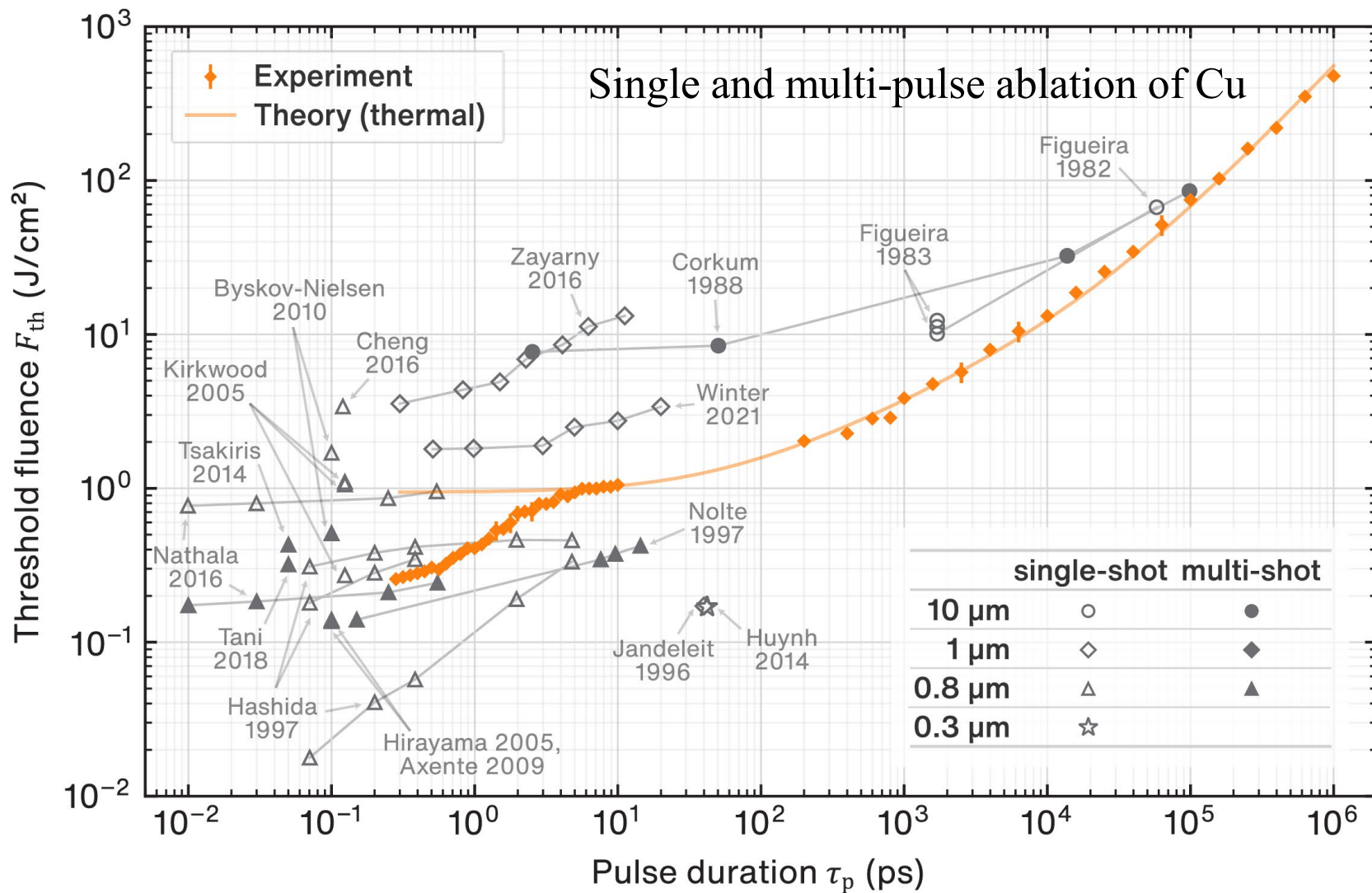
Dimensionality of heat transfer: Implications for $F_{th}(\tau_p)$



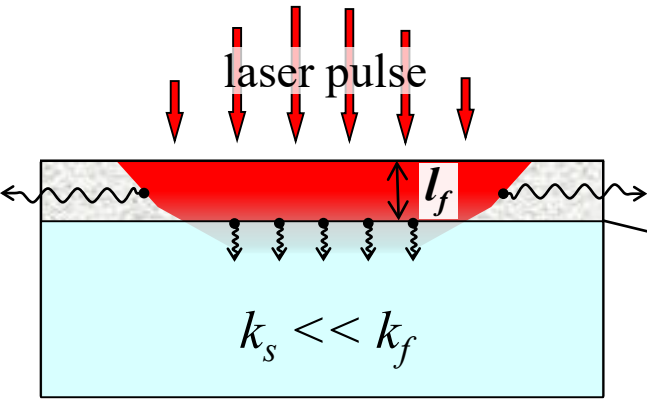
nonthermal
ablation ?

Tsubasa Endo *et al.*, *Optics Express* **31**, 36027, 2023

Dimensionality of heat transfer: Implications for F_{th} (τ_p)



Dimensionality of heat transfer

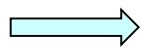


high- k film on a low- k substrate: 2D lateral heat transfer + 1D (for large R_s) heat transfer to the substrate

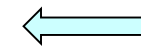
$T_f = T_s$ may not be valid, *i.e.*, $\Delta T = T_s - T_f \neq 0$

Thermal boundary resistance R (Kapitza resistance):

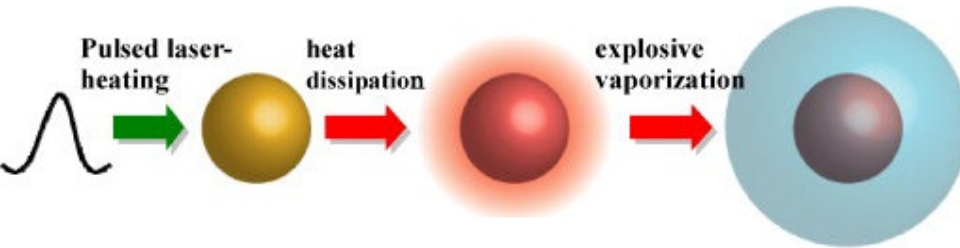
$$q = -k \Delta T / \Delta x$$



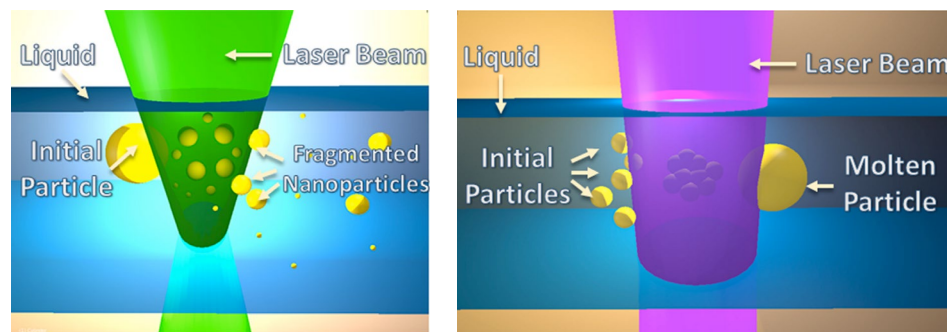
equivalent depth: $kR = \Delta x$



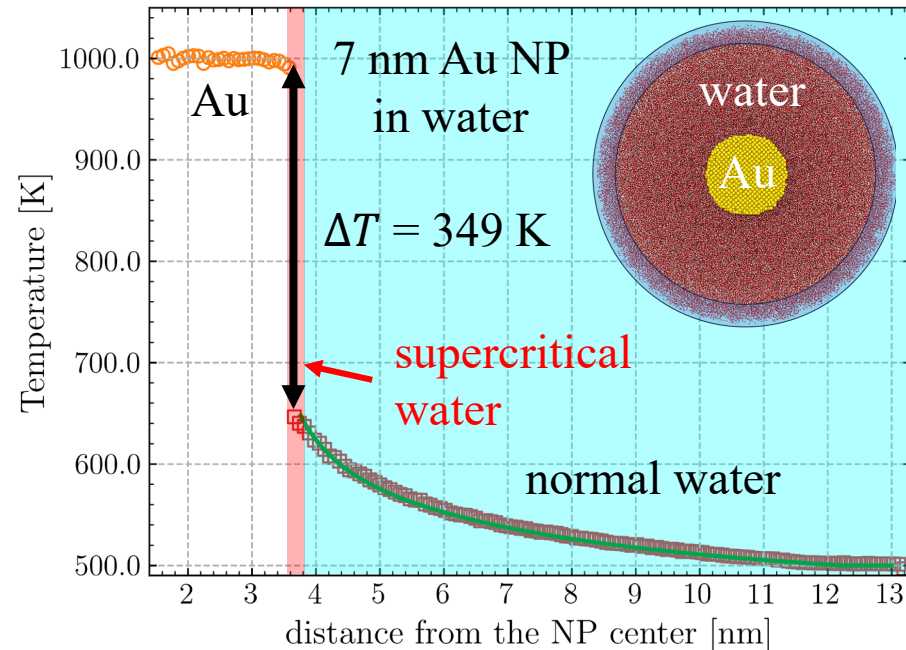
$$q = -\Delta T / R$$



Hashimoto *et al.*, *J. Photochem. Photobiol. C* **13**, 28, 2012



Zhang, Gökce, Barcikowski, *Chem. Rev.* **117**, 3990, 2017



MD simulations, Mikhail Arefev, current work

Laser energy deposition and heat transfer

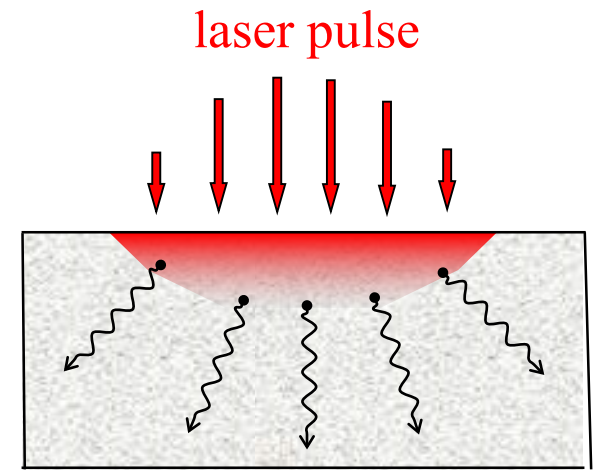
phonons (in non-metals)

phonons

electrons (in metals)

electrons

$$\rho c_p \frac{\partial T(\vec{r}, t)}{\partial t} = \nabla \cdot [k(T) \nabla T(\vec{r}, t)] + S(\vec{r}, t)$$



What are the *dominant* heat carriers?

- phonons in dielectrics & semiconductors
- electrons in metals

Example: Silicon

Diffusion of electron-hole pairs accounts for $\sim 30\text{-}40\%$ of k of solid Si close to T_m ;
jump from 20.4 to $56.5 \text{ Wm}^{-1}\text{K}^{-1}$ at 1700 K is due to transition to metallic state upon melting

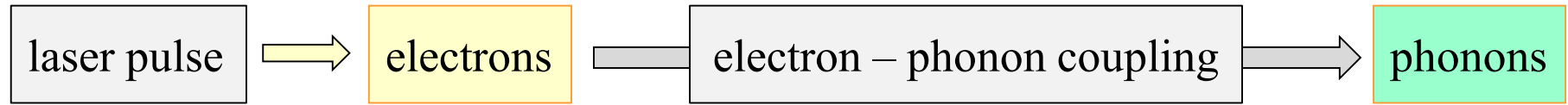
[Fulkerson *et al.*, *Phys. Rev.* **167**, 765, 1968] [Yamasue *et al.*, *J. Crystal Growth* **234**, 121, 2002]

Why do we care?

Energy is stored in atomic vibrations (phonons), but laser deposits energy to electrons \rightarrow **conditions for electron-phonon nonequilibrium**

Laser energy deposition & heat transfer: Electron-phonon nonequilibrium

Energy pathway:



Laser excitation can create conditions of electron – phonon nonequilibrium
(electron and lattice temperatures are not equal to each other)

For metals: two-temperature model (TTM) [Anisimov *et al.*, *Sov. Phys. JETP* **39**, 375, 1974]

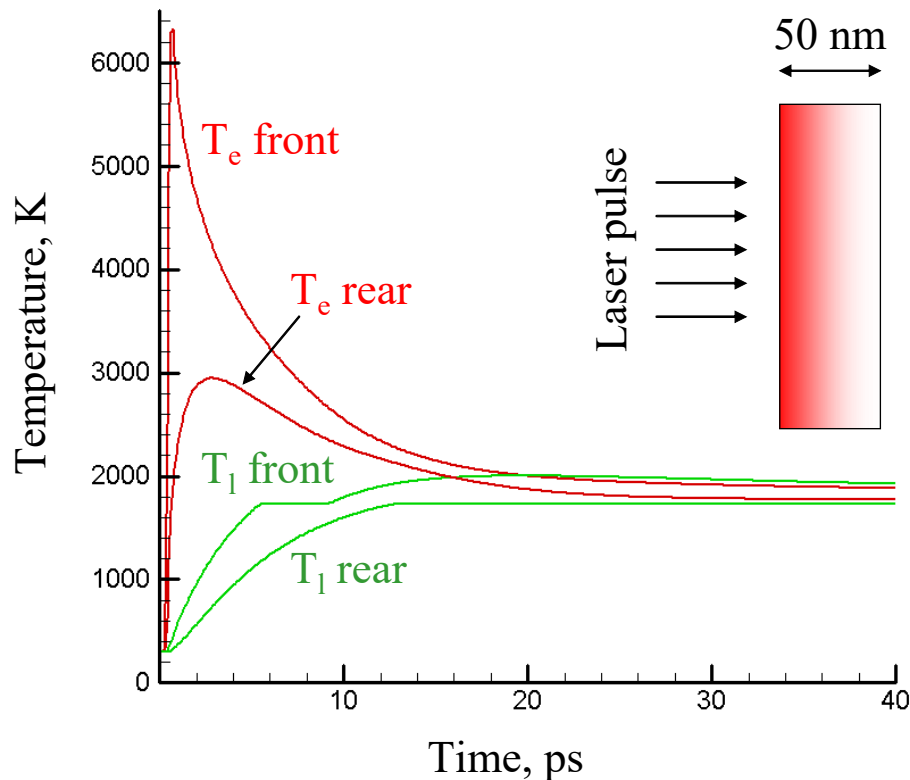
$$c_e(T_e) \frac{\partial T_e(\vec{r}, t)}{\partial t} = \underbrace{\nabla \cdot [k_e(T_e, T_l) \nabla T_e(\vec{r}, t)]}_{\text{transport}} - G(T_e)(T_e - T_l) + S(\vec{r}, t)$$
$$\underbrace{c_l(T_l) \frac{\partial T_l(\vec{r}, t)}{\partial t}}_{\text{storage}} = \nabla \cdot [\cancel{k_l(T_l) \nabla T_l(\vec{r}, t)}]_{\text{metals}} + \underbrace{G(T_e)(T_e - T_l)}_{\text{energy exchange}}$$

Heat diffusion equations written for T_e and T_l + **additional terms** accounting for electron-phonon energy exchange

Laser energy deposition & heat transfer: Electron-phonon nonequilibrium

$$c_e(T_e) \frac{\partial T_e(\vec{r}, t)}{\partial t} = \nabla \cdot [k_e(T_e, T_l) \nabla T_e(\vec{r}, t)] - G(T_e)(T_e - T_l) + S(\vec{r}, t)$$

$$c_l(T_l) \frac{\partial T_l(\vec{r}, t)}{\partial t} = \nabla \cdot [k_l(T_l) \nabla T_l(\vec{r}, t)] + G(T_e)(T_e - T_l)$$

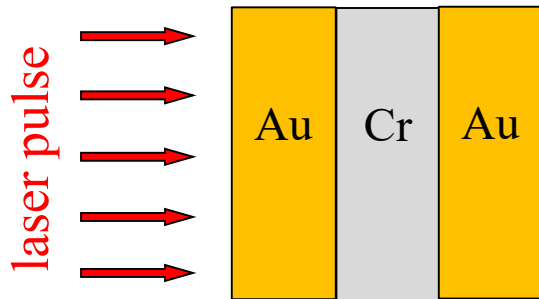


50 nm Ni film irradiated by
200 fs pulse at absorbed
fluence of 430 J/m²

Are there any practical
implications?

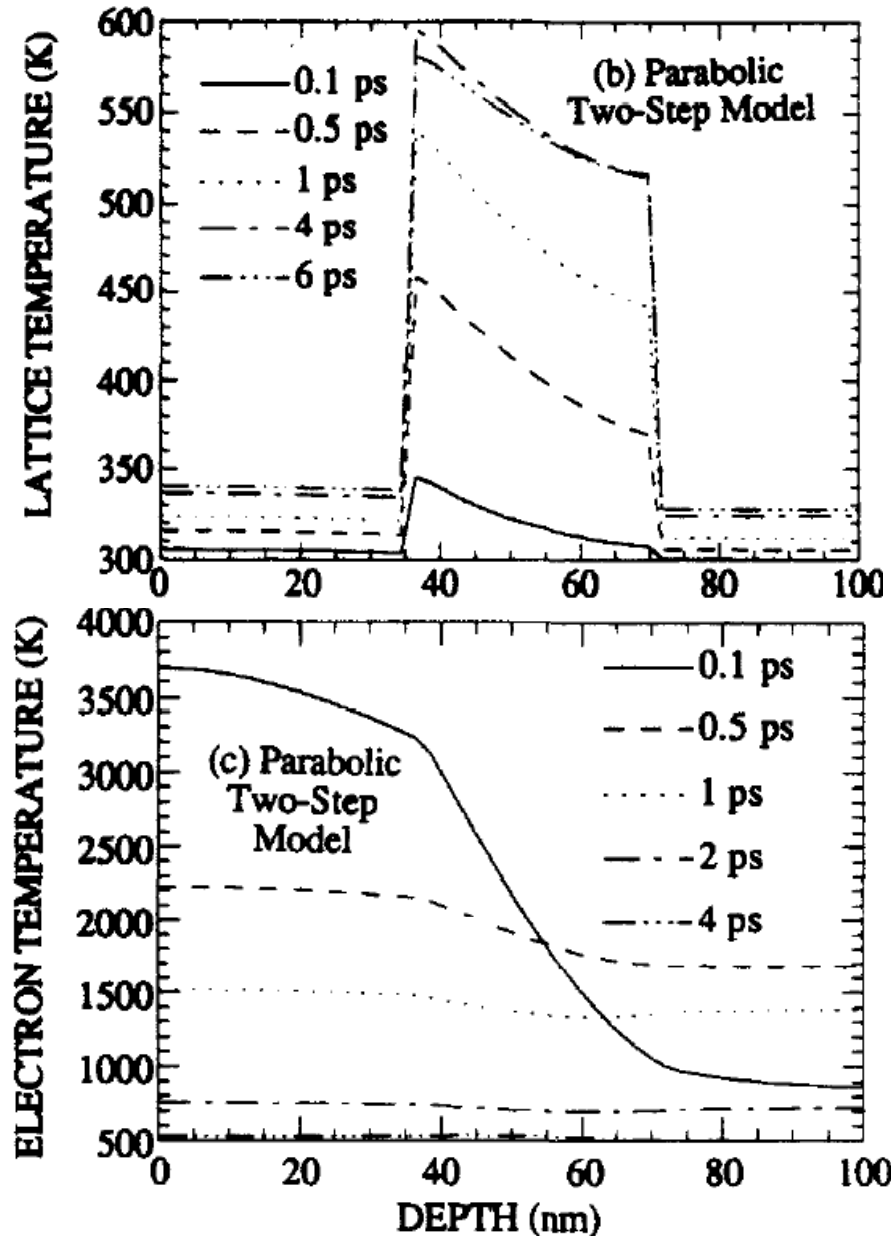
Peculiarities of energy redistribution in two-temperature state

33 nm Au – 33 nm Cr – 33 nm Au
three-layer film irradiated by 100 fs
pulse at a fluence of 500 J/m²

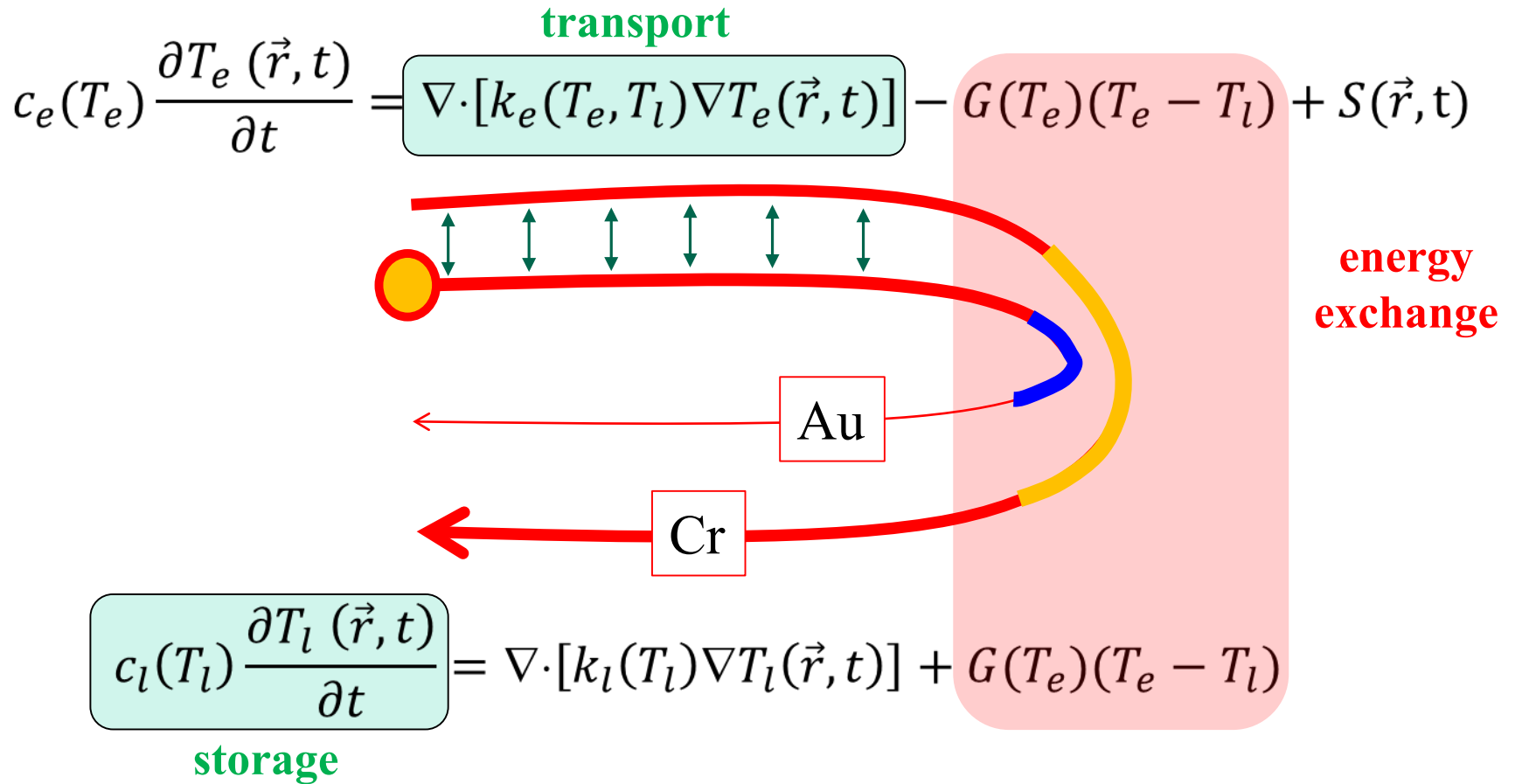


The results of pump-probe thermo-reflectivity measurements can only be explained if the preferential heating of Cr layer is accounted for.

Qiu and Tien,
Int. J. Heat Mass Transfer **37**, 2789, 1994



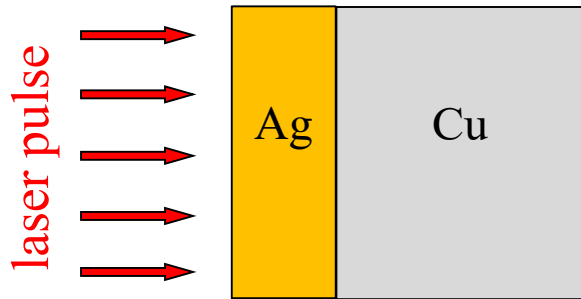
Peculiarities of energy redistribution in two-temperature state



G for Cr \gg G for Au

Peculiarities of energy redistribution in two-temperature state

30 nm Ag film deposited on Cu substrate
and irradiated by 200 fs pulse at an
absorbed fluence of 1300 J/m²



higher strength of e-ph coupling in Cu



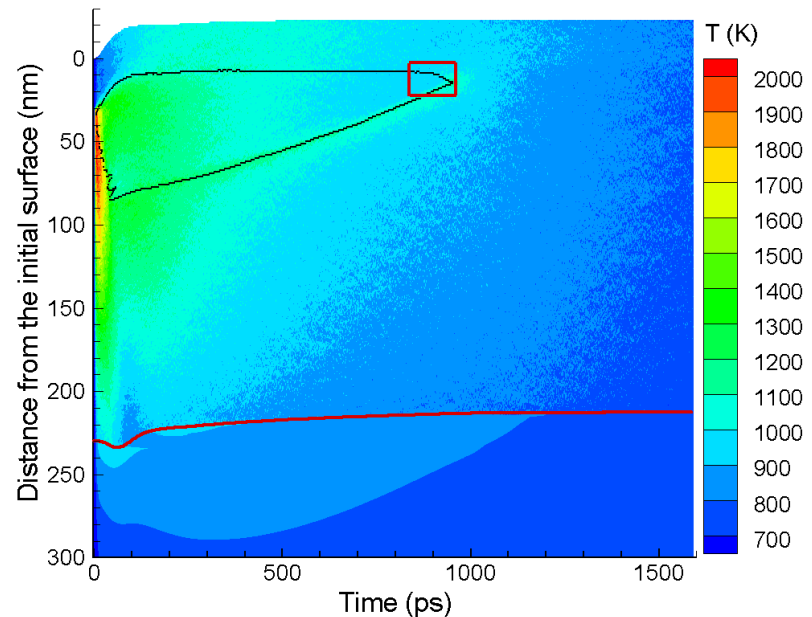
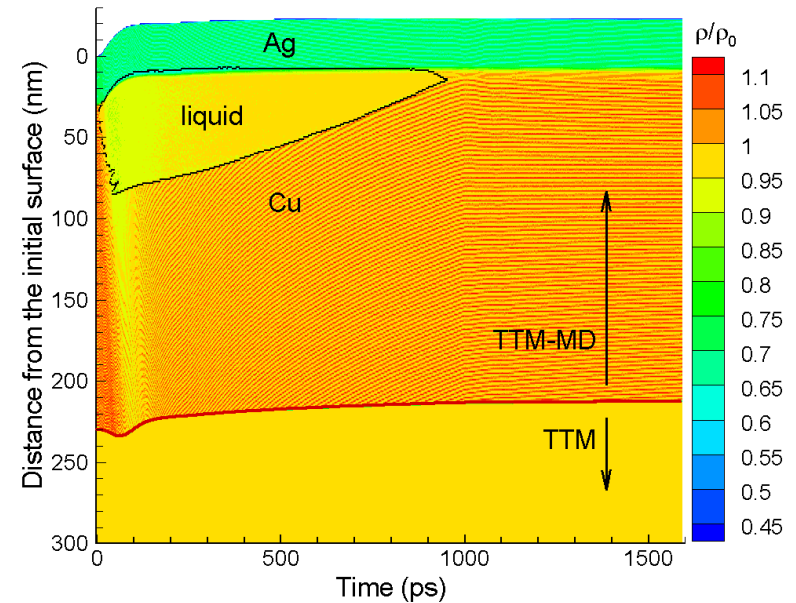
preferential sub-surface heating &
melting of Cu substrate

even though $T_m^{\text{Ag}} < T_m^{\text{Cu}}$

Thomas *et al.*, *Appl. Surf. Sci.* **255**, 9605, 2009

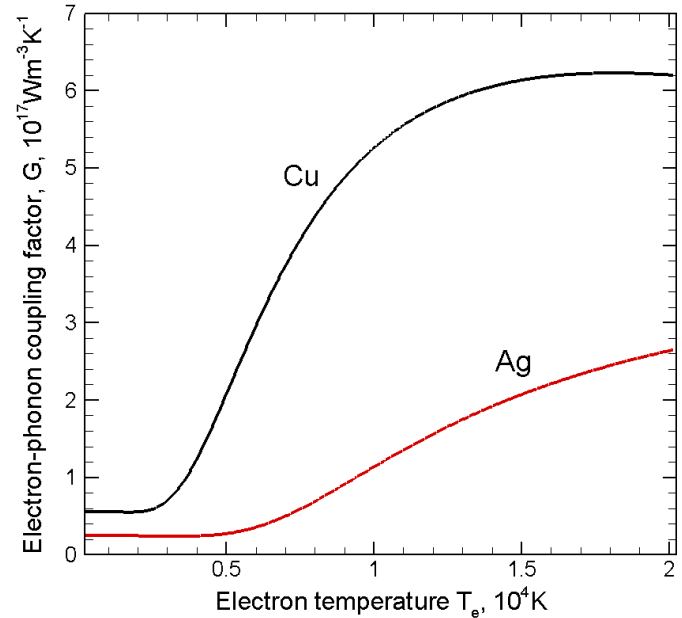
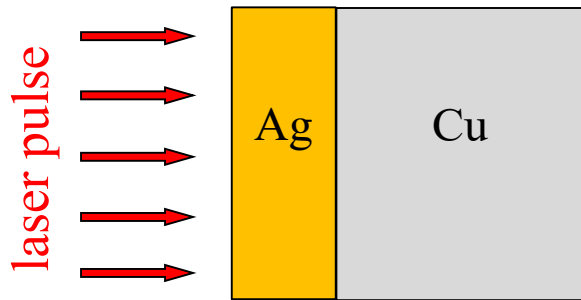
Wu *et al.*, *Appl. Phys. A* **104**, 781, 2011

Naghilou *et al.*, *Phys. Chem. Chem. Phys.* **21**, 11846, 2019



Peculiarities of energy redistribution in two-temperature state

30 nm Ag film deposited on Cu substrate
and irradiated by 200 fs pulse at an
absorbed fluence of 1300 J/m²



higher strength of e-ph coupling in Cu



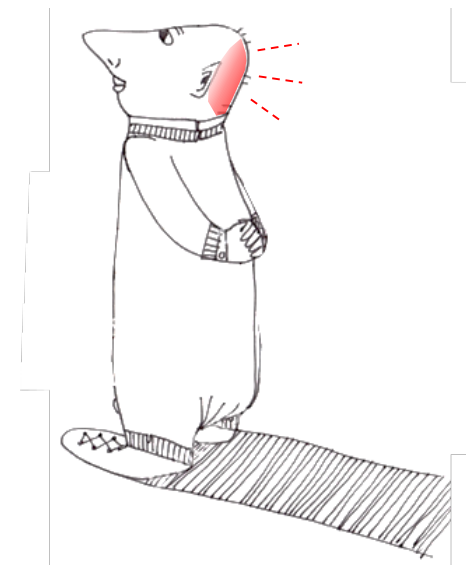
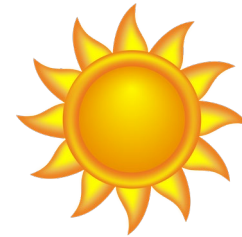
preferential sub-surface heating &
melting of Cu substrate

even though $T_m^{\text{Ag}} < T_m^{\text{Cu}}$

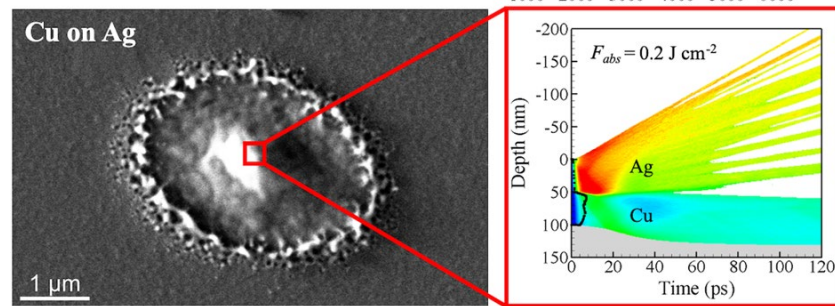
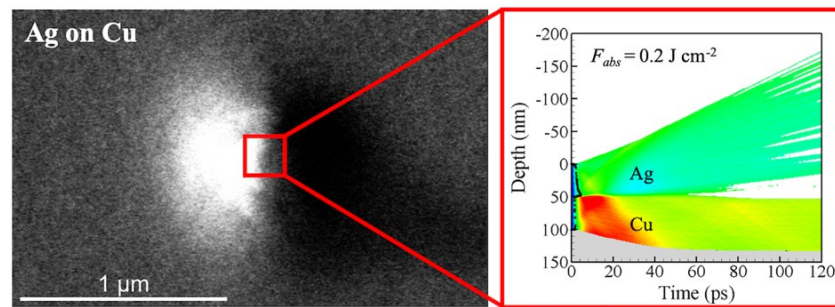
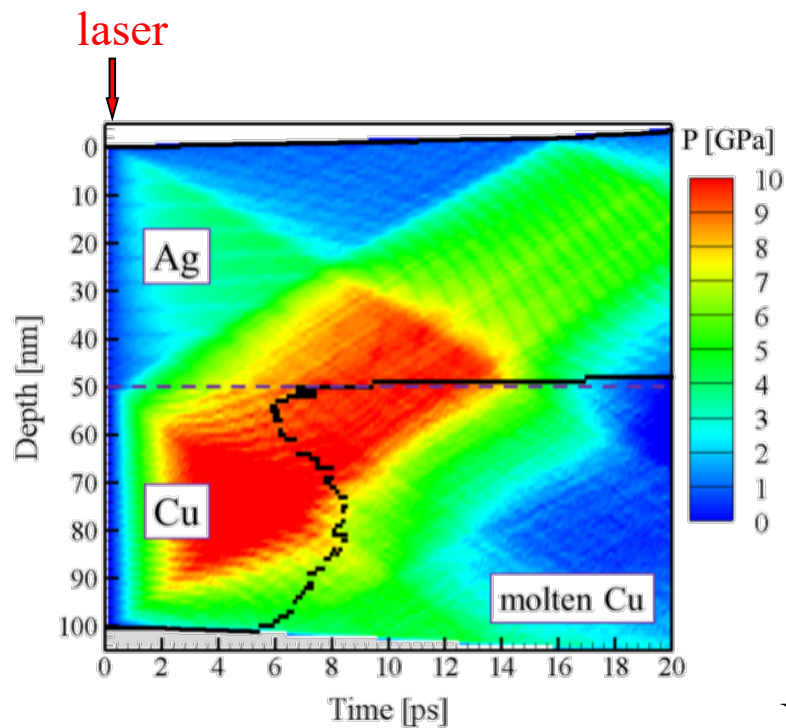
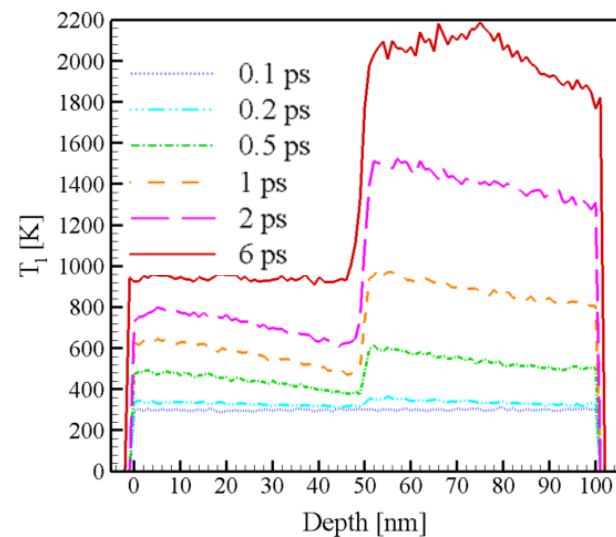
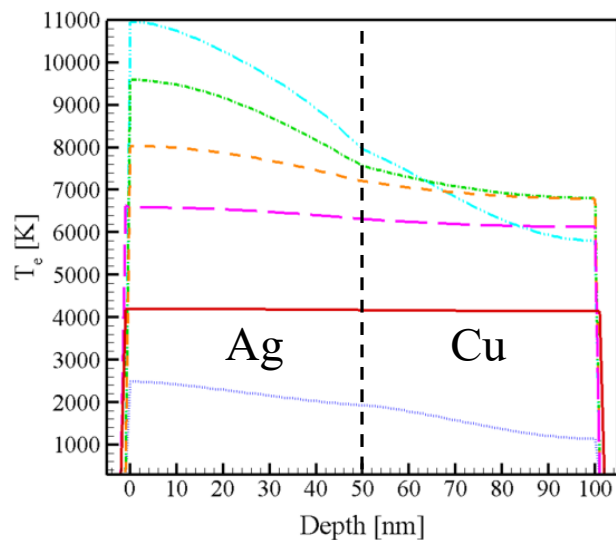
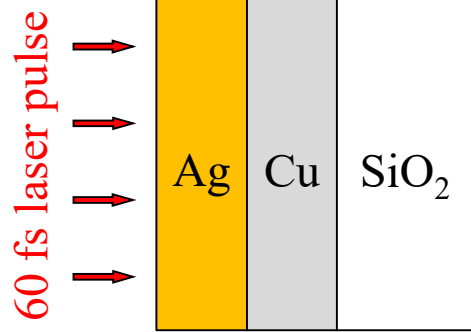
Thomas *et al.*, *Appl. Surf. Sci.* **255**, 9605, 2009

Wu *et al.*, *Appl. Phys. A* **104**, 781, 2011

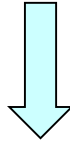
Naghilou *et al.*, *Phys. Chem. Chem. Phys.* **21**, 11846, 2019



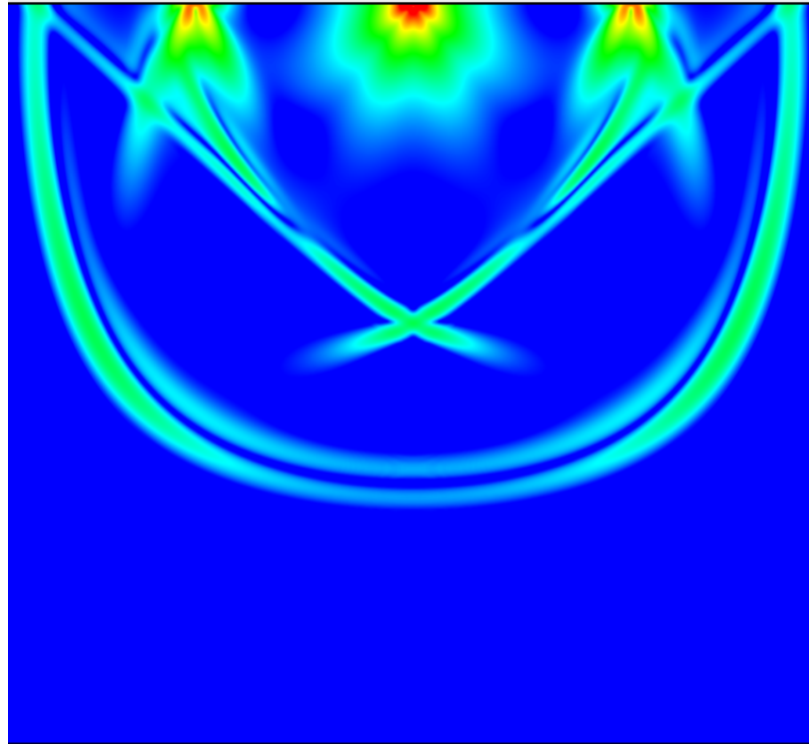
Peculiarities of energy redistribution in two-temperature state



Rapid, localized heating by laser pulses

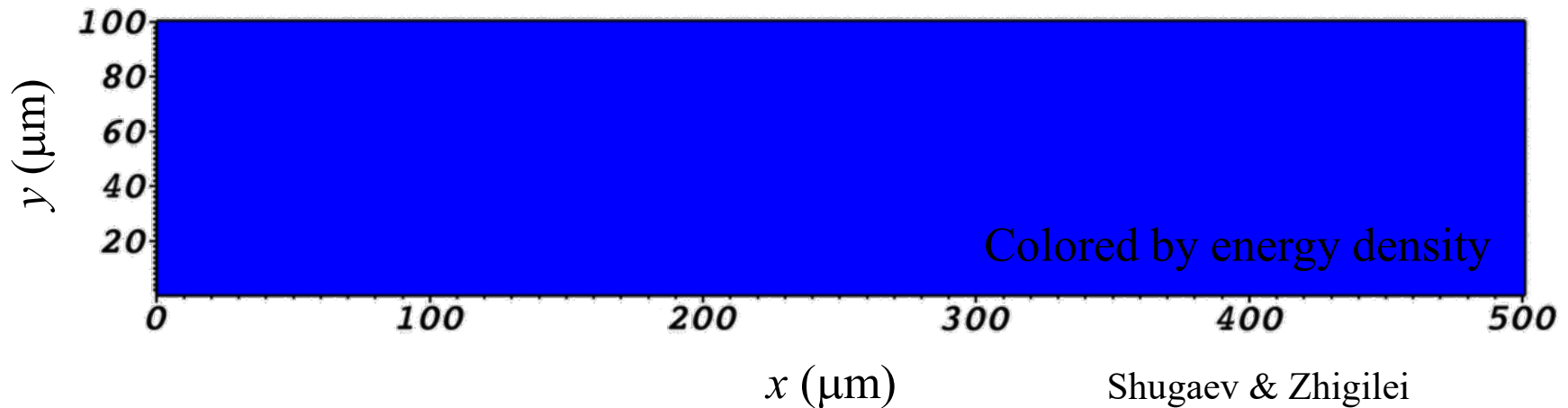


Generation of stresses and stress waves



Laser-induced stresses and stress waves

Continuum-level simulation: Silica substrate, Gaussian laser pulse, $100\ \mu\text{m} \times 500\ \mu\text{m}$ computational domain
($d = 21\ \mu\text{m}$, $L_p = 10\ \mu\text{m}$, $\tau = 100\ \text{ps}$, $I_{abs} = 10\ \text{J}/\text{cm}^2$, Beer's law absorption)



Types and sources of laser-induced stresses:

- Dynamic transient stresses generated due to the conditions of **stress confinement**
- Ablation or vaporization recoil pressure
- Long-term quasi-static thermo-elastic stresses due to the temperature gradients
- Residual stresses due to the laser-induced structural changes (defects) in the material

Condition of stress confinement: $\tau_h = \max\{\tau_p, \tau_{e-ph}\} \leq \tau_s$, where $\tau_s \sim \delta_{\text{eff}}/C_s$

Paltauf and Dyer, *Chem. Rev.* **103**, 487, 2003

Leveugle *et al.*, *Appl. Phys. A* **79**, 1643, 2004

Photoacoustic probing and imaging

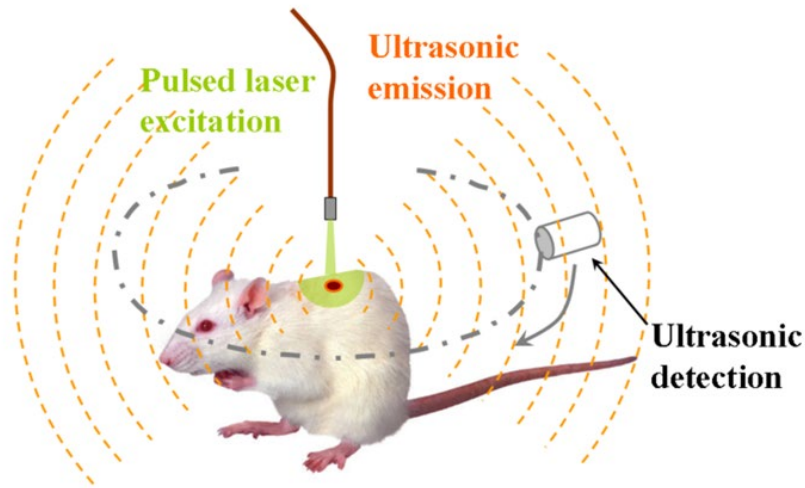
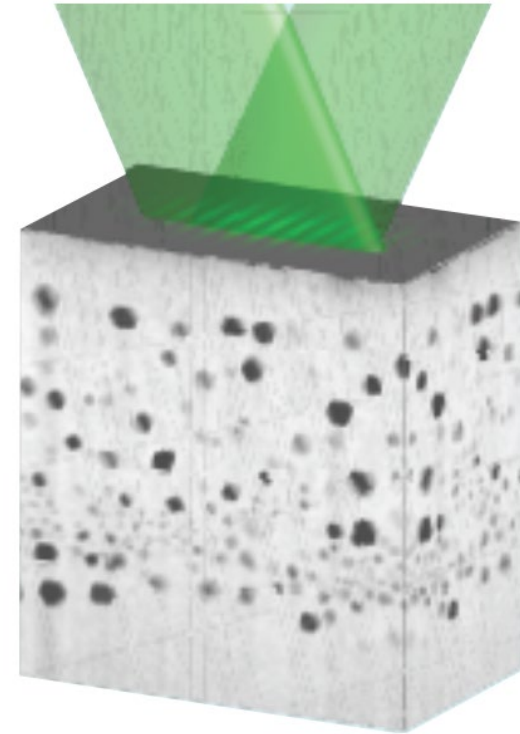
transient grating spectroscopy

optical generation & probing of surface acoustic waves

in situ / in operando characterization of evolving subsurface microstructure on sub- μs timescale & with tunable depth resolution, *e.g.*, probing of accumulation of radiation damage

Dennett and Short, *J. Appl. Phys.* **123**, 215109, 2018

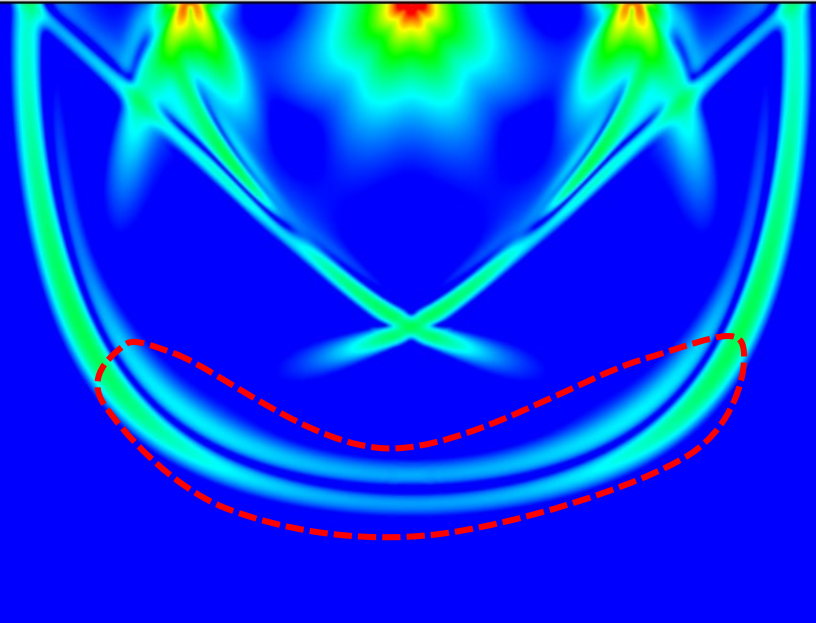
Dennett *et al.*, *Nucl. Instrum. Methods Phys. Res. B* **440**, 126, 2019



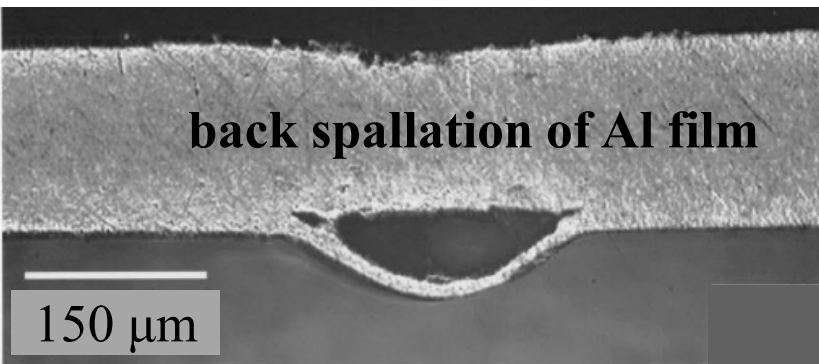
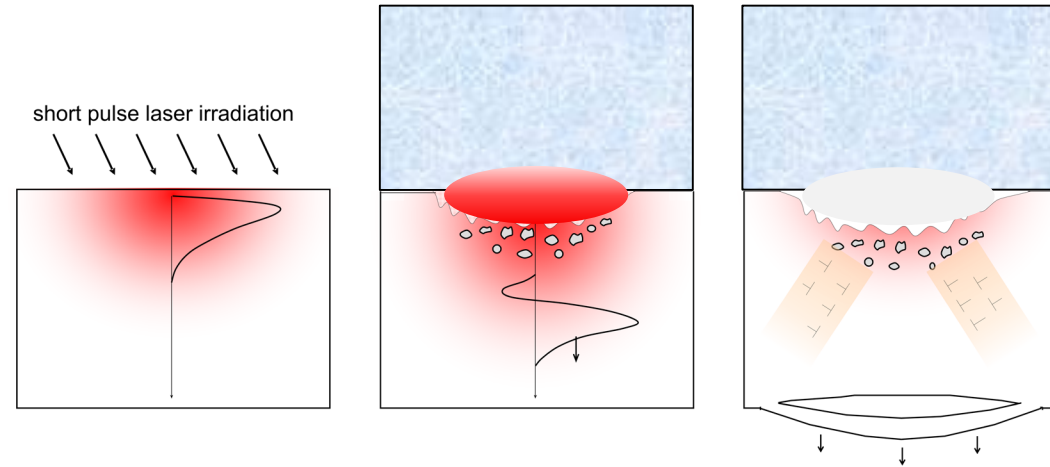
photoacoustic imaging of biological tissue

Selective laser heating (due to the natural optical contrast or embedded nanoparticles) leads to thermal expansion or nanobubbles formation \rightarrow acoustic signal \rightarrow 3D image

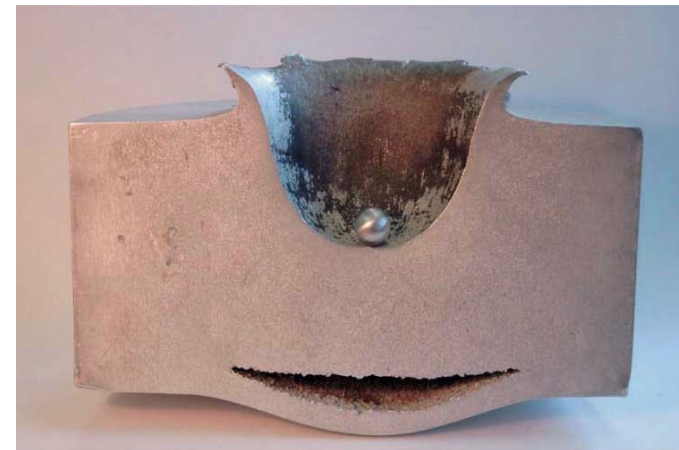
Laser-induced stress waves → **back surface spallation**



Back surface spallation: dynamic fracture due to reflection of a shock wave from a back surface of a sample

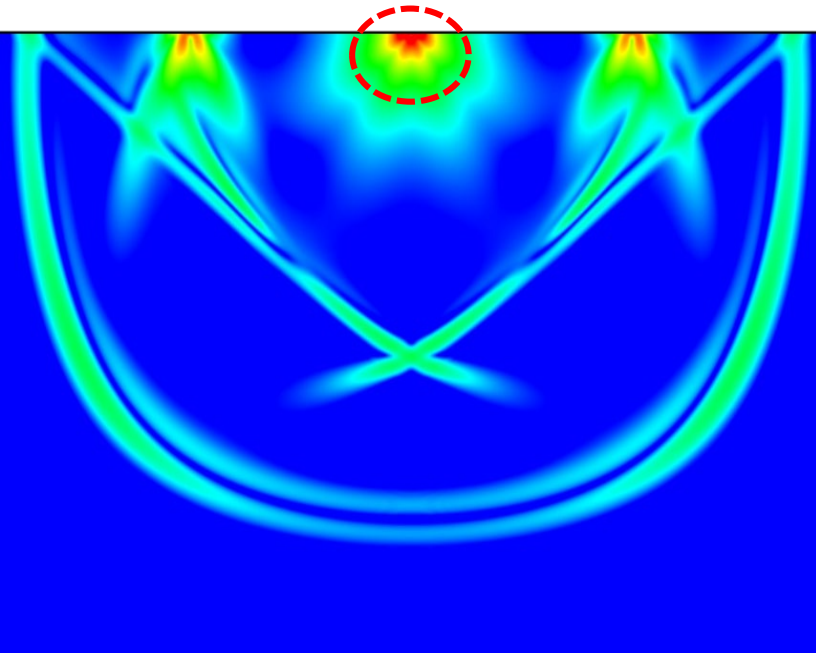


Tamura *et al.*, *J. Appl. Phys.* **89**, 3520, 2001

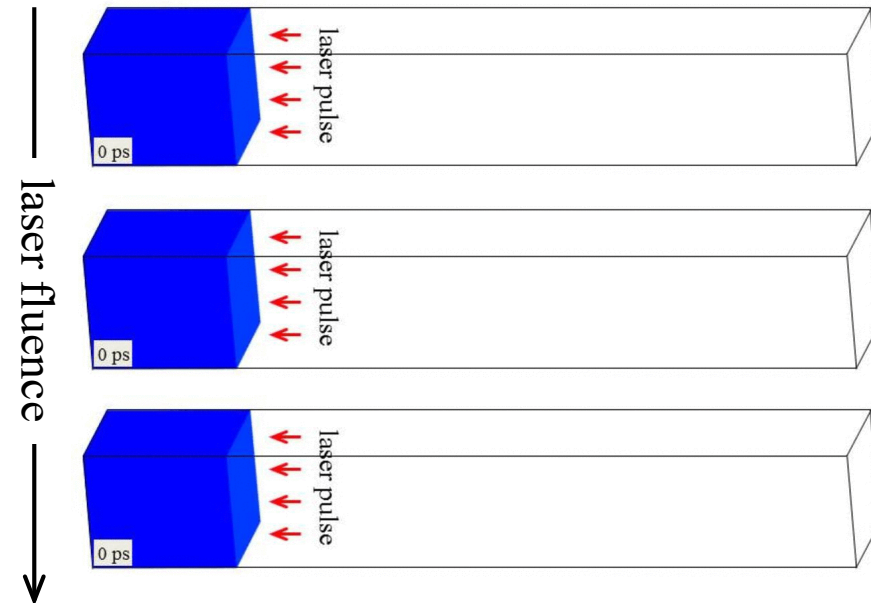
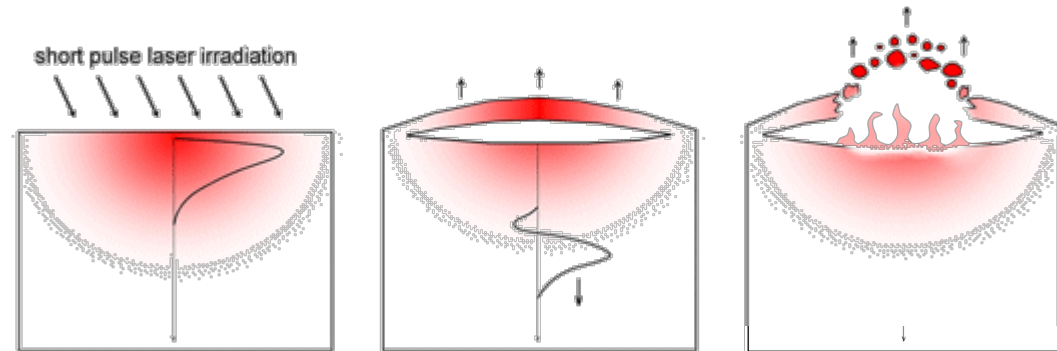


Al block impacted by 1.2 cm Al ball at 6.8 km/s
European Space Agency

Laser-induced stress waves → **front surface spallation**

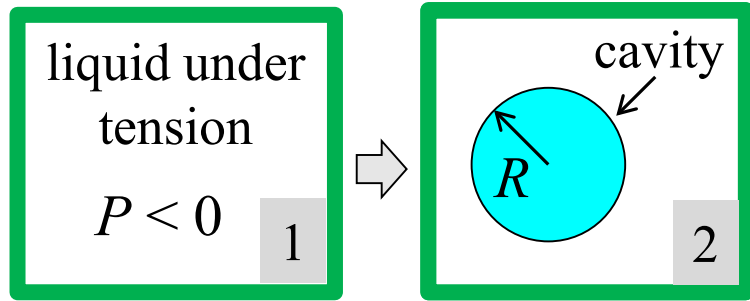


Front surface spallation: subsurface cavitation and ejection of a thin molten layer from the irradiated target



Laser-induced stress waves → front surface spallation

Thermodynamic analysis

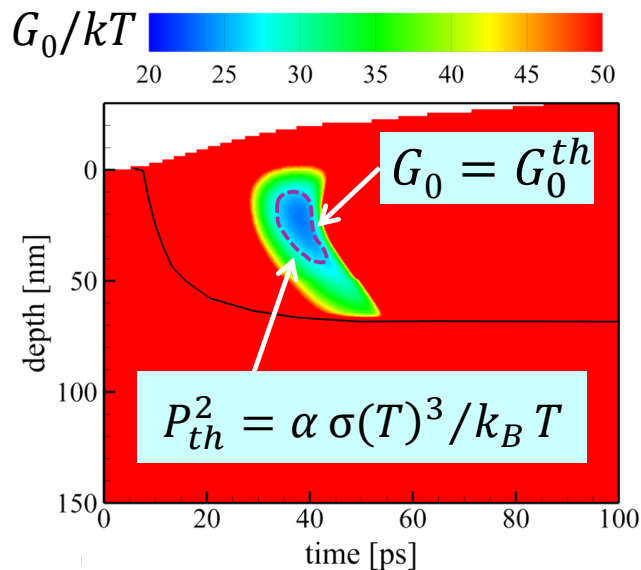
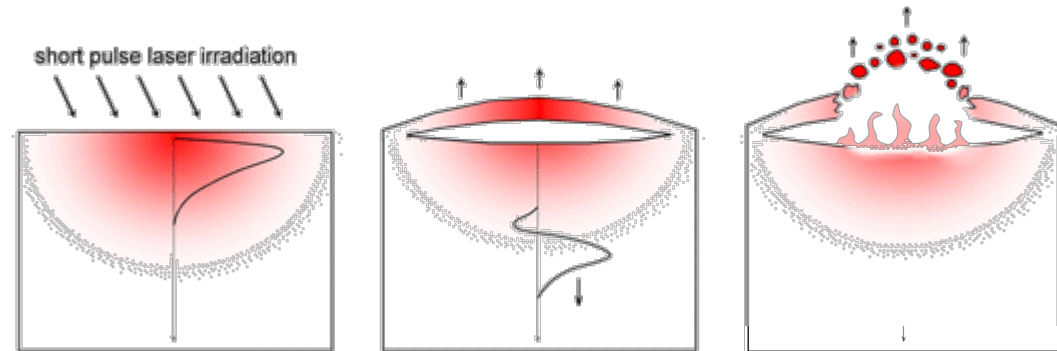


$$\Delta G = G_2 - G_1 \approx 0$$

$$= \frac{4}{3} \pi R^3 (P - P_v) + 4\pi R^2 \sigma$$

negative positive

Front surface spallation: subsurface cavitation and ejection of a thin molten layer from the irradiated target



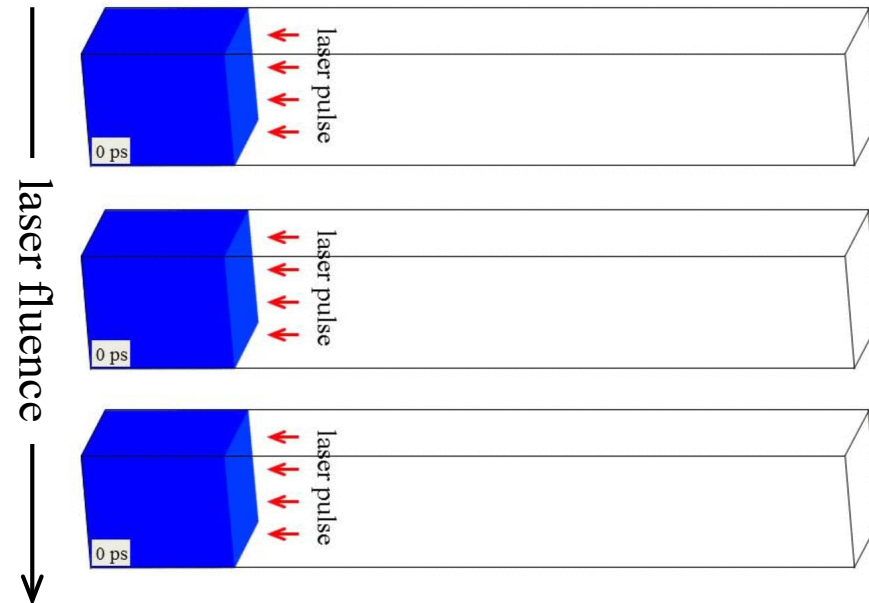
$$R_c = -\frac{2\sigma}{P}$$

$$G_0 = \Delta G(R_c)$$

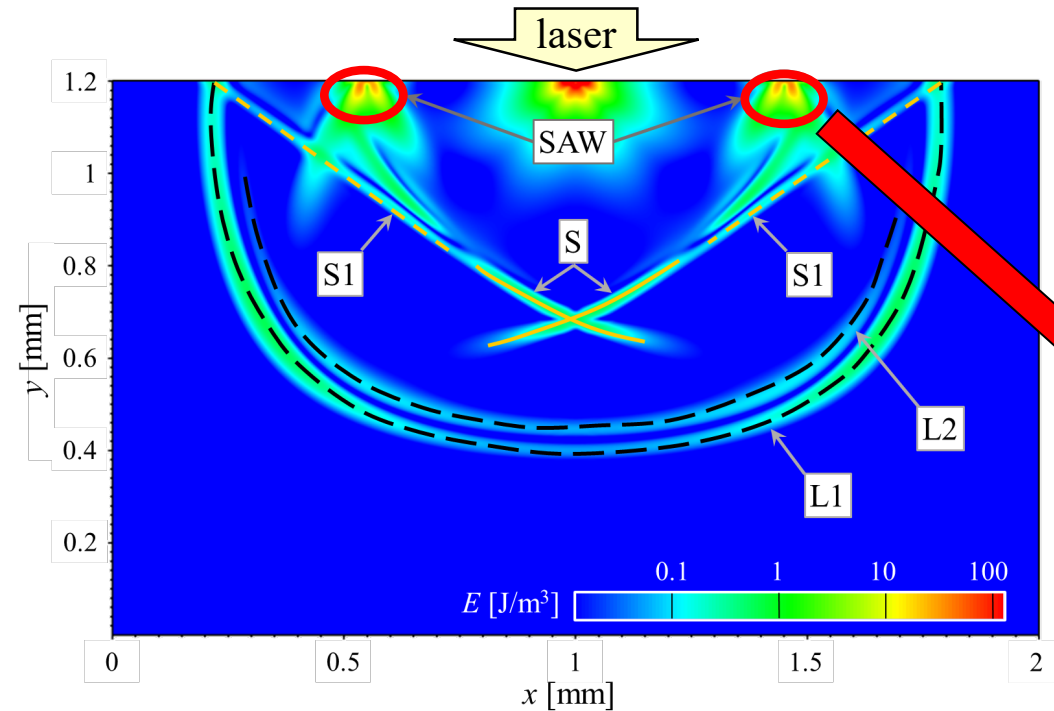
$$= \frac{16\pi\sigma^3}{3P^2}$$

Rate of void nucleation:

$$R = R_0 e^{-\frac{G_0}{k_B T}}$$

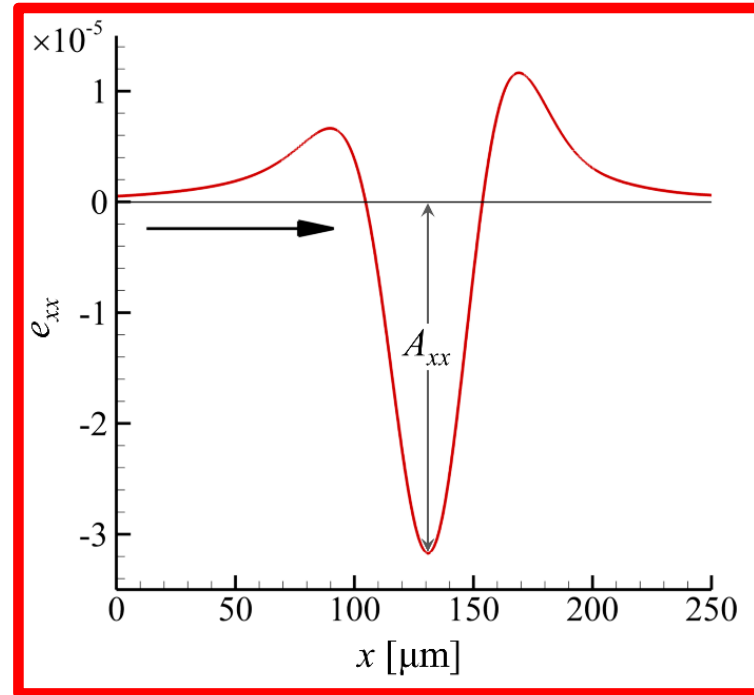


Can laser-generated SAWs contribute to target surface modification?

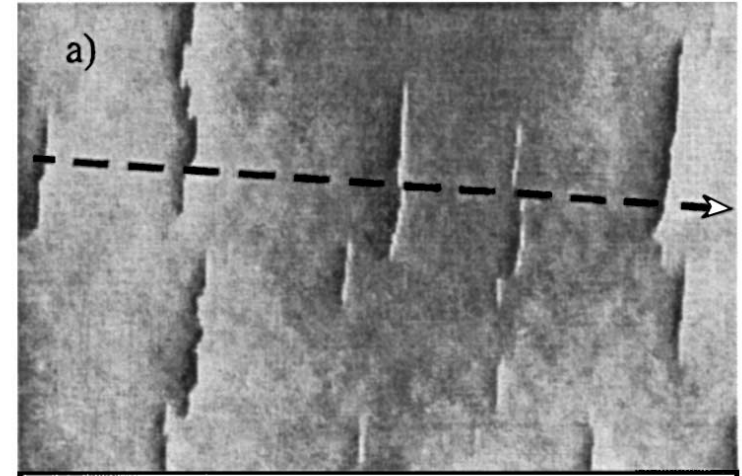
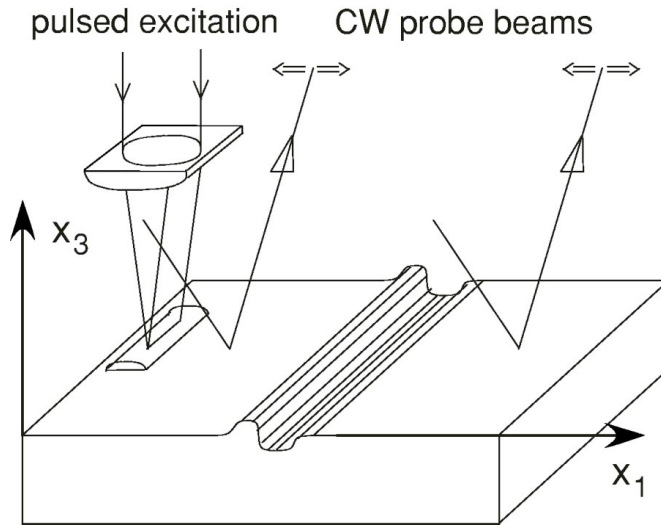


Si(100) substrate irradiated by 6 ns pulse at 355 nm and fluence of 0.25 J/cm², snapshot taken at 100 ns.

Shugaev & Zhigilei, *J. Appl. Phys.* **130**, 185108, 2021



Probing ultimate strength under conditions of ultrafast mechanical loading

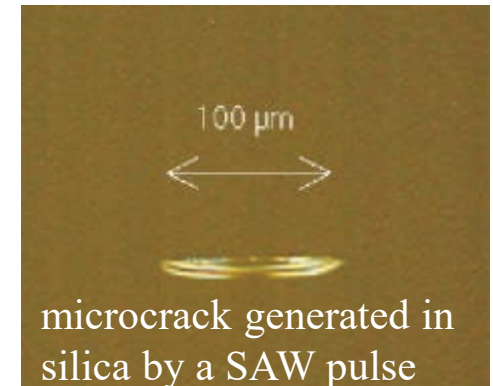


Probing ideal fracture strength of brittle materials

Impulsive fracture without notching using the effect of gradual growth of stress in the strongly nonlinear SAW pulses - **critical tensile stress of dynamic fracture** obtained

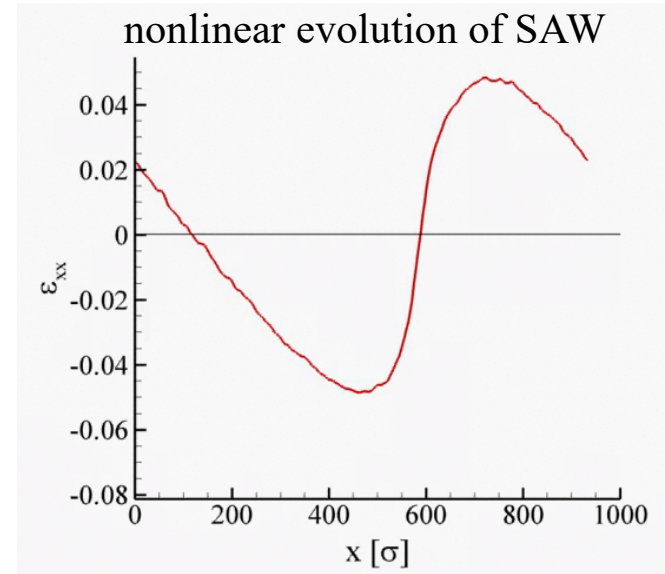
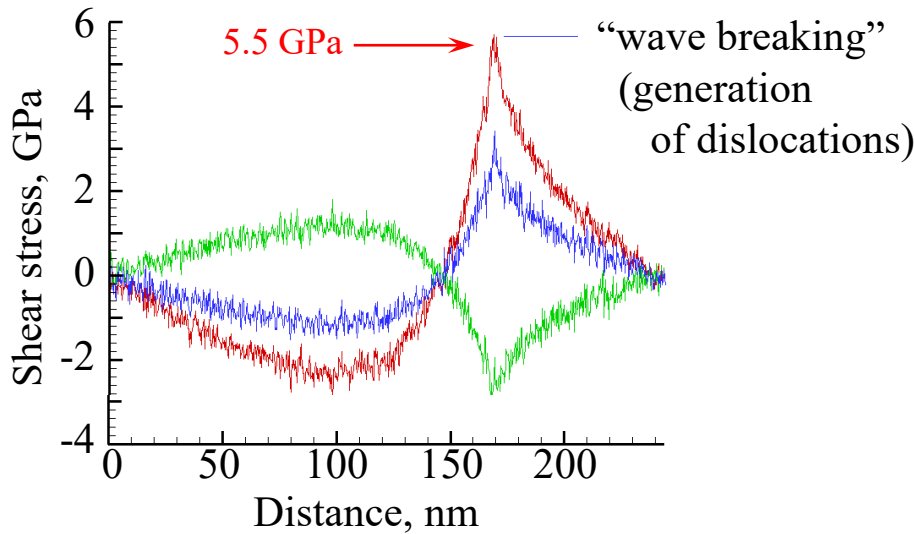
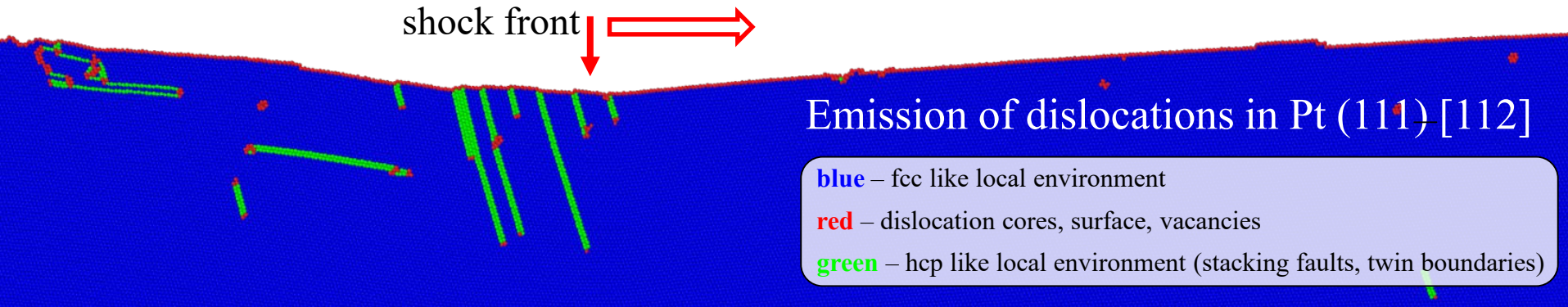
Silicon: Lomonosov and Hess, *PRL* **89**, 095501, 2002

Diamond: Hess, *Diam. Relat. Mater.* **18**, 186, 2009



Modern Acoustical Techniques for the Measurement of Mechanical Properties
(Academic, New York, 2001)

Nonlinear sharpening of SAWs: Generation of dislocations

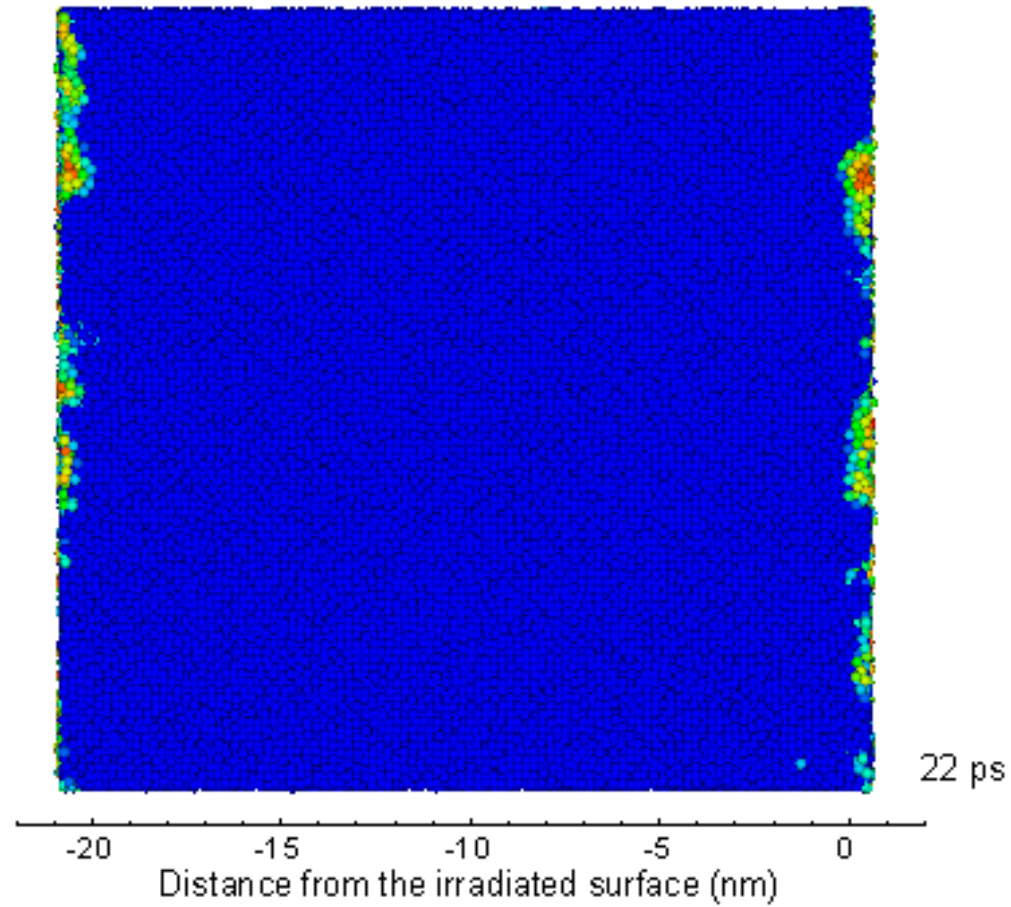


Yuan Xu,
current work

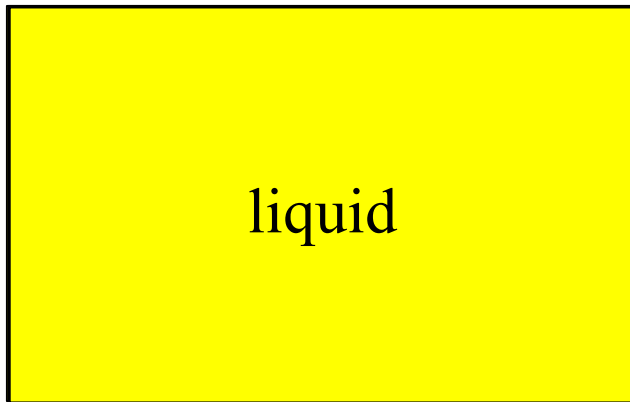
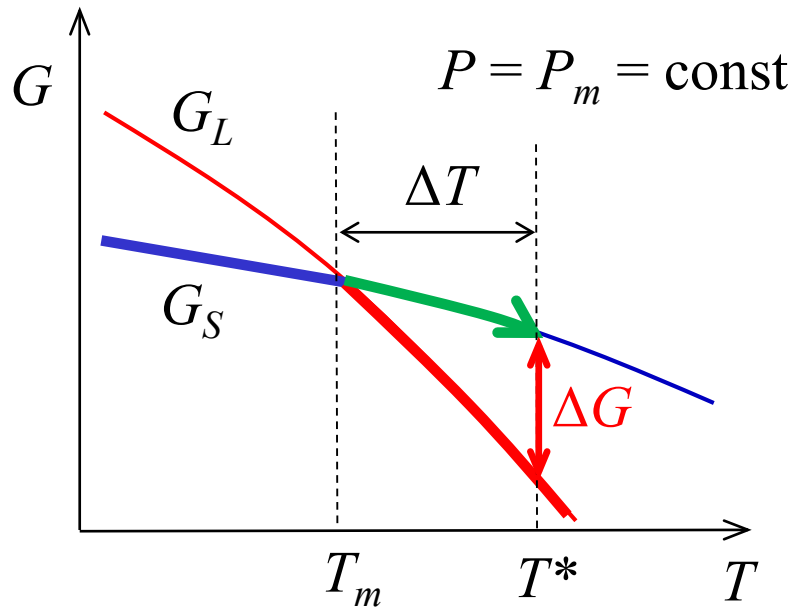
Atomic-scale roughening of the surface due to the SAW-induced generation of dislocations is a possible mechanism of the promotion of surface catalytic activity.

von Boehn *et al.*, *Angew. Chem. Int. Ed.* **59**, 20224, 2020

Laser-induced phase transformations: Melting

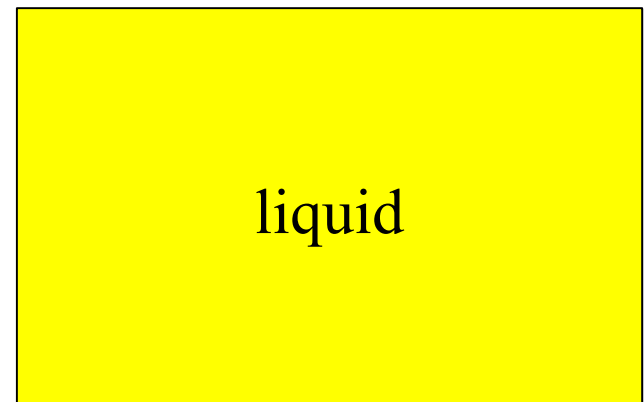
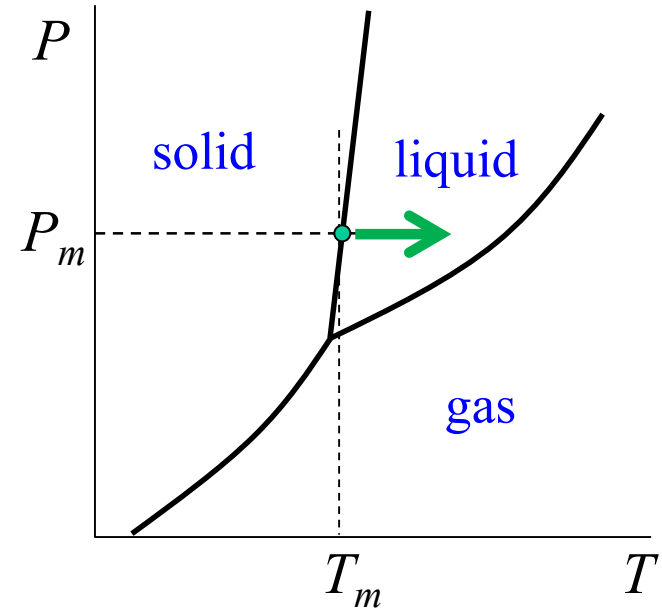


Basic thermodynamics of phase transformations



Heterogeneous melting: propagation of melting front from the surface

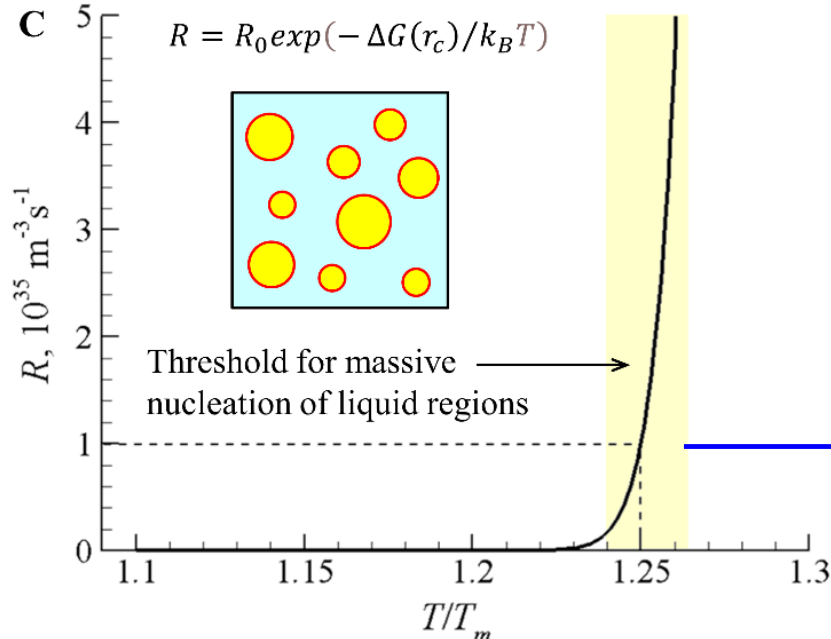
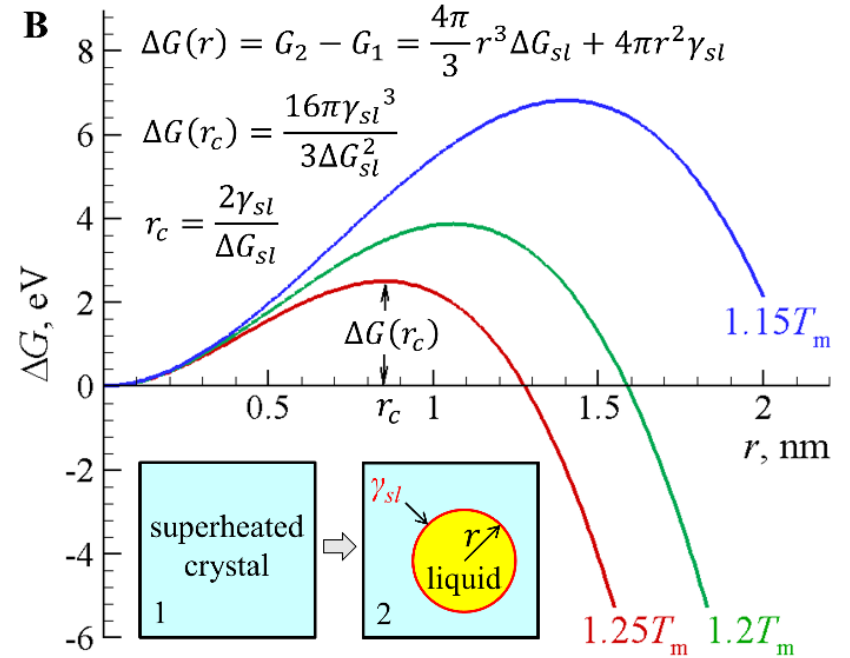
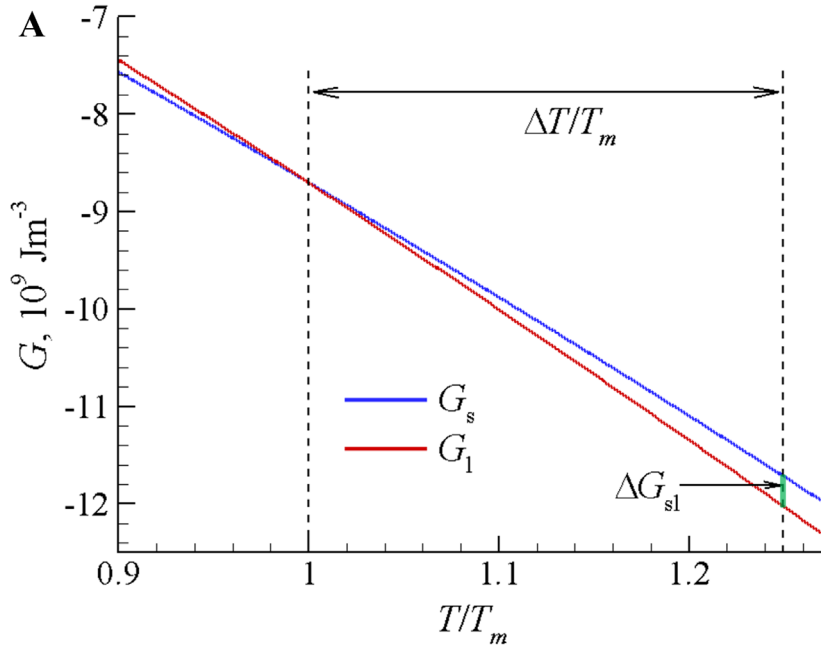
melting front velocity $v = \mu \Delta T$



Homogeneous melting: nucleation inside the superheated crystal (*i.e.*, at T^*)

how does the nucleation rate depends on T^* ?

Classical Nucleation Theory: Homogeneous Melting – case study of Au



calculations done with the experimental thermodynamic properties of Au

Arefev *et al.*, *Sci. Adv.* **8**, eabo2621, 2022

$R \approx 10^{35} \text{ s}^{-1} \text{ m}^{-3} = \text{one nucleus in a volume of } (10 \text{ nm})^3 \text{ every } 10 \text{ ps}$

Laser melting of Au films: Experiments and simulations

Electron diffraction experiments for Au 20 films

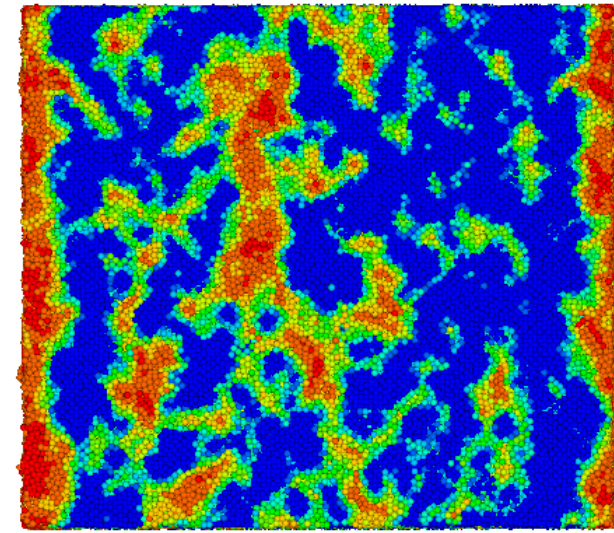
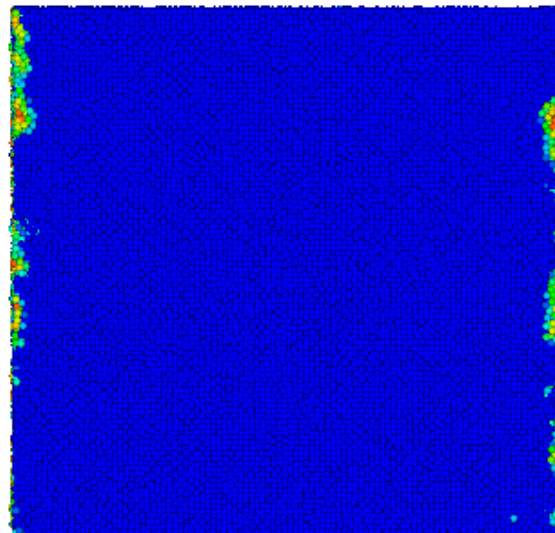
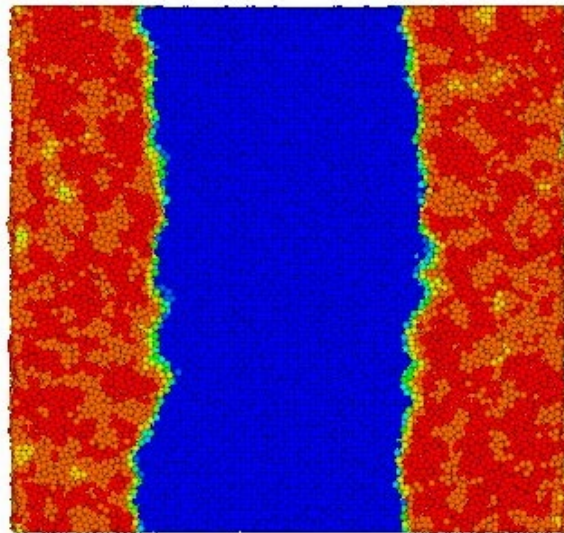
Dwyer et al., *Philos. Trans. R. Soc. London, Ser. A* **364**, 741, 2006.

Gold \Rightarrow weak electron-phonon coupling \Rightarrow separation of the timescales for lattice heating and melting

slow heterogeneous melting



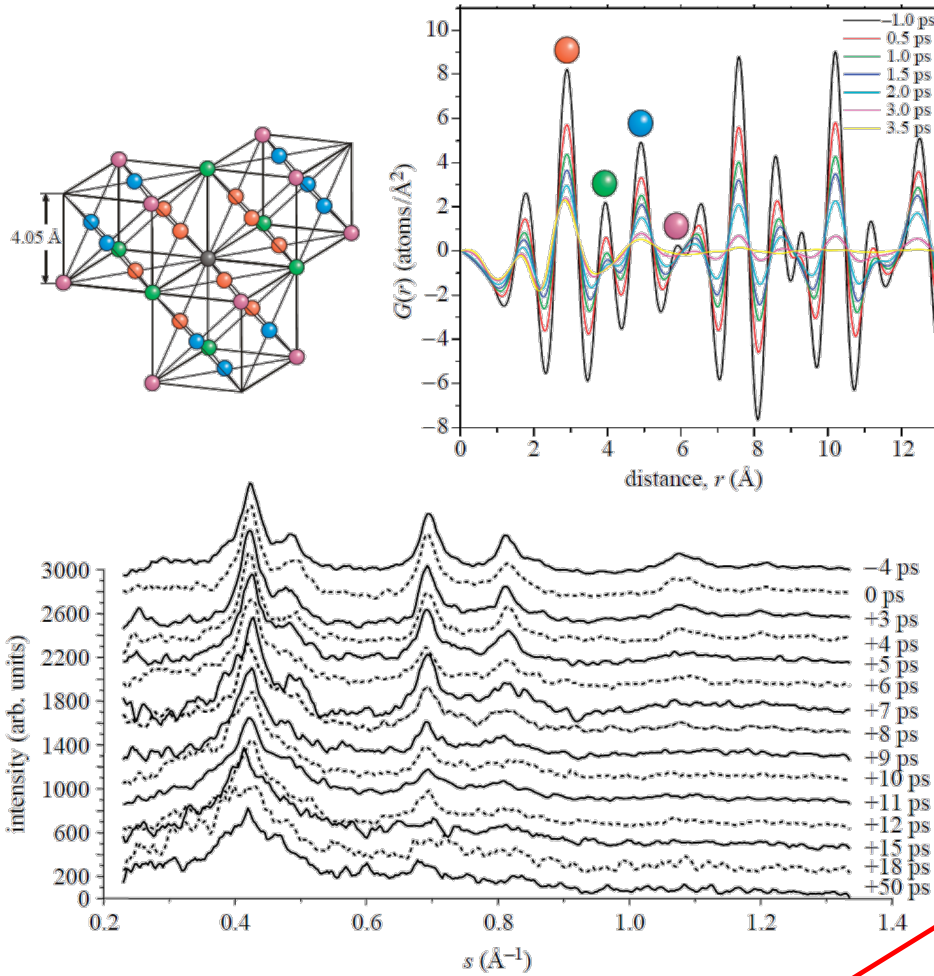
fast homogeneous melting



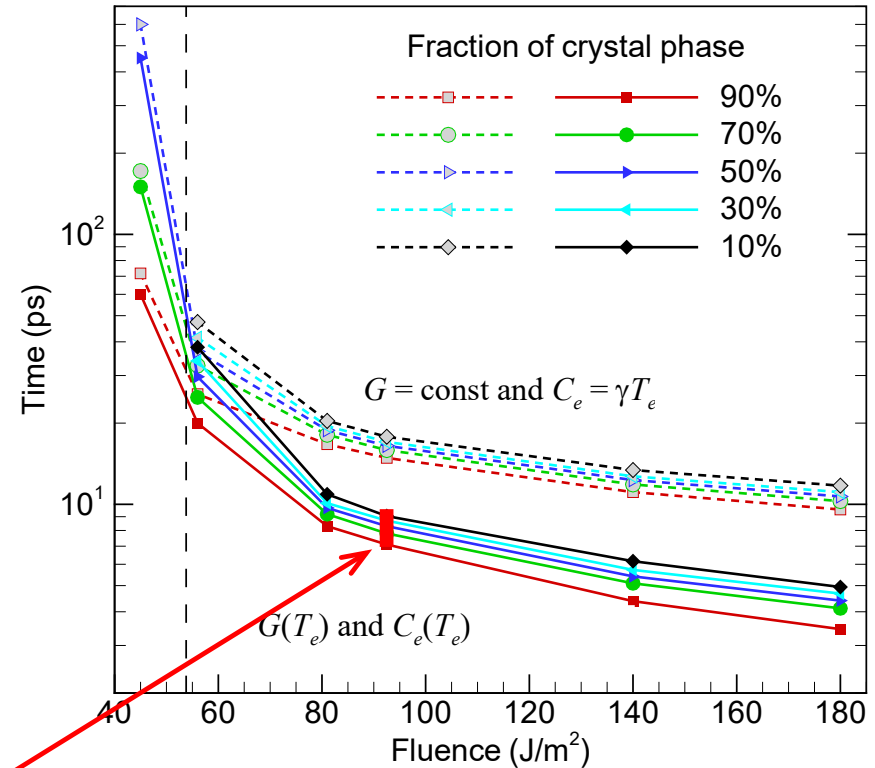
laser fluence \rightarrow

Laser melting of Au films: Experimental probing and simulations

Siwick *et al.*, *Science* **302**, 1382, 2003



timescales of melting in a 20 nm single crystal Au film (200 fs pulse)



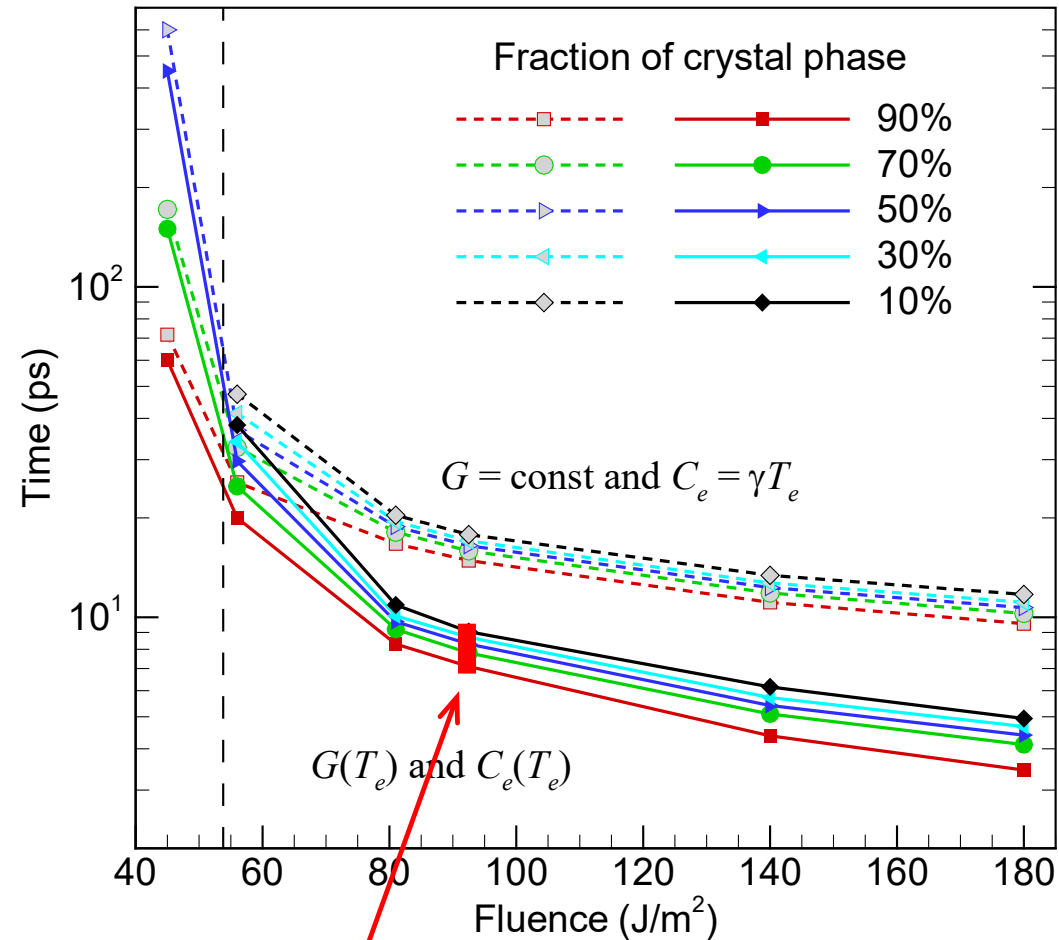
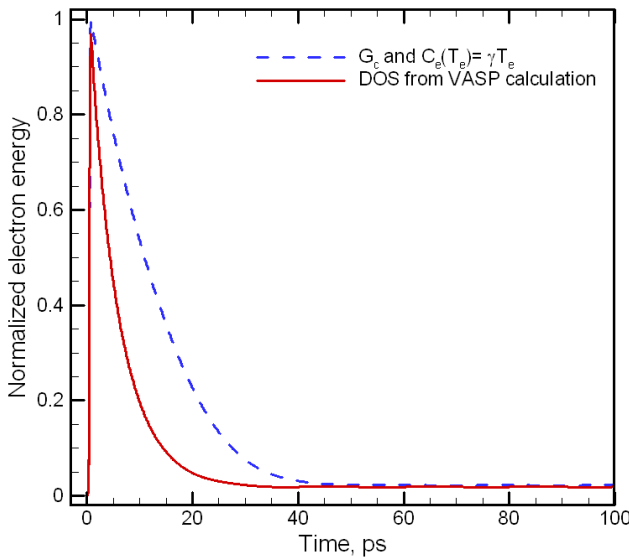
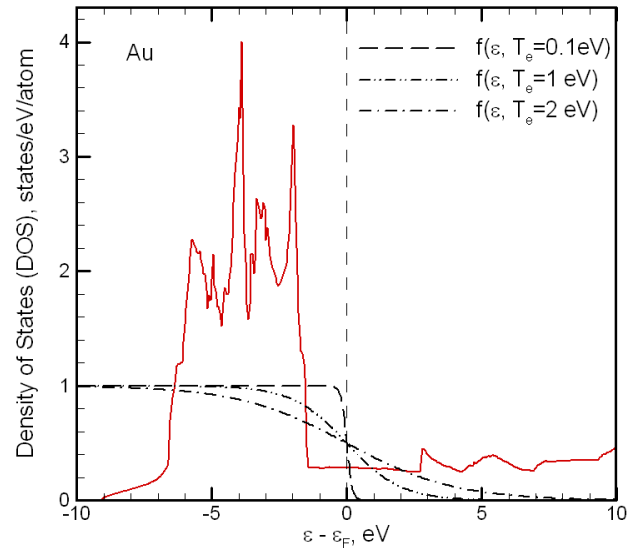
Lin *et al.*, *J. Phys. Chem. C* **114**, 5686, 2010

Experiment: Dwyer *et al.*, *Philos. Trans. R. Soc. London, Ser. A* **364**, 741 (2006)

Quantitative comparison to experiments: Laser melting of Au films

excitation of 5d electrons: $G(T_e)$ and $C_e(T_e)$

timescales of melting in a 20 nm single crystal Au film (200 fs pulse)

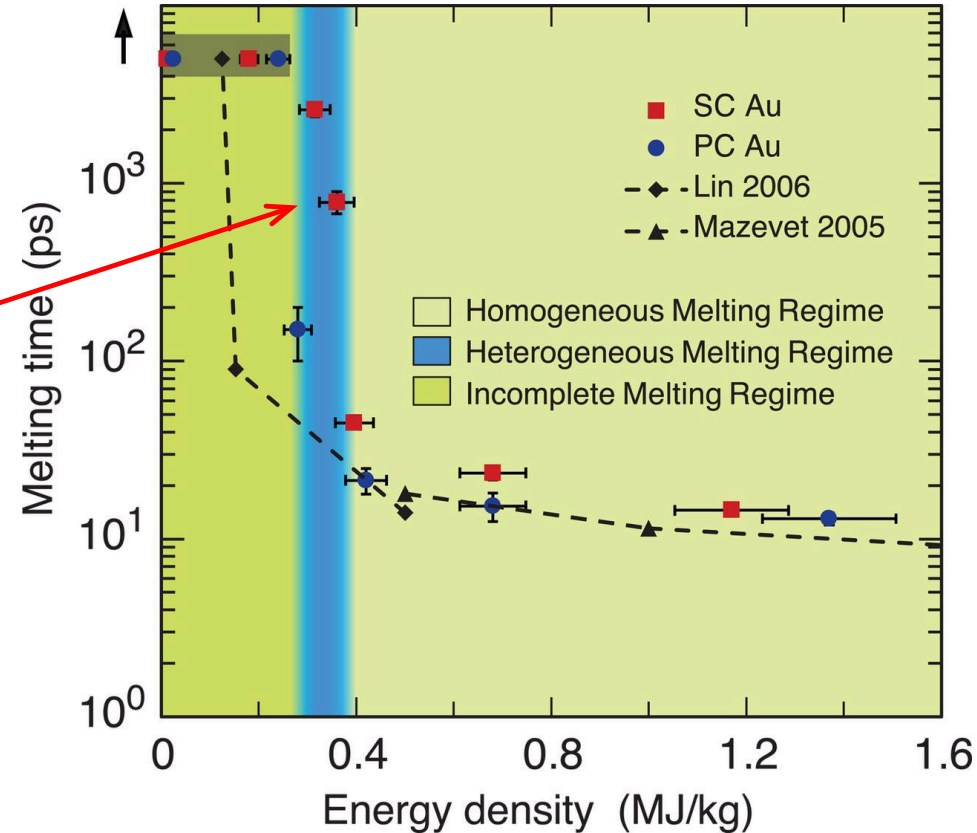


Experiment: Dwyer et al., *Philos. Trans. R. Soc. London, Ser. A* **364**, 741 (2006)

New results for Au films: **Very slow** heterogeneous melting

At a general level, the results are consistent with earlier experiments and simulations

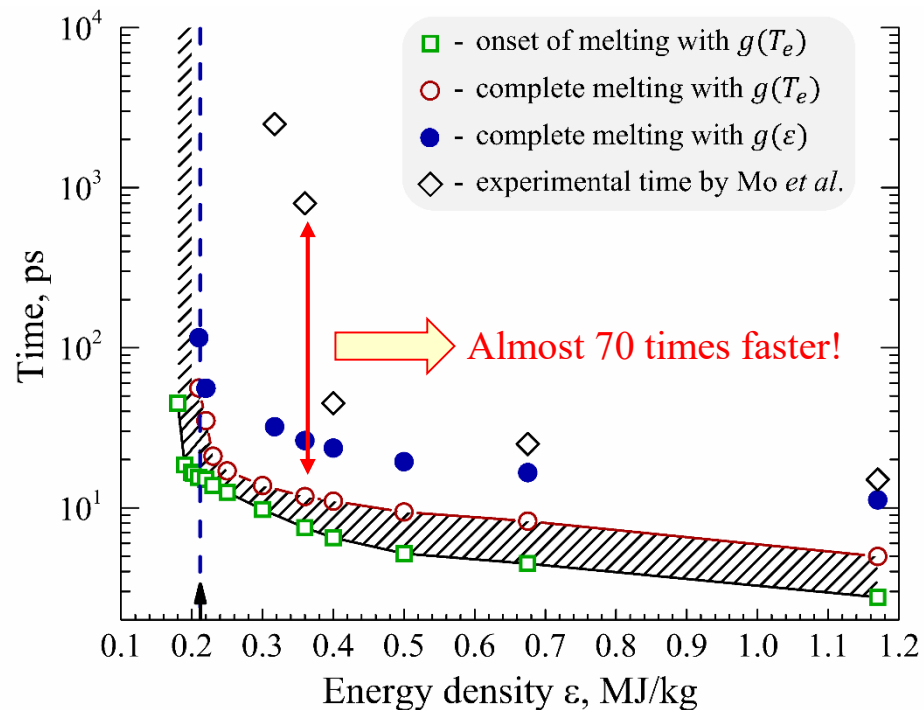
slow heterogeneous melting: takes > 800 ps to melt 35-nm-thick Au film at fluence **45% above threshold** for complete melting.



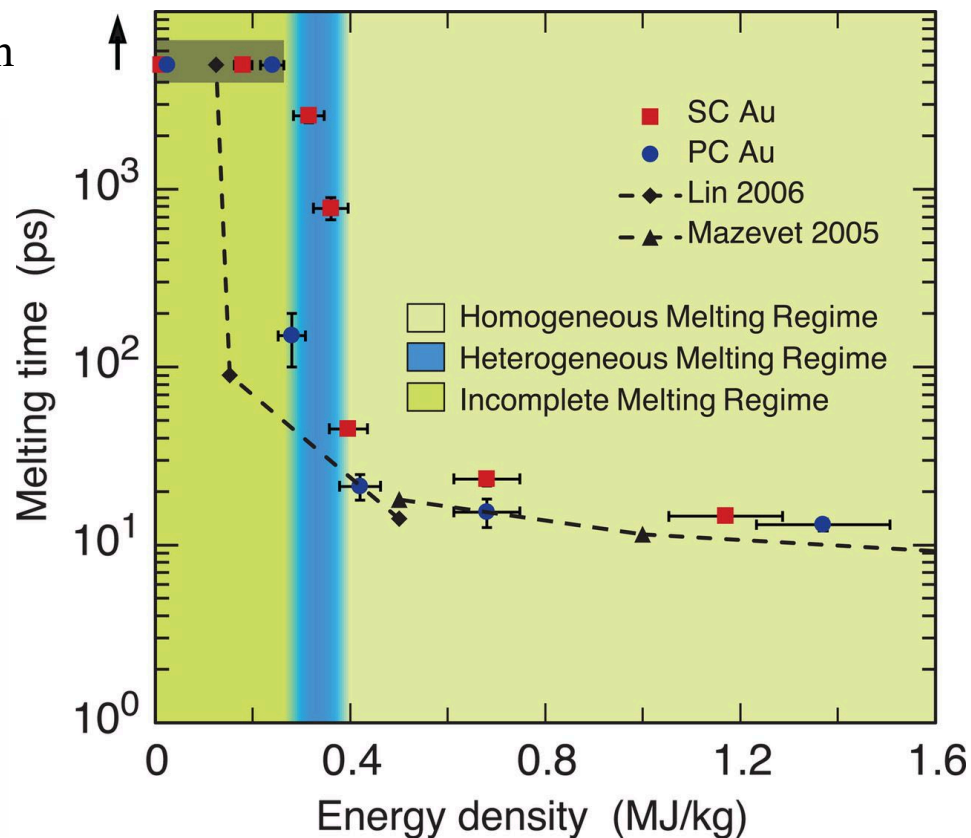
Mo *et al.*, *Science* **360**, 1451, 2018

Kinetics of laser-induced melting of thin gold film: **How slow can it get?**

Atomistic modeling of melting of 35 nm Au film



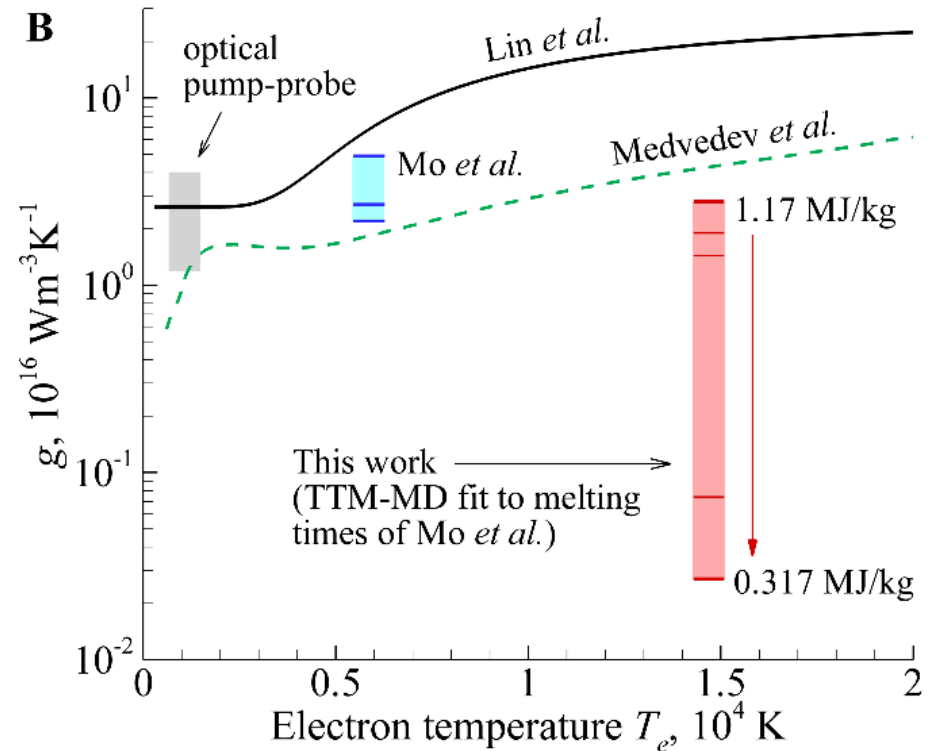
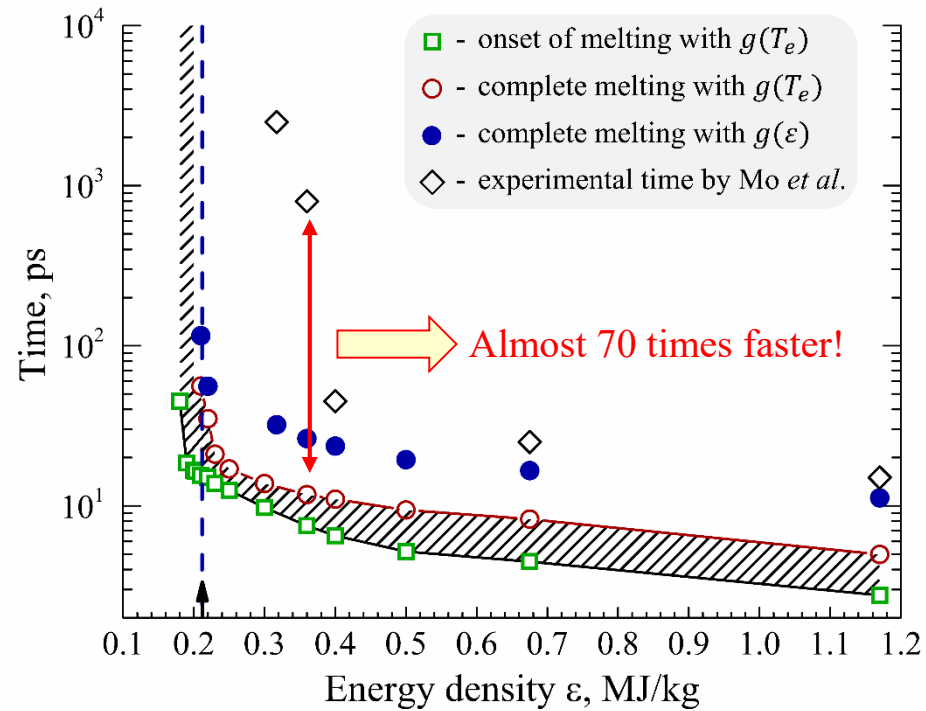
Arefev *et al.*, *Sci. Adv.* **8**, eabo2621, 2022



Mo *et al.*, *Science* **360**, 1451, 2018

Kinetics of laser-induced melting of thin gold film: **How slow can it get?**

Atomistic modeling of melting of 35 nm Au film

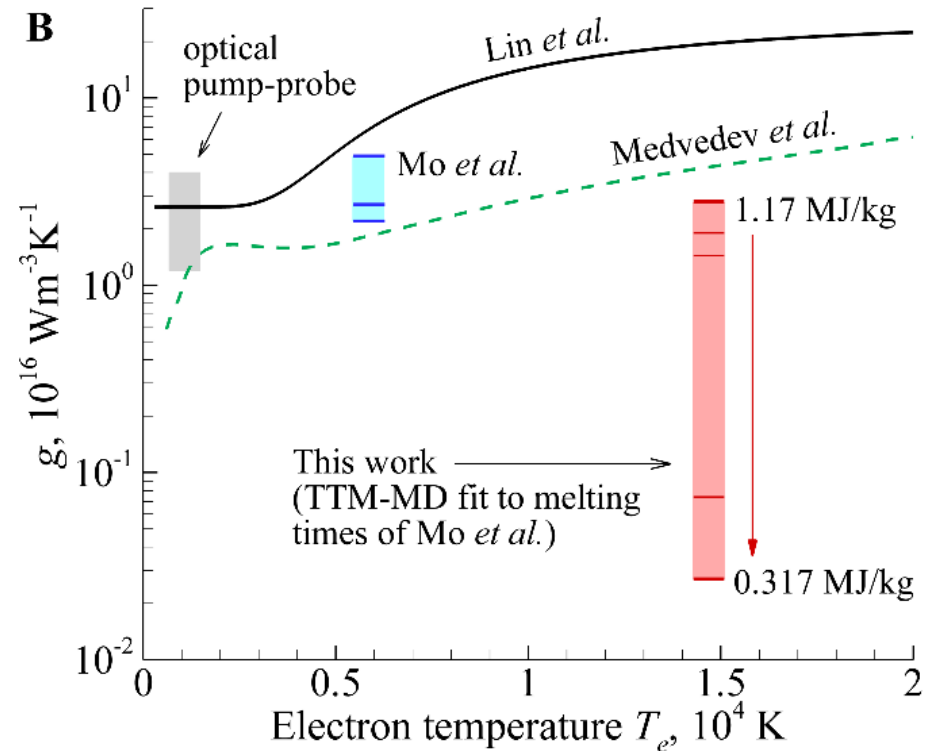
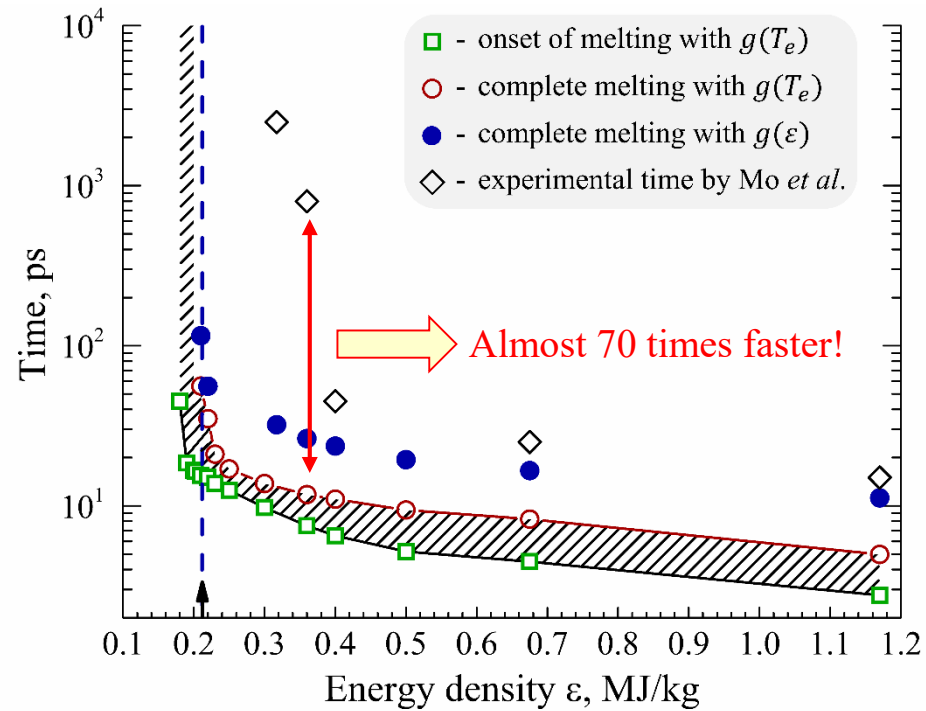


Arefev *et al.*, *Sci. Adv.* **8**, eabo2621, 2022

Ultra-slow melting cannot be explained by modeling with any reasonable value of G

Kinetics of laser-induced melting of thin gold film: **How slow can it get?**

Atomistic modeling of melting of 35 nm Au film

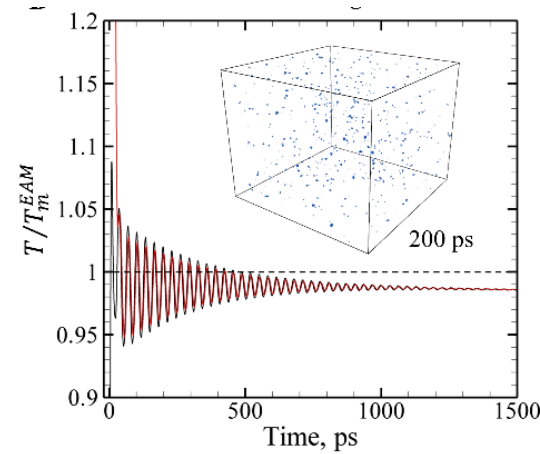
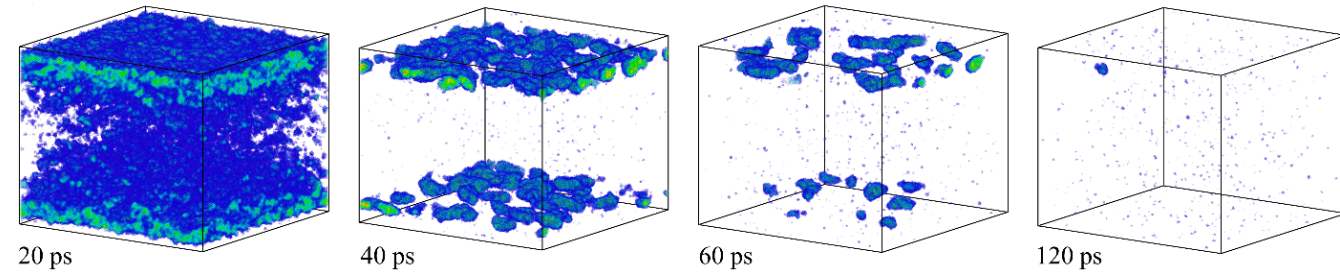


“Never trust an experimental result until it has been confirmed by theory”

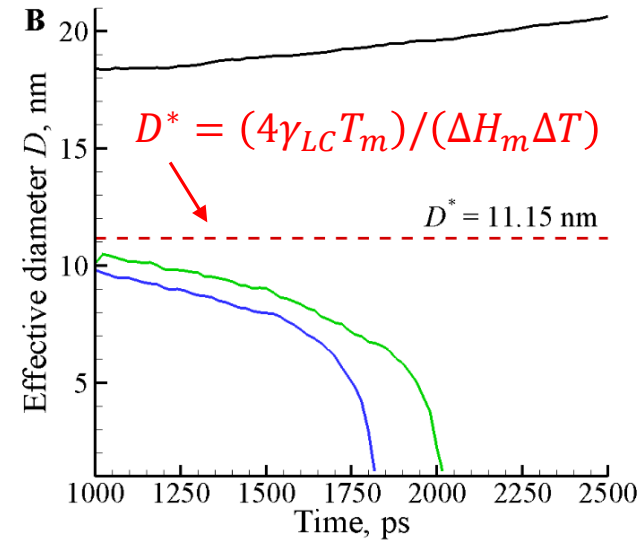
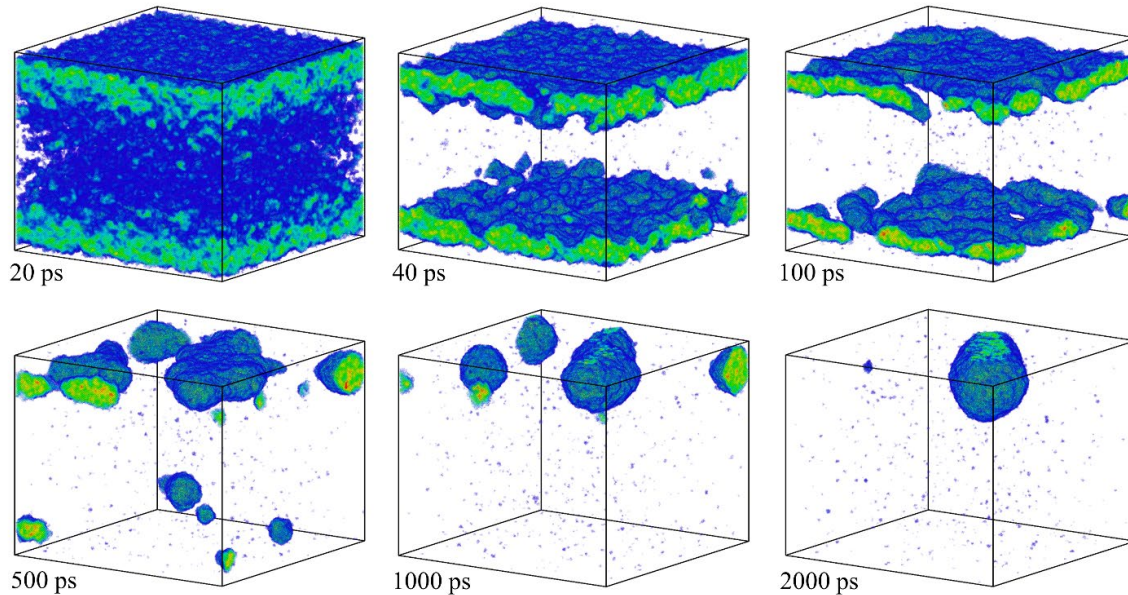
Sir Arthur Stanley Eddington

Kinetics of laser-induced melting of thin gold film: **How slow can it get?**

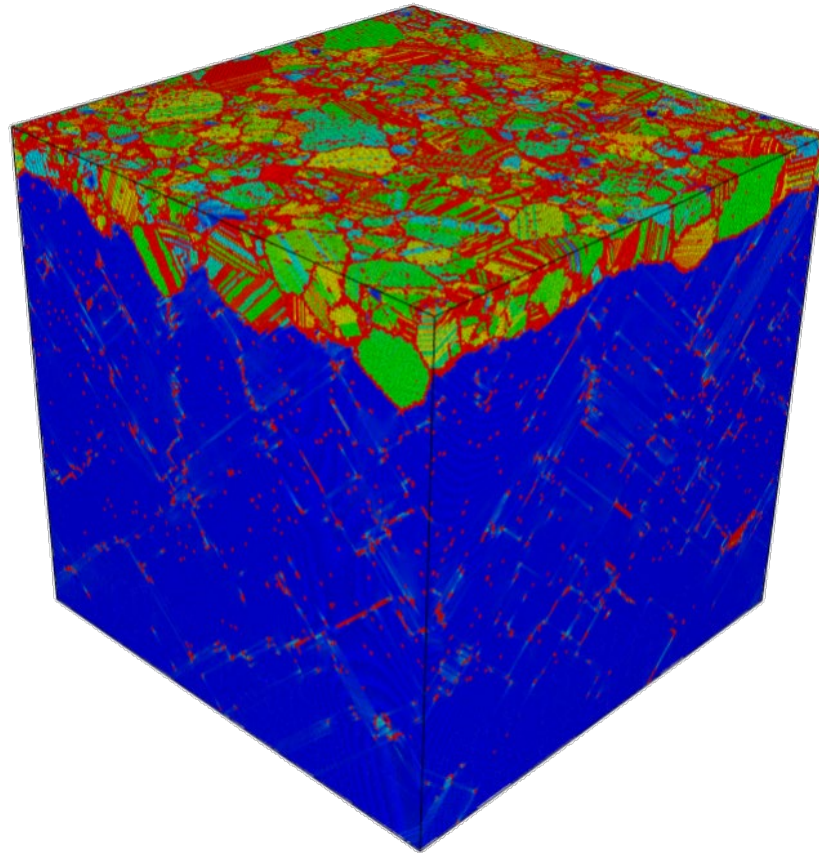
absorbed energy density of $0.21 \text{ MJ/kg} = 0.99\epsilon_m$



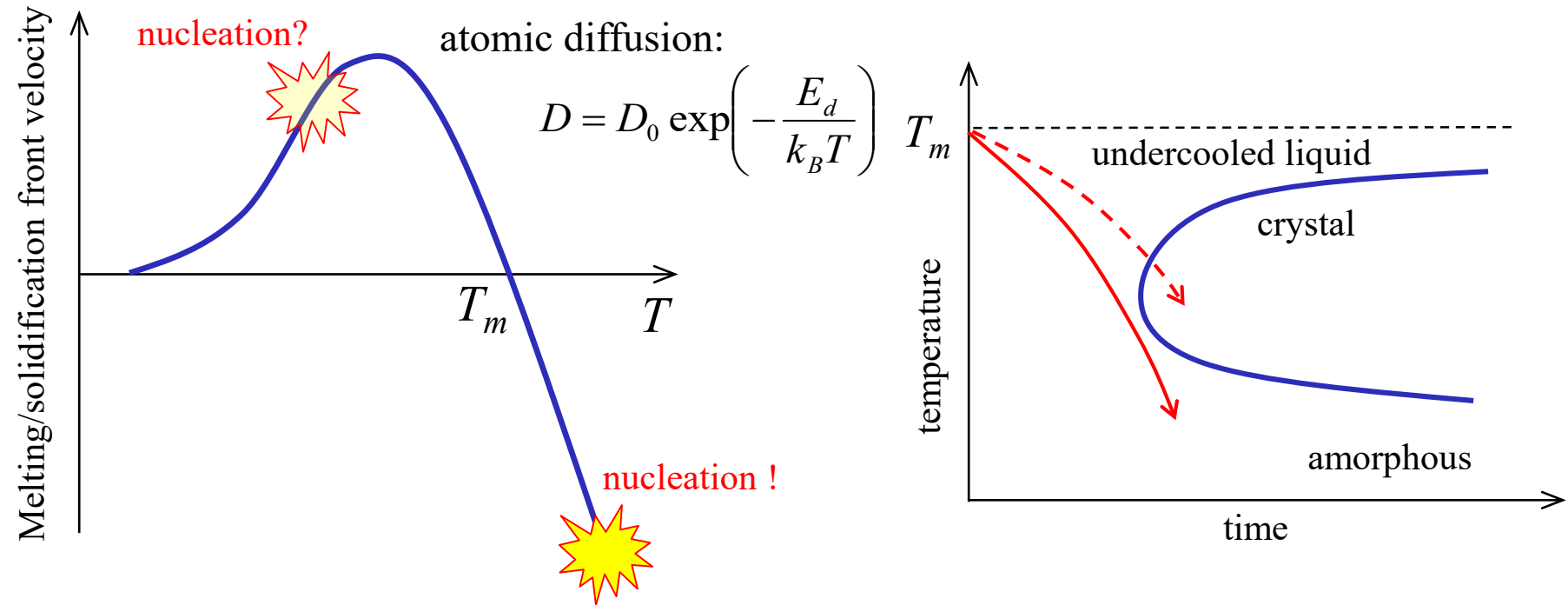
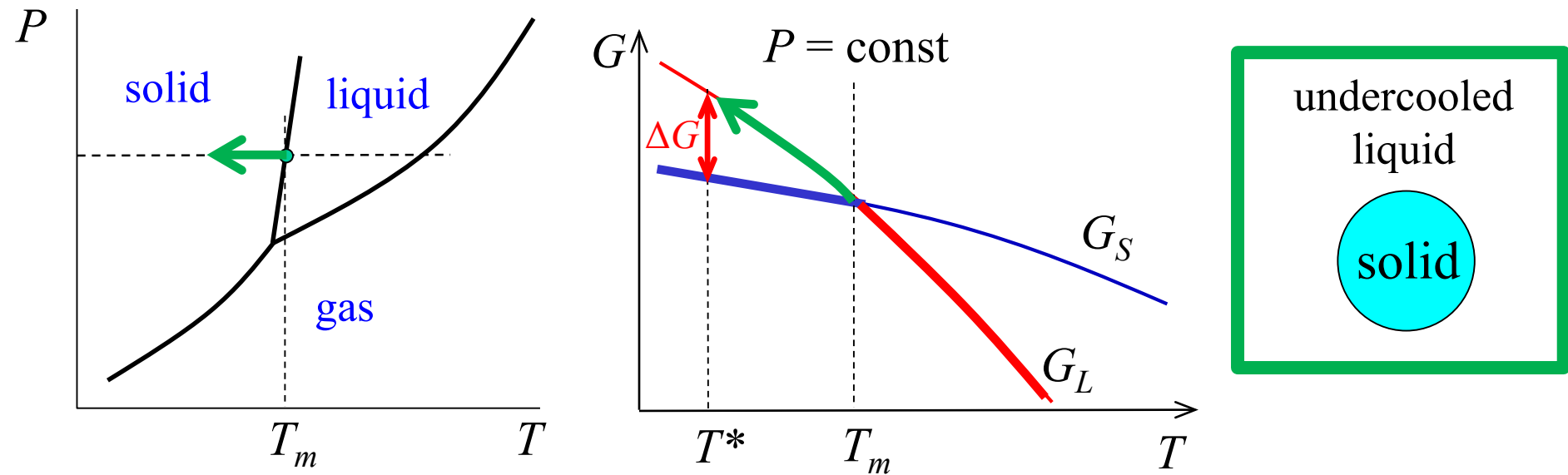
absorbed energy density of $0.2 \text{ MJ/kg} = 0.94\epsilon_m$



Laser-induced phase transformations: Solidification

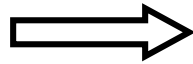


Laser-induced phase transformations: Solidification



Laser-induced phase transformations: Solidification

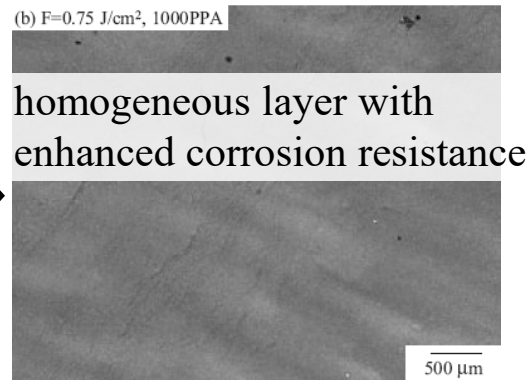
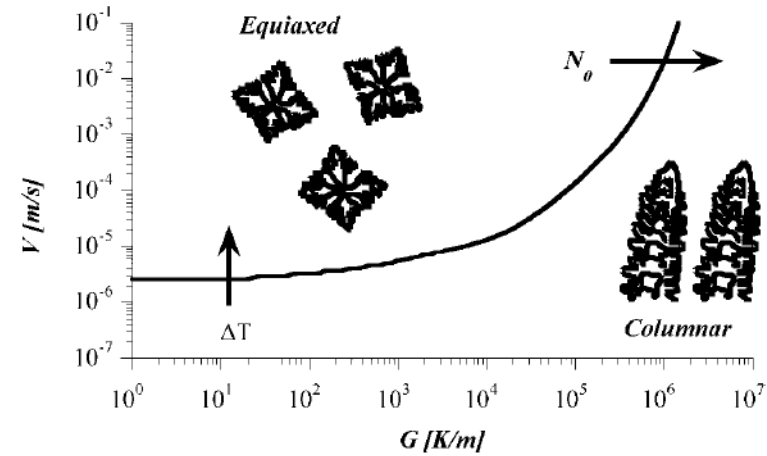
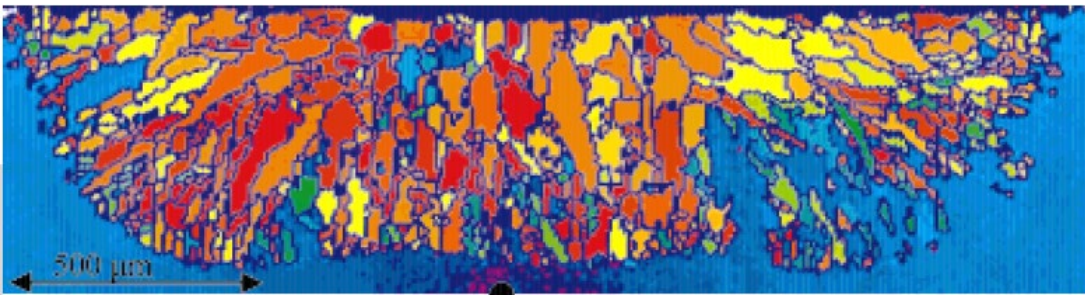
Fast heating and cooling
Melting and resolidification



Modification of surface microstructure
surface alloying, annealing, hardening

Examples:

solidification microstructure – processing maps
Kurtz, *Adv. Eng. Mat.* **3**, 443, 2001



Transition from columnar to equiaxed
microstructure in laser-processed Ni-based
superalloy

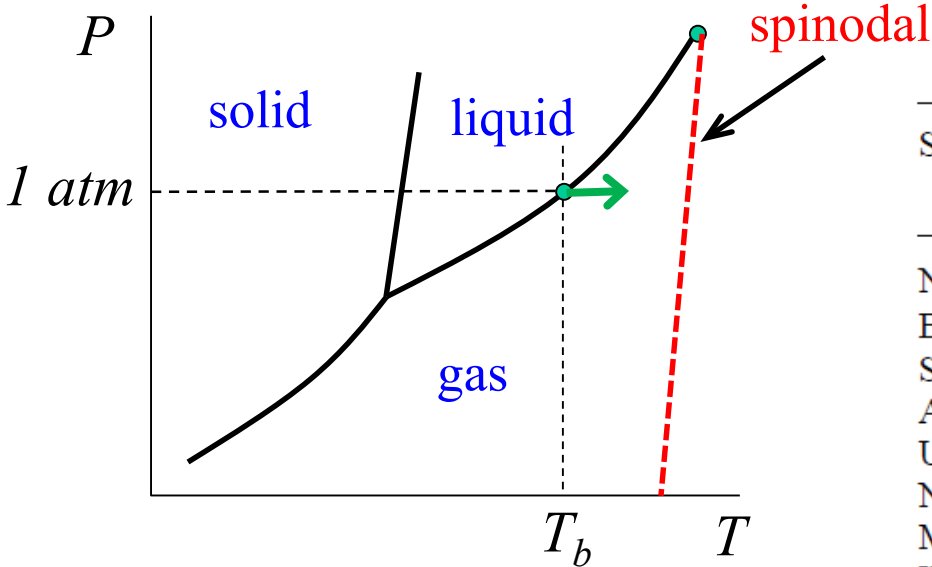
Hoekstra *et al.*, *Adv. Eng. Mat.* **7**, 805, 2005

Clear understanding of the
connections between laser processing
conditions and microstructure is
critical for the actively evolving area
of **additive manufacturing**

Laser-induced phase transformations: Vaporization



“Conventional” vaporization of superheated liquid



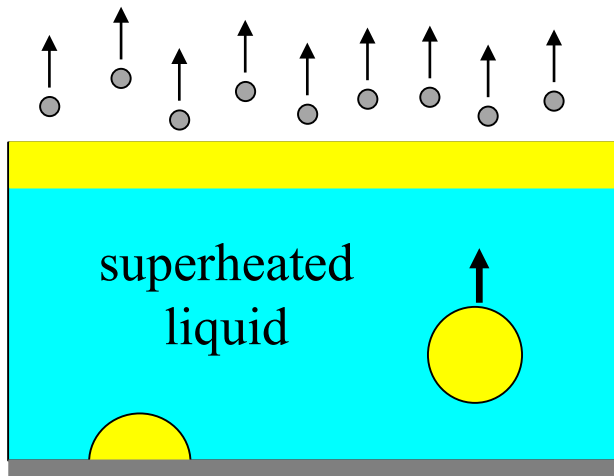
1. Evaporation from the surface

Substance	T_b K	T K	Atom layers in 1 ns	Atom layers in 100 ns
Na	1156	1500	0.78	78
Bi ^(a)	1837	2000	0.058	5.80
Sb ^(b)	1860	2000	0.047	4.7
Ag	2435	3000	0.31	30.5
U	4404	5000	0.069	6.9
Nb	5017	5500	0.069	6.9
Mo	4912	5000	0.028	2.8
W	5828	6000	0.010	1.04

Miotello & Kelly, *Appl. Phys. A* **69**, S67, 1999

2. Normal boiling

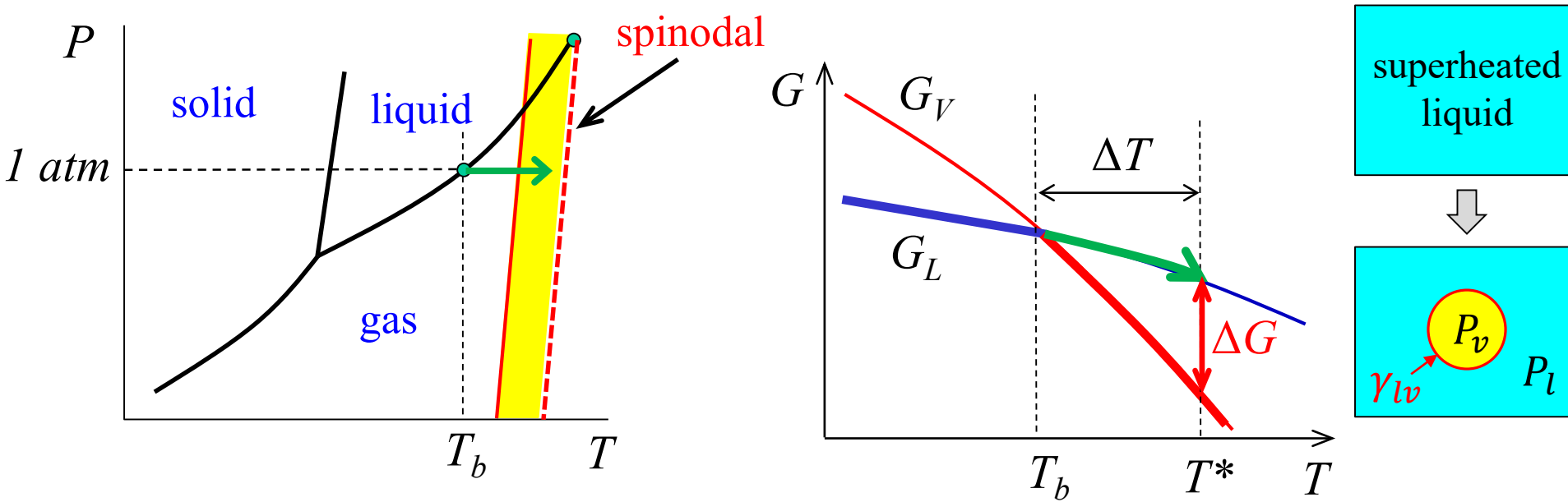
normal boiling is subject to a major kinetic bottleneck in the process of bubble diffusion - distances travelled by a bubble in 100 ns are atomically small at $2T_m$



Surface evaporation and normal boiling are not relevant for ns pulses

Surface evaporation becomes important for 100s ns pulses and longer, can also lead to melt expulsion due to vapor recoil pressure

Vaporization of superheated liquid: Transition to “explosive boiling”



Thermodynamic analysis

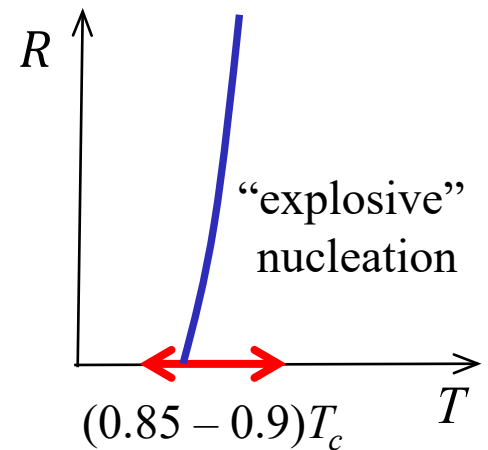
$$\Delta G(r) = 4\pi r^2 \gamma_{lv} - (P_v - P_l) \frac{4}{3} \pi r^3 + (\mu_v - \mu_l) \frac{P_v}{k_B T} \cdot \frac{4}{3} \pi r^3$$

positive
negative

Nucleation rate:

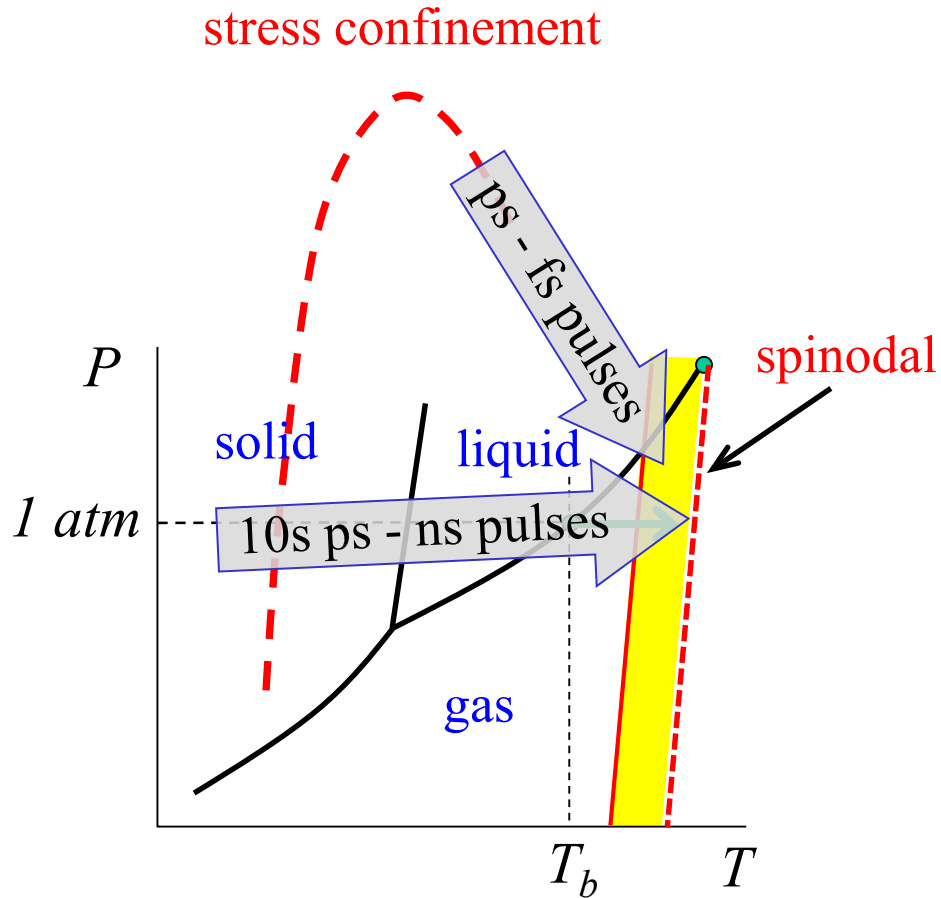
$$R = n_l \sqrt{6 \gamma_{lv} / [(2 + P_l / P_v) \pi m]} e^{-\Delta H_v / k_B T} e^{-\Delta G^* / k_B T}$$

$$\gamma_{lv} \rightarrow 0 \text{ and } \Delta G^* \rightarrow 0 \text{ as } T \rightarrow T_c \quad R \sim \exp\left(-\frac{\Delta G^*}{RT}\right) \rightarrow \infty$$

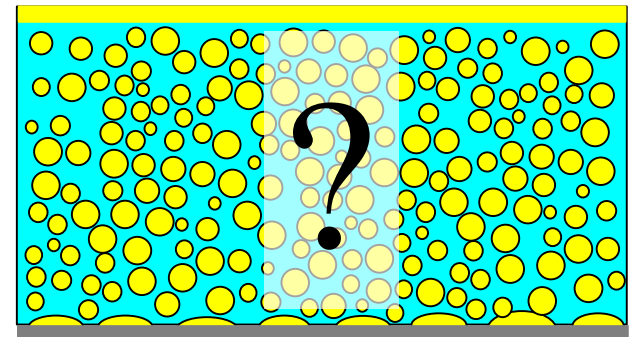
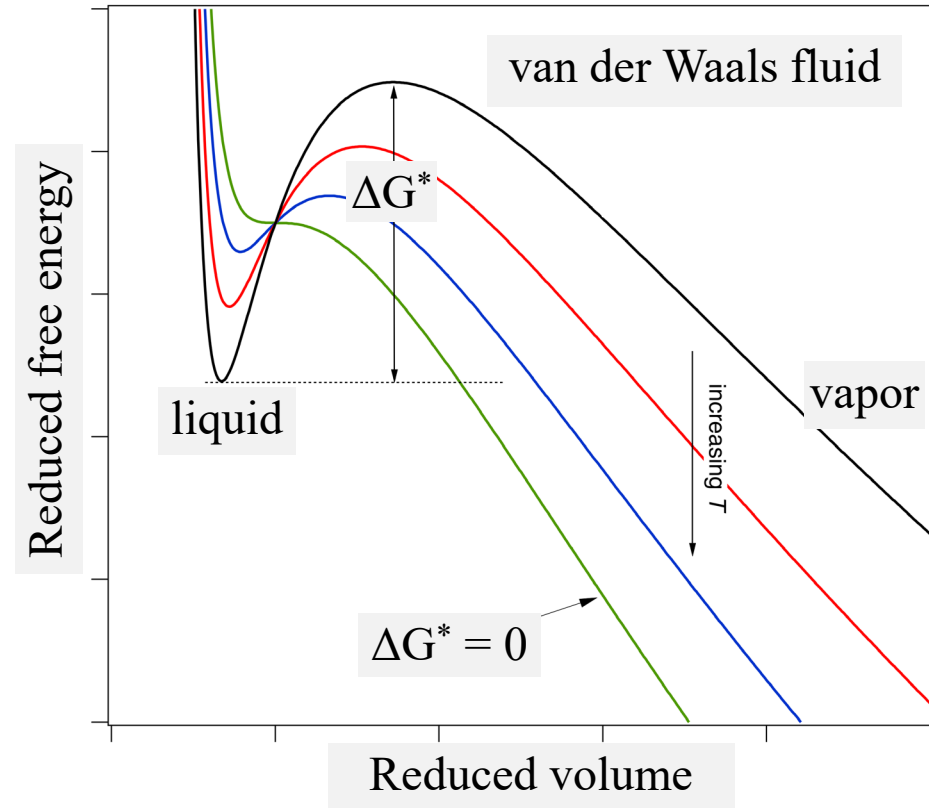


very strong temperature dependence!

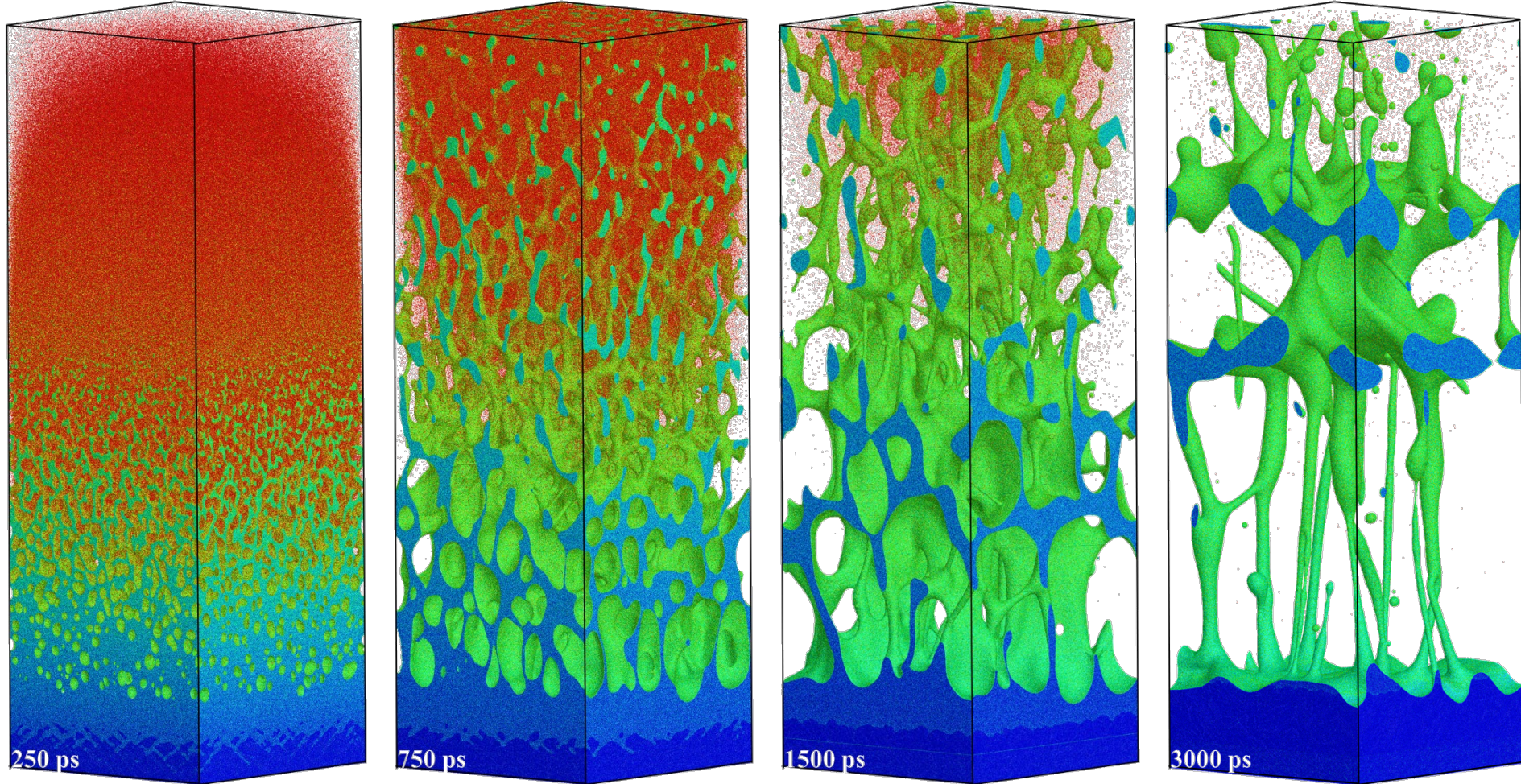
What is “explosive boiling,” also known as “phase explosion” ?



explosive boiling of liquid
superheated up to the limit of
thermodynamic stability

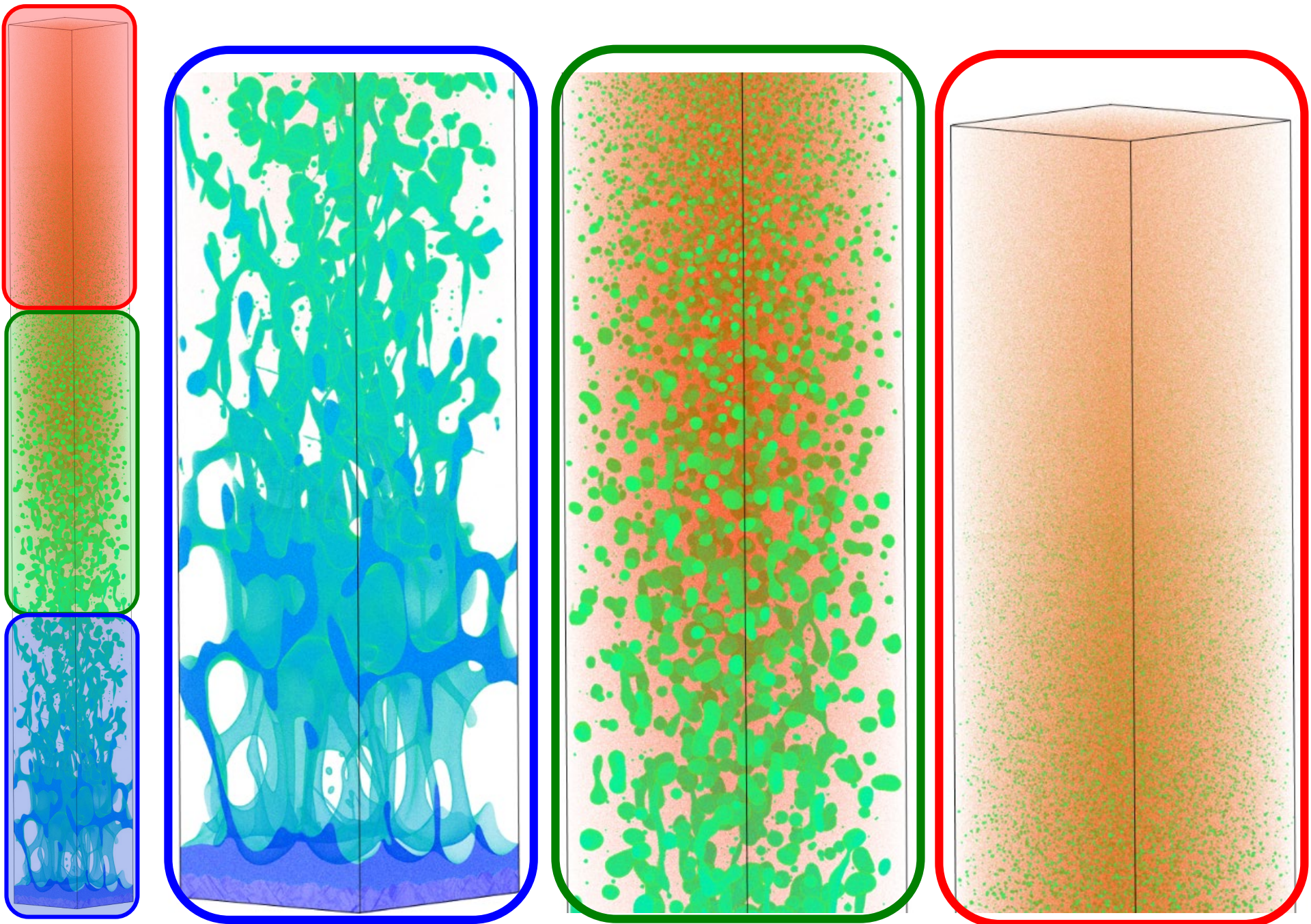


Visual picture of phase explosion from large-scale atomistic simulations

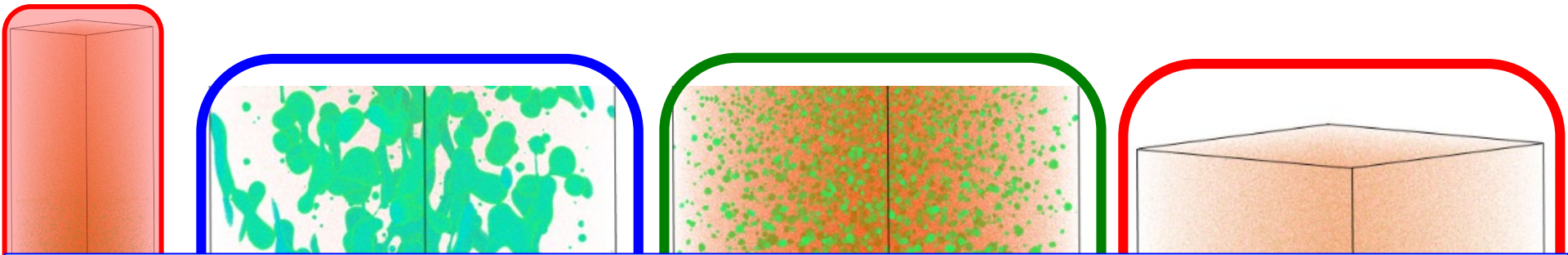


Homogeneous boiling (phase explosion): liquid superheated to $\sim 90\%$ of the spinodal temperature rapidly decomposes into vapor and liquid droplets.

Analysis of the ablation plume from large-scale MD simulations



Analysis of the ablation plume from large-scale MD simulations



Plume imaging: splitting of the plume into a fast component (optical emission of neutral atoms) and a slow component (blackbody-like emission \rightarrow presence of hot clusters)

Albert *et al.*, *Appl. Phys. A* **76**, 319, 2003

Okano *et al.*, *Appl. Phys. Lett.* **89**, 221502, 2006

Noël *et al.*, *Appl. Surf. Sci.* **253**, 6310, 2007

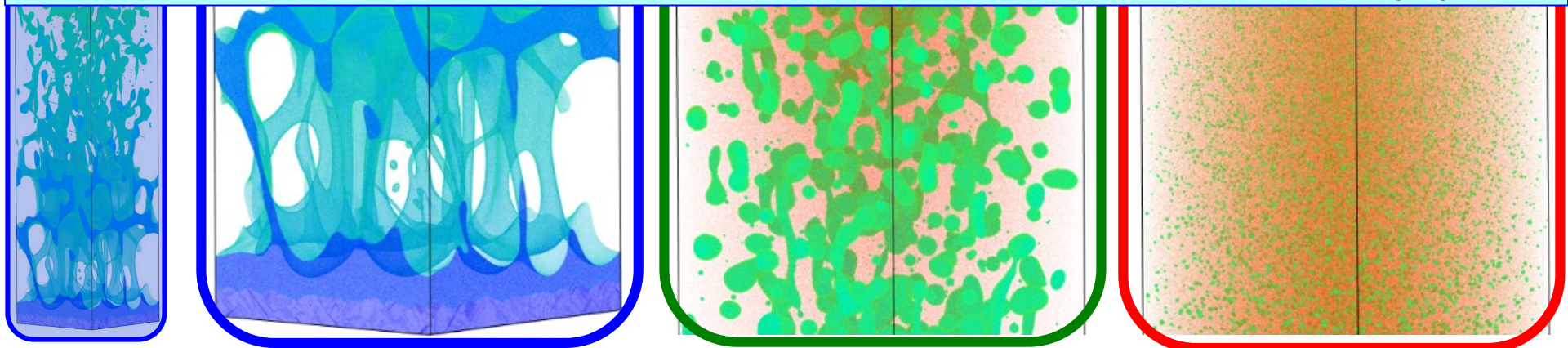
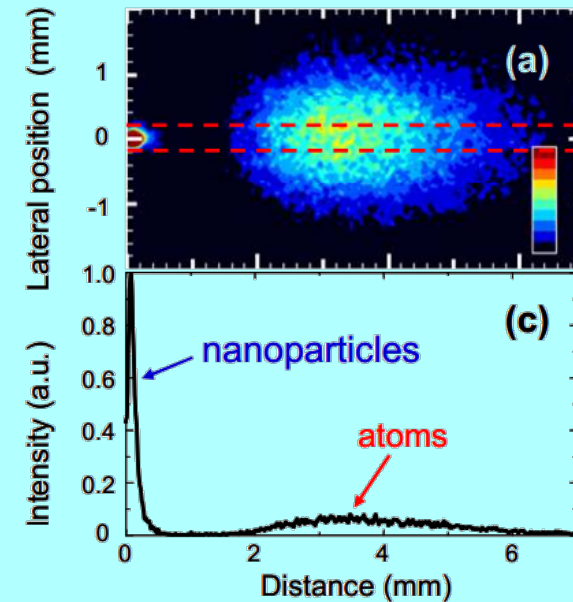
Itina *et al.*, *Appl. Surf. Sci.* **253**, 7656, 2007

Amoruso *et al.*, *Appl. Phys. A* **89**, 1017, 2007

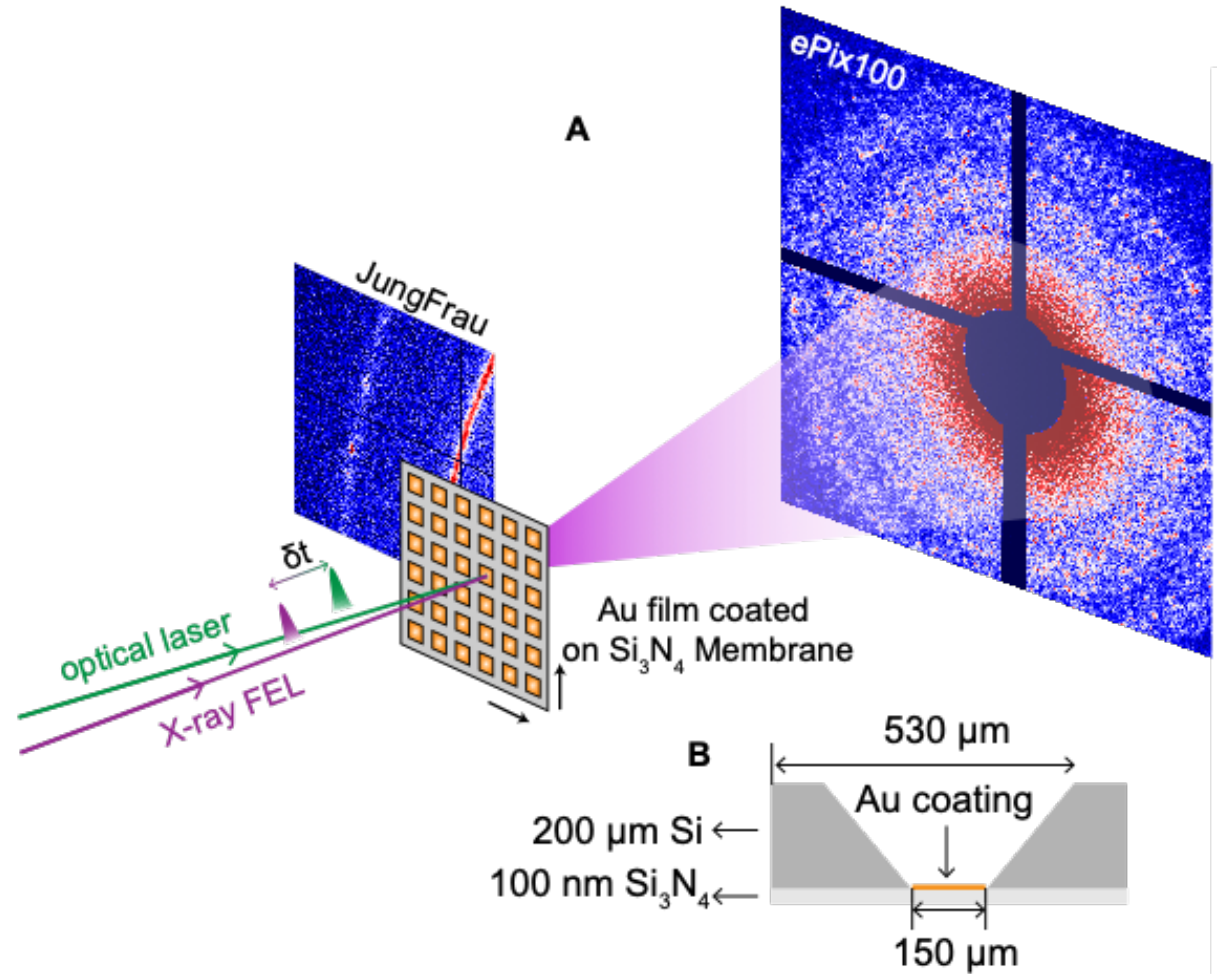
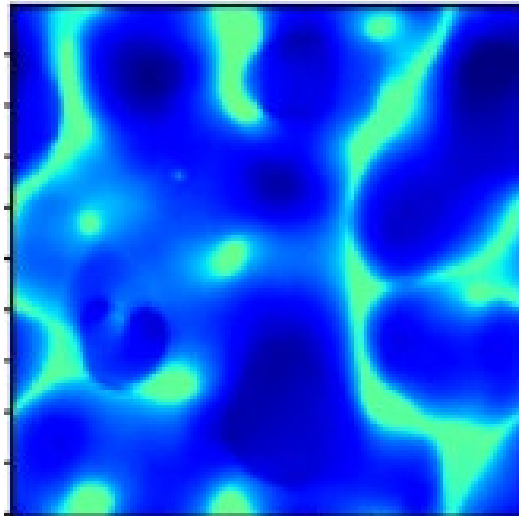
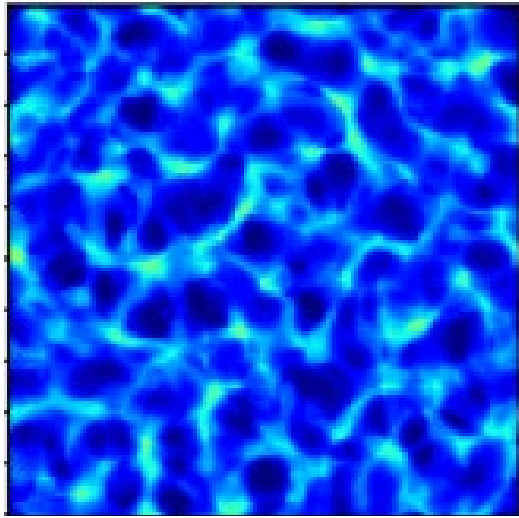
Jegenyes *et al.*, *Appl. Phys. A* **91**, 385, 2008

Nakano *et al.*, *Appl. Phys. A* **101**, 523, 2010

Hermann *et al.*, *J. Phys.: Conf. Ser.* **399**, 012006, 2012



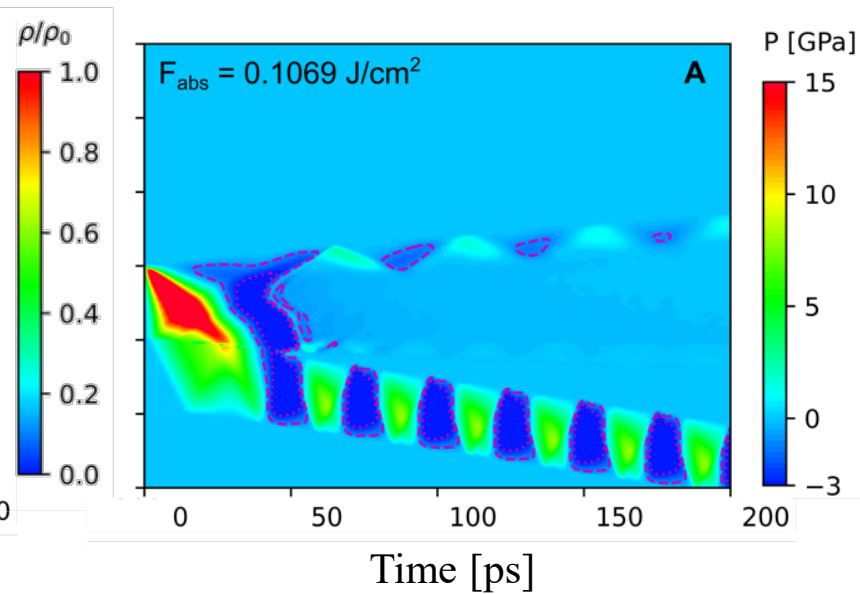
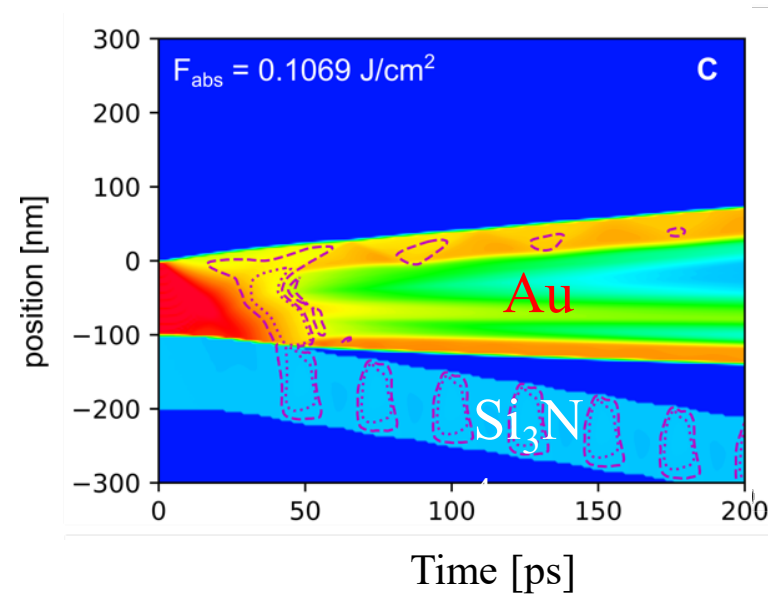
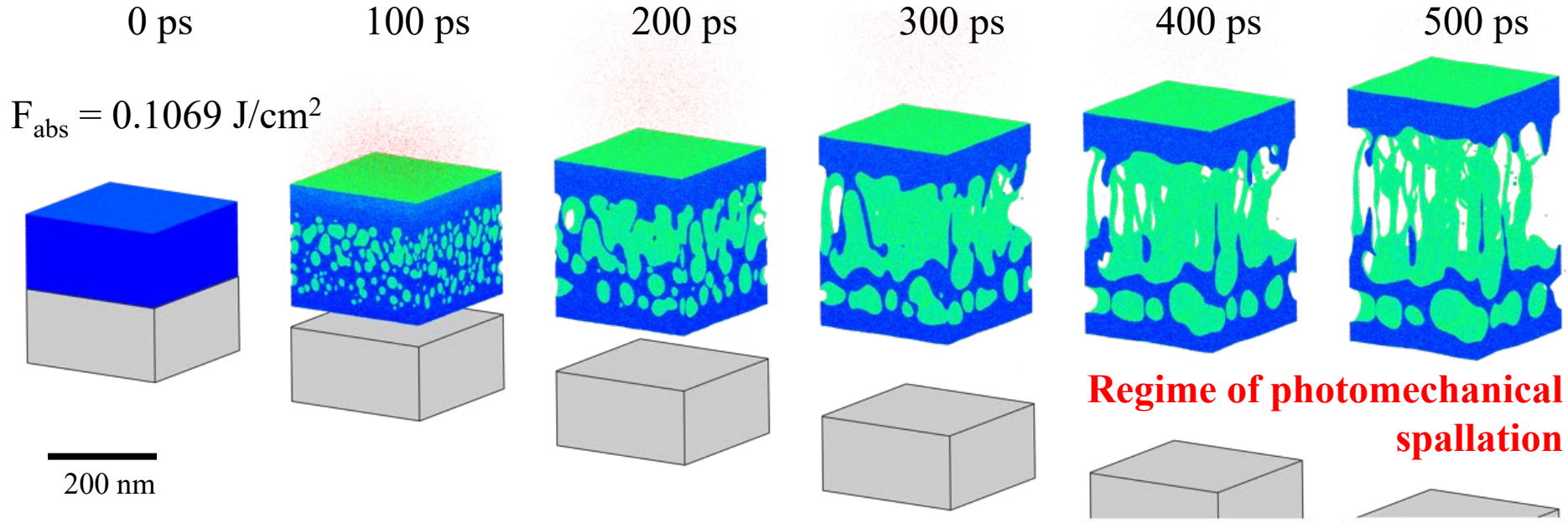
Dynamics of nanoscale phase decomposition in laser ablation



Experiments at SLAC

by Yanwen Sun, Klaus Sokolowski-Tinten *et al.*

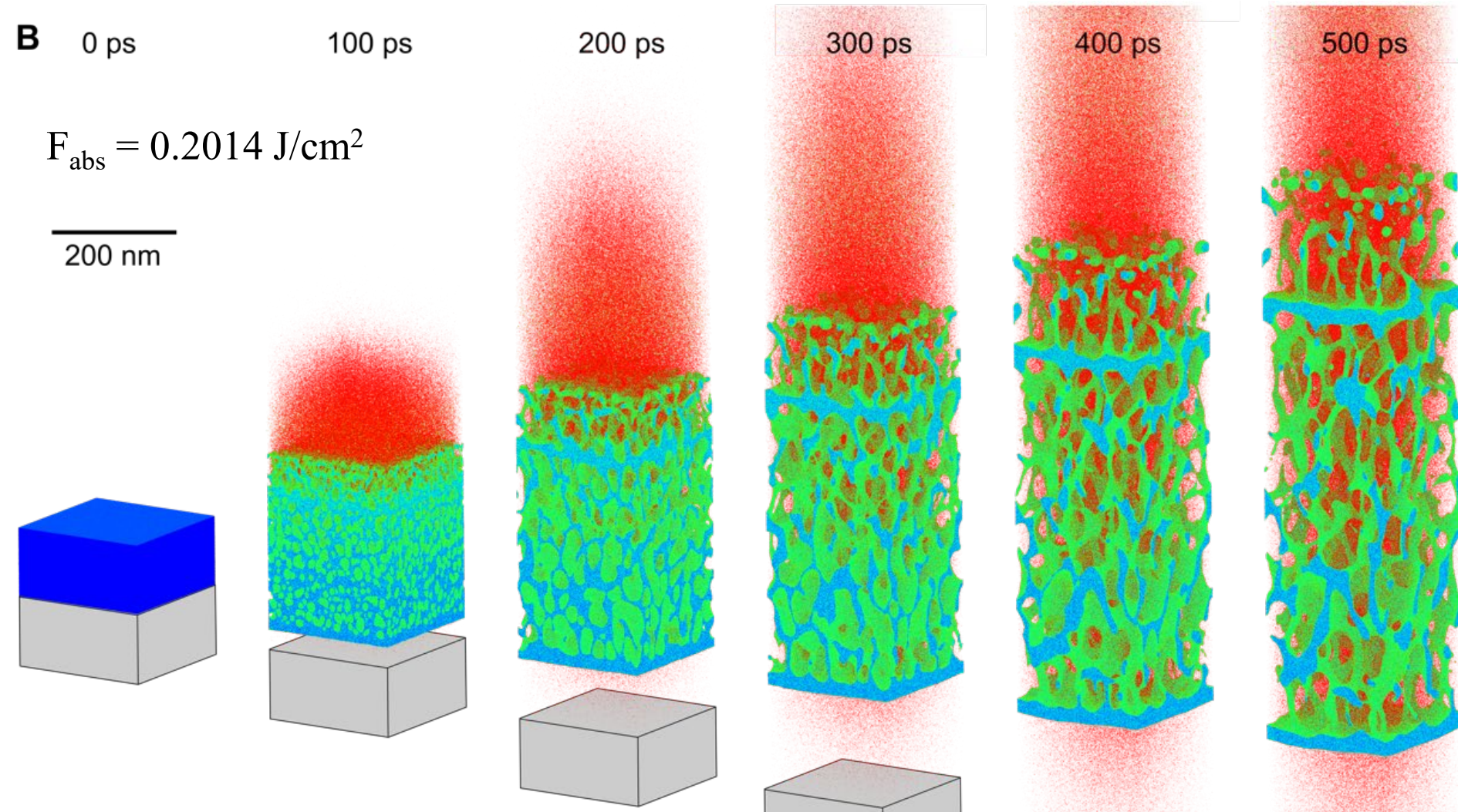
Dynamics of nanoscale phase decomposition in laser ablation



Chaobo
Chen

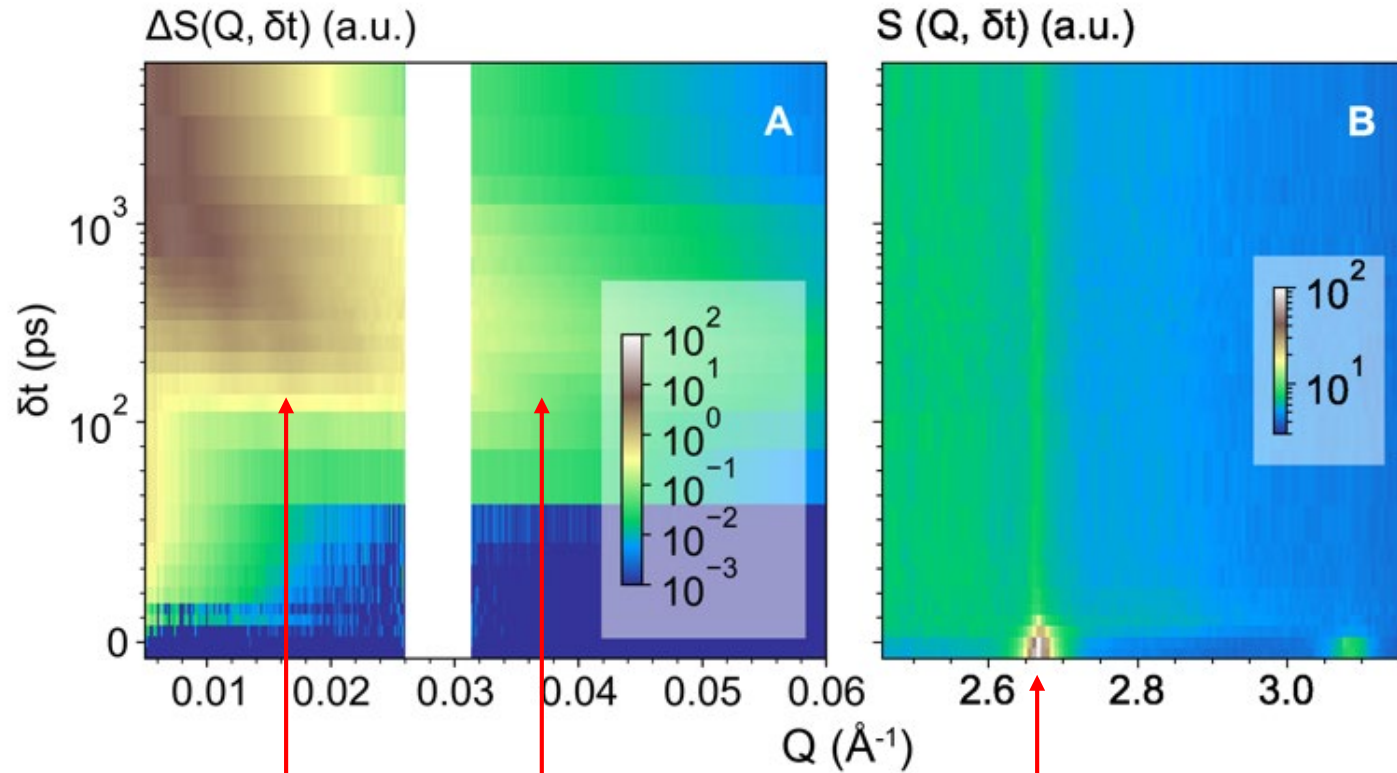
Dynamics of nanoscale phase decomposition in laser ablation

Transition from photomechanical spallation to phase explosion



Dynamics of nanoscale phase decomposition in laser ablation

Experiments at SLAC by Yanwen Sun, Klaus Sokolowski-Tinten *et al.*

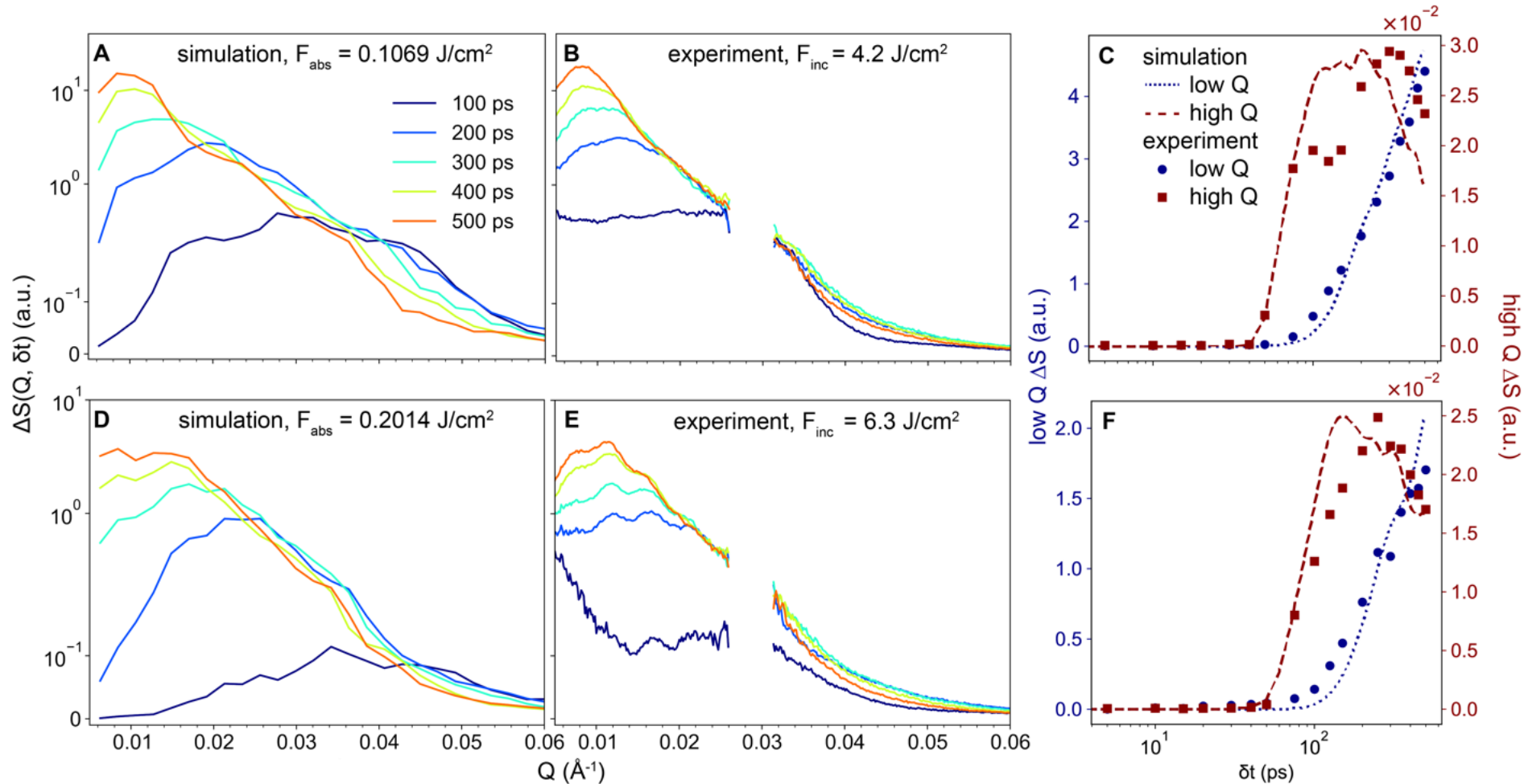


(2) then, low- Q signal appears, signifying emergence of nanoscale density variation

(1) first film fully melts

length-scale d that corresponds to Q : $d = \frac{2\pi}{Q}$

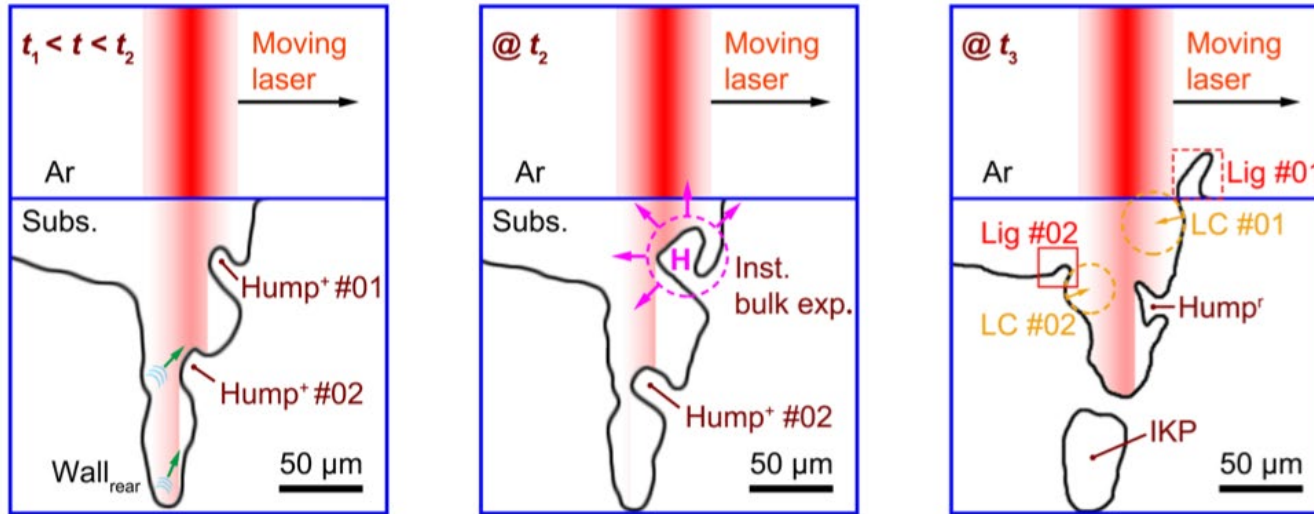
Dynamics of nanoscale phase decomposition in laser ablation: Direct verification of computational predictions



...except that *something strange* is going on in the low-Q region:
Increase at $Q \sim 0.005 - 0.02 \text{ \AA}^{-1}$ ($d \sim 30 - 125 \text{ nm}$) within 100 ps

What is the lower limit on the heating rate for triggering phase explosion?

In-situ X-ray probing of **CW additive manufacturing**: sudden disappearance of keyhole protrusions and metal spattering - evidence of the phase explosion.



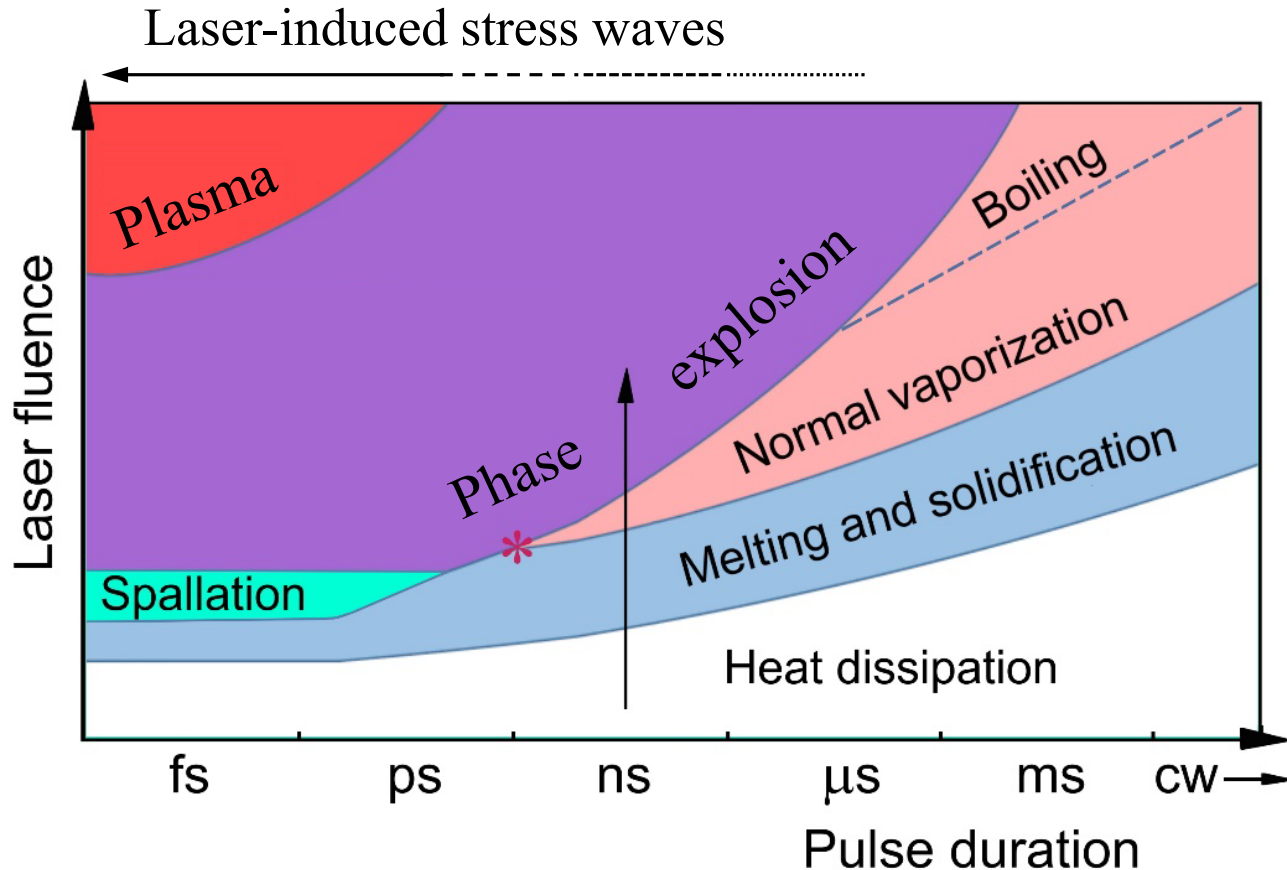
Zhao et al., *Phys. Rev. X* **9**, 021052, 2019;
Science **370**, 1080, 2020.

Nahen and Vogel, *J. Biomed. Opt.* **7**, 165, 2002: phase explosion in laser ablation of gelatin and biological tissue induced by **100 μs laser pulses**

Possible question for classroom discussion

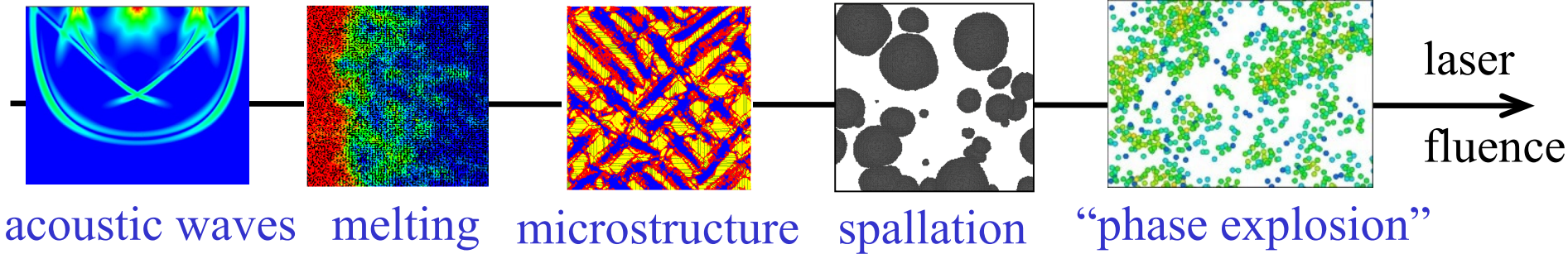
What is (or is there) an upper limit for the laser pulse duration for triggering the phase explosion?

Thermal processes at different laser fluences and pulse durations



M. V. **Shugaev**, M. **He**, Y. **Levy**, A. **Mazzi**, A. **Miotello**, N. M. **Bulgakova**, and L. V. **Zhigilei**, Laser-induced thermal processes: Heat transfer, generation of stresses, melting and solidification, vaporization and phase explosion, in: *Handbook of Laser Micro- and Nano-Engineering*, Edited by K. **Sugioka** (Springer, Cham, Switzerland, 2021), pp. 83-163.

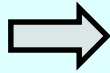
Summary on laser-induced thermal processes



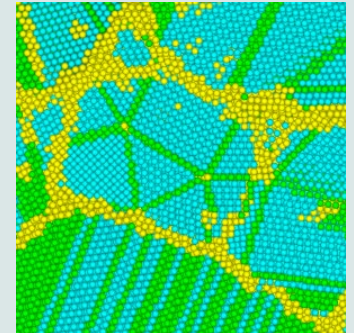
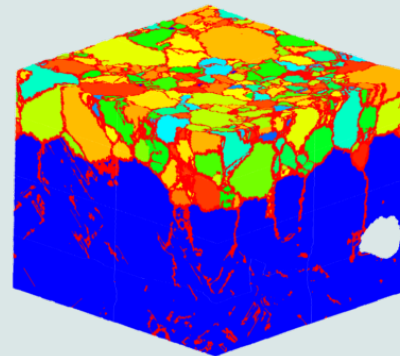
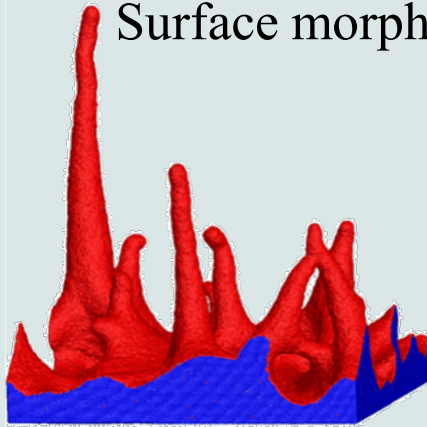
thermal spike

rapid melting
& solidification

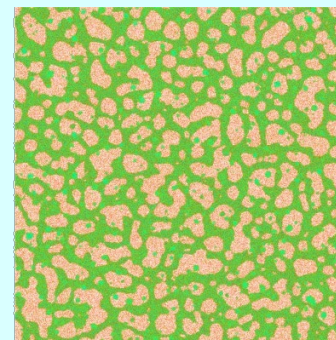
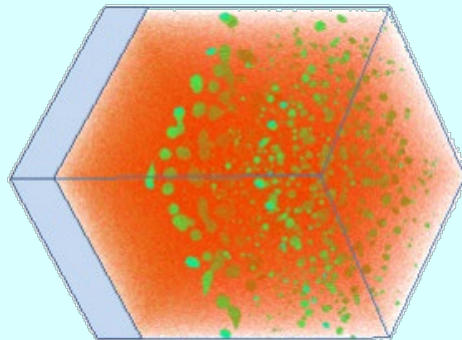
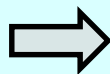
laser-induced
stresses



Surface morphology, crystal defects, metastable phases



vaporization
phase
explosion



parameters of the
ablation plume
and generation of
nanoparticles